On the physiology of artificial hibernation

Dirkes, M.C.

Publication date
2018
Document Version
Final published version
License
Other

On the Physiology of Artificial Hibernation

Marcel C. Dirkes

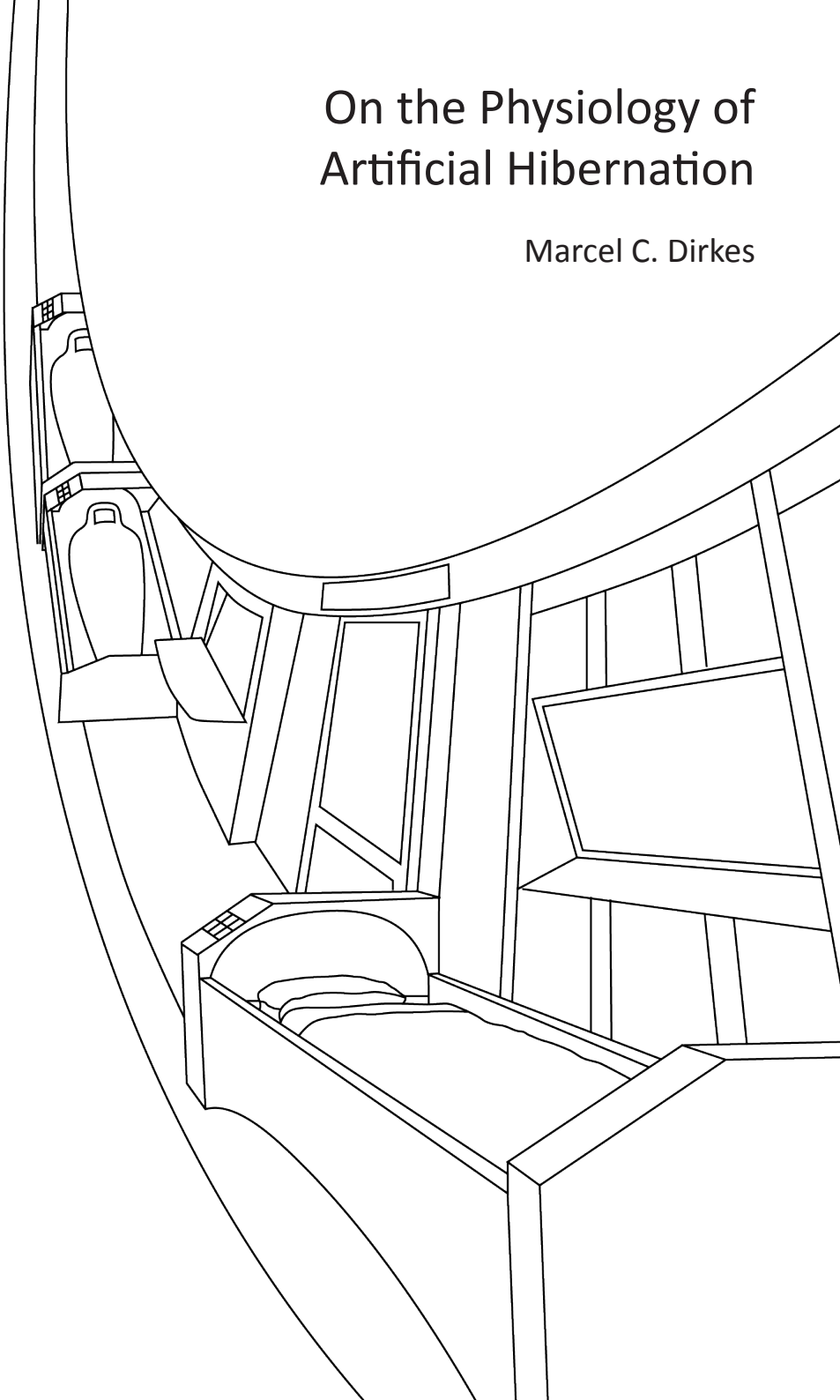

On the Physiology of Artificial Hibernation

Marcel C. Dirkes

All reported studies were performed at the Surgical Laboratory of the Academic Medical Center, University of Amsterdam, Amsterdam, The Netherlands

This research was supported by:

- **Roba Metals BV**
  IJsselstein, The Netherlands
- **Mediphenix Holding BV**
  Zoeterwoude, The Netherlands

On the Physiology of Artificial Hibernation

UNIVERSITY OF AMSTERDAM

ACADEMISCH PROEFSCHRIFT

Ter verkrijging van de graad van doctor
aan de Universiteit van Amsterdam
Op gezag van de Rector Magnificus prof. dr. ir. K.I.J. Maex
ten overstaan van een door het College voor Promoties
ingestelde commissie, in het openbaar te verdedigen in de
Agnietenkapel op Donderdag 27 november 2018, te 10.00
uur

door Marcel Cornelis Dirkes
Geboren te Veldhoven

Promotiecommissie

Promotores:	prof. dr. T.M. van Gulik	AMC-UvA
Co-promotores:	dr. M. Heger	AMC-UvA
Overige leden:	prof. dr. E.L. Swart	Vrije Universiteit Amsterdam
	prof. dr. ir. C. Ince	AMC-UvA
	prof. dr. N.P. Juffermans	AMC-UvA
	prof. dr. R.P.J. Oude Elferink	AMC-UvA
	prof. dr. H.G.D. Leuvenink	Rijksuniversiteit Groningen
	dr. A.G. Baranski	Universiteit Leiden

Faculteit der Geneeskunde

CONTENT TABLE

Content table

Part III Single organ application

INTRODUCTION

MEDICAL NOTES IN PARLIAMENT.

HUMAN HIBERNATION.

A PRACTICE closely akin to hibernation is said to be general among Russian peasants in the Pskov Government, where food is scanty to a degree almost equivalent to chronic famine. Not having provisions enough to carry them through the whole year, they adopt the economical expedient of spending one half of it in sleep. This custom has existed among them from time immemorial. At the first fall of snow the whole family gathers round the stove, lies down, ceases to wrestle with the problems of human existence, and quietly goes to sleep. Once a day every one wakes up to eat a piece of hard bread, of which an amount sufficient to last six months has providently been baked in the previous autumn. When the bread has been washed down with a draught of water, everyone goes to sleep again. The members of the family take it in turn to watch and keep the fire alight. After six months of this reposeful existence the family wakes up, shakes itself, goes out to see if the grass is growing, and by-and-by sets to work at summer tasks. The country remains comparatively lively till the following winter, when again all signs of life disappear and all is silent, except we presume for the snores of the sleepers. This winter sleep is called *lotska*. These simple folk evidently come within the terms of Touchstone's definition of a natural philosopher; and many whose lot is cast in places where men are breathless with the fierce race for power or glory or wealth would doubtless be disposed to say of them, *O fortunatos nimium sua si bona norint!* In addition to the economic advantages of hibernation, the mere thought of a sleep which knits up the ravelled sleeve of care for half a year on end is calculated to fill our harassed souls with envy. We, doomed to dwell here where men sit and hear each other groan, can scarce imagine what it must be for six whole months out of the twelve to be in the state of Nirvana longed for by Eastern sages, free from the stress of life, from the need to labour, from the multitudinous burdens, anxieties, and vexations of existence.

JUNE 23, 1900.

Introduction

During the turn of the 20th century, a brief account of human hibernation appeared in the British Medical Journal. Published in full on the previous page, it describes the observations of an anonymous explorer who came across a practice in Russia to combat the winter that bears a likeliness to hibernation.

Looking back, it is safe to say that these observations were less of a scientific report, and more a reflection of the author's personal yearn to escape the daily stresses of life. But it still raises the question of how much progress we have made over the past century. How far have we come to realize hibernation in humans?

Our understanding of natural hibernation has vastly improved over the last century. Zoological research has documented countless of hibernating species and unraveled many of the underlying principles. All amidst a growing prospect of human application, ranging from organ preservation prior to transplantation, to its potential impact on long term spaceflight. Yet it takes little effort to see that these applications have yet to materialize.

So what is holding us back? There is no evidence that indicates hibernation is dependent on factors that would exclude humans from entering such a state. And this optimism is further substantiated by the diverse set of animals that display hibernation or similar states of low metabolism.

Many of these animals demonstrate comparable, but seemingly unconnected, attributes. For example, hibernation seems to be under neurological control, it appears to be unrelated to body size, and metabolic depression seems to precede the characteristic drop in body temperature. But as these appear to be relevant attributes, their interrelations and dependencies are left up to theory.

In the last decades, there is a growing interest in an old attribute: (bio) chemical agents that have the ability to lower metabolism in animal models. Dubbed hibernation induction trigger in the late sixties, it now causes a renewed attention for the translation of hibernation to humans. In the wake of this attention, new experimental evidence surfaces all over the map. In particular of hydrogen sulfide, an otherwise toxic gas, that became a notable

centre of attention in hypometabolic research.

However, in contrast to much of the early work in the field of hibernation, new experimental evidence focuses on cellular pathways and tissue-isolated effects, leaving some of the important physiological effects aside.

This dissertation aims to complement and clarify the already existing findings and place them in context of a new model to advance our view on possible interrelations and dependencies. It remains unclear whether the renewed interest in hibernation moves the needle any closer to understanding how to translate hibernation to humans, but as you may find in this dissertation, it seems to have paved a way of new avenues to explore.

OUTLINE

Outline

The work described in this dissertation, On the Physiology of Artificial Hibernation, aims to translate insights from the physiology of natural hibernators to a model of artificial hibernation that could aid clinical applications.

In **Part I**, the governing physiological elements that are responsible for the induction of (artificial) hibernation are discussed. Translation to its artificial counterpart is currently hampered by incomplete understanding of the exact mechanisms responsible for induction of hibernation. To facilitate this translation, in **Chapter 1**, a model is presented that identifies the necessary physiological changes for induction of artificial hibernation. This model interrelates six essential components: metabolism, body temperature, thermoneutral zone, substrate, ambient temperature, and hibernation-inducing agents. Then, **Chapter 2** dives deeper into one of the critical elements to gain control over this model: (bio)chemical and pharmacological agents with thermoregulatory properties. To identify the potential of pharmacological agents to induce anapyrexic signaling, i.e. to signal a lowering of the thermoneutral zone, experimental findings of over a thousand pharmacologically active compounds were analyzed for their ability to induce anapyrexia in different animals.

In **Part II**, the effects of a popular biochemical agent, hydrogen sulfide (H_2S), are evaluated for its potential to induce artificial hibernation in large and small animals. **Chapter 3** starts with a series of experiments in large animals (pigs), studying the effects of H_2S on systemic, pneumocardial, hematological, biochemical, microvascular, and histological parameters. On the basis of our findings and the literature, a mechanistic explanation is provided for the differential manifestation of hypometabolism between small and large animals upon exposure to H_2S. **Chapter 4**, subsequently, goes back to a small-animal model (mice) and compares the effects of H_2S to – what turns out to be – the more potent effects of hypoxia for the induction of artificial hibernation.

Part III ends with a description of practical systems and strategies for bringing this model to single organ application in the liver, ultimately to be

used to improve organ viability and transplantation success rates in clinical scenarios. **Chapter 5** describes the necessary preparations to the liver to maintain stable extracorporeal hepatic physiological function. In this context, the ideal pressure, temperature and solution to wash a liver clean of red blood cells is studied in a rat liver model. **Chapter 6** closes with the proposal of a novel, portable, pressure-regulated, and oxygenated machine perfusion system that allows extended extracorporeal perfusion of the liver via the portal vein. This final chapter demonstrated how several of the model's elements can be controlled in an extracorporeal environment.

PART I
THE PHYSIOLOGY OF ARTIFICIAL HIBERNATION

Chapter 1
Governing the physiology of artificial hibernation

Adapted from

M.C. Dirkes, T.M. van Gulik, M. Heger
J Clin Trans Res 2015(2): 78-93

ABSTRACT

Incomplete understanding of the mechanisms responsible for induction of hibernation prevent translation of natural hibernation to its artificial counterpart. To facilitate this translation, a model was developed that identifies the necessary physiological changes for induction of artificial hibernation. This model encompasses six essential components: metabolism (anabolism and catabolism), body temperature, thermoneutral zone, substrate, ambient temperature, and hibernation-inducing agents. The individual components are interrelated and collectively govern the induction and sustenance of a hypometabolic state. To illustrate the potential validity of this model, various pharmacological agents (hibernation induction trigger, delta-opioid, hydrogen sulfide, 5'-adenosine monophosphate, thyronamine, 2-deoxyglucose, magnesium) are described in terms of their influence on specific components of the model and corollary effects on metabolism.

INTRODUCTION

Metabolic homeostasis is key to physical function, justifying its meticulous regulation and powerful governing mechanisms in every living cell. The ability to artificially and reversibly reduce metabolism could provide many advantages for medicine, sports, and aviation [Ratigan and McKay, 2016; Bereiter-Hahn et al., 2015]. However, despite a growing understanding of our ability to regulate the mechanisms that govern metabolism at the cellular level, translation of metabolic control in cells to a whole organism has remained beyond our reach.

In nature, reversible states of hypometabolism are a common trait. Members of eight species, including a variety of rodents, carnivores (bears), and primates (lemurs) are known to exhibit a type of hypometabolism [Geiser, 2004]. Although biological vernacular varies between many different types of hypometabolism (Figure 1), two types can generally be distinguished within animals that have an endogenous thermoregulatory system: a deep and a shallow type of hypometabolism. The difference lies in the depth of the drop in body temperature (T_b) and the duration. Shallow hypometabolism represents a temporary type, as exhibited during torpor by e.g., the house mouse, whereas deep hypometabolism is a more sustainable type, as is found in e.g., the hibernating ground squirrel [Geiser 2004; Hudson and Scott, 1979].

The mechanism(s) responsible for the induction of hypometabolism remain(s) controversial [Geiser, 2004]. Unfavorable environmental circumstances appear to be a common denominator in hibernating animals, including seasonal cooling, light deprivation, and prolonged starvation. However, the use of such external triggers to induce artificial hibernation in humans has proven to be of no avail. Irrespective of the external cues, an internal physiological signal, or perhaps a concerted cascade of signals, must initiate, propagate, govern, and sustain hypometabolic signaling in vivo. In an attempt to find such a signal, much research has focused on (bio)chemical signaling during hibernation and its induction, leading to the identification of several hypometabolic agents [Blackstone et al., 2005; Dark et al., 1994; Horton et al., 1998; Scanlan et al., 2004; Zhang et al., 2006].

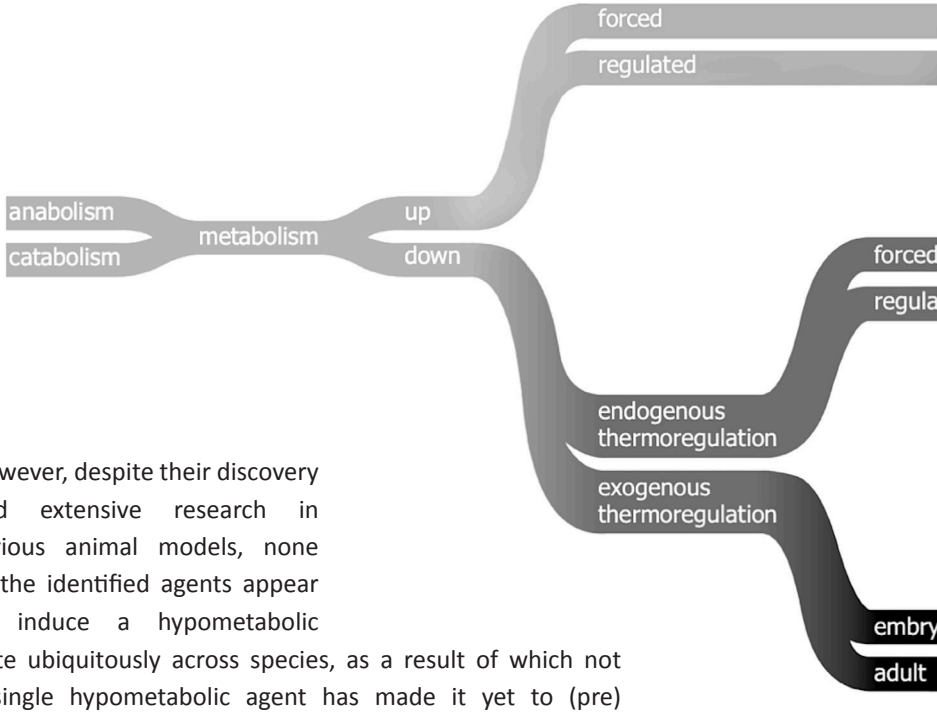

However, despite their discovery and extensive research in various animal models, none of the identified agents appear to induce a hypometabolic state ubiquitously across species, as a result of which not a single hypometabolic agent has made it yet to (pre) clinical application. Currently, the only metabolic control that is clinically employed is forced hypothermia-induced hypometabolism, although this type of hypometabolism fails to achieve the depth found in natural hibernators and comes with challenging limitations.

In an attempt to expand on current insights into hypometabolism, this review addresses the conditions necessary for the induction of hypometabolism and the possible initial (biochemical) triggers. Accordingly, a theorem on the induction of hypometabolism is presented, whereby the relationship between key physiological and environmental factors is provided as a framework to explain the physiological cascade that leads to a sustainable and reversible state of hypometabolism in mammals. Readers should note that the focus of this paper is on mainly the physiological and biochemical conditions required for the induction of hypometabolism.

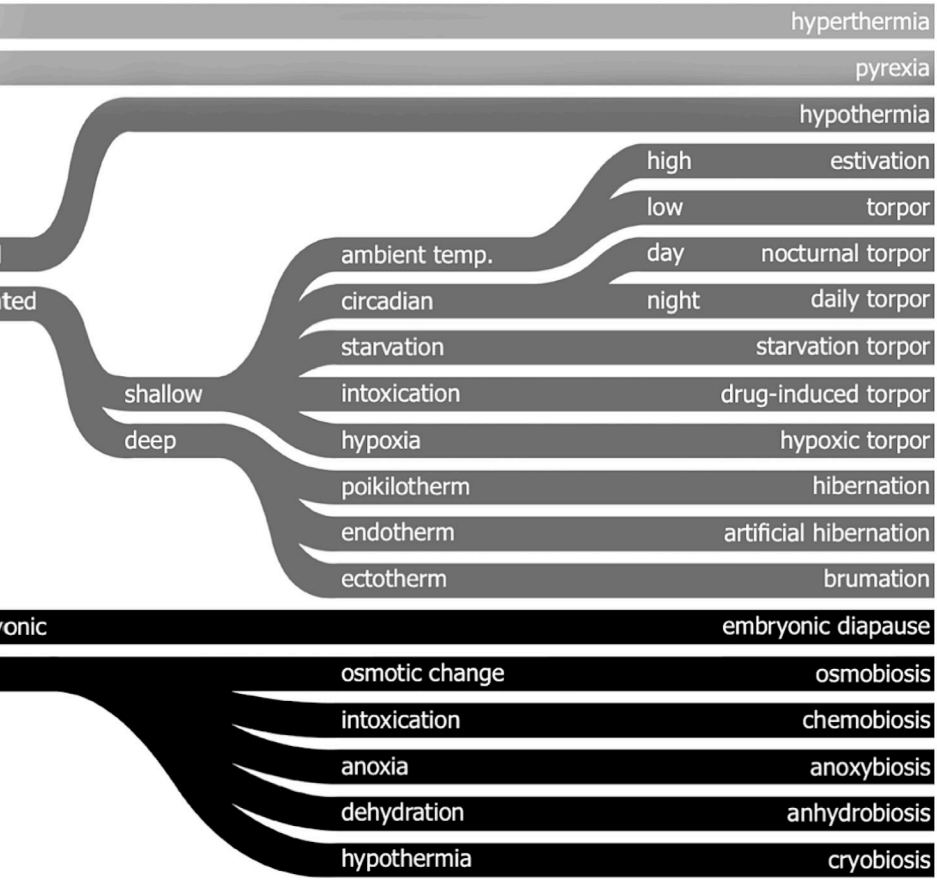

Figure 1. Classification of the different types of hyper- and hypometabolism and the official biological vernacular. Endogenous thermoregulation occurs through the modulation of the thermoneutral zone (Z_{tn}) and thermal effectors, whereas exogenous thermoregulation is dependent on the ambient temperature (T_a) and exogenous triggers but not the Z_{tn}.

Although neurological signal relay is key to convey, propagate, and sustain a state of hypothermia and hypometabolism, the responsible neurological pathways have only been superficially addressed. These pathways will be elaborated in more detail in a subsequent, separate review.

A MODEL FOR HYPOMETABOLIC INDUCTION

Control of metabolism through temperature and substrate availability

A pivotal step in the induction of artificial hypometabolism is gaining control over the most important factors that regulate metabolism (Q), namely the availability of substrate (S, i.e., oxygen and glucose) and the rate of adenosine triphosphate (ATP) production (anabolism, A) and consumption (catabolism, C), which are both influenced by the core body temperature (T_b). Hence, a direct relationship exists between T_b and Q (Figure 2) as well as between S and A (Figure 2). The relationship between T_b and Q essentially abides by Arrhenius' law, which states that the chemical (i.e., enzymatic) reaction rate, Q, is reduced as a result of lowering of temperature (Equation 1).

Although the magnitude of Q varies among enzymes, all have in common that Q is temperature-dependent and therefore relies on T_b. The directly proportional effect of T_b on Q is in turn affected by the ambient temperature (T_a), which impacts T_b and hence Q through heat exchange (Figure 2). The (T_a—) T_b—Q relationship is widely exploited in the clinical setting, as exemplified by the contrived reduction in patients' T_b through direct or indirect cooling (e.g., reduction in T_a by means of breathing cold air, cutaneous cooling, organ perfusion with a cold solution, or intravascular cooling) as a protective strategy in surgery [Azoulay et al., 2005; Reniers et al., 2014], neurology [Axelrod and Diringer, 2008], cardiology [Holzer and Behringer, 2008], trauma

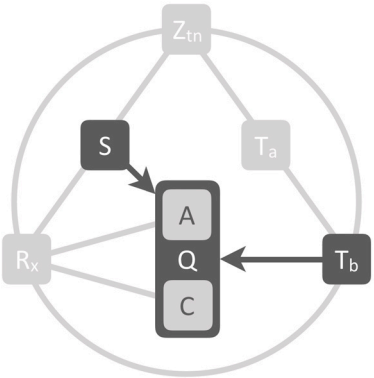

Figure 2. Substrate and temperature effects on metabolism. The S—Q relationship relies on substrate (S) availability to support anabolism (A). The T_b—Q relationship is dictated by the Arrhenius equation (Equation 1, where k is equal to Q in this model), which governs the relation between body temperature (T_b) and chemical reaction speed (Q). Catabolism (C) is directly affected by T_b, but not by S.

[Bernard et al., 2002], and intensive care [Polderman, 2004]. The protective effects of mild to moderate hypothermia (T_b reduction to ~35-32 °C) have been ascribed to lower radical production rates, ameliorated mitochondrial injury/dysfunction, reduced ion pump dysfunction, and cell membrane leakage, amongst others [Polderman, 2009]. The majority of these factors is directly related to the rate at which chemical reactions proceed, whereby cytoprotection is conferred by a T_b-mediated reduction in Q in accordance with the Arrhenius equation (Equation 1).

The generally protective effects of hypothermia notwithstanding, the advantage of clinically forced hypothermia-induced hypometabolism is questionable in some instances. At mild hypothermia (~35 °C), serum concentrations of norepinephrine start to rise in response to hypothermic stress, coagulopathy starts to develop, susceptibility to infections increases, and mortality rates are negatively affected [Frank et al., 1995; Jurkovich et al., 1987; Sajid et al., 2009]. When the T_b is lowered further to ~30 °C, severe hypothermia-related complications may occur, including ventilatory and cardiac arrest [Polderman, 2009; Ivanov, 2000]. An even more profound

---

Arrhenius equation

$$k = Ae^{-\frac{E_a}{RT}}$$

k	Rate constant (S^{-1}), identical to Q in the proposed model (Figure 11)
A	Prefactor (S^{-1})
E_a	Activation energy ($J \bullet M^{-1}$), potentially affected by R_x in the proposed model (Figure 11)
T	Temperature (K), determined by T_b in the proposed model (Figure 11)
R	Universal gas constant ($J \bullet K^{-1} \bullet M^{-1}$)

---

reduction in T_b would require mechanical ventilation with extensive monitoring and would considerably increase procedural risks. Accordingly, in the last five decades, the limit of ~30 °C has not been adjusted downward in the clinical setting as much as it has been refined, despite of successful animal experiments with much deeper hypothermia [Ananiadou et al., 2008, Letsou et al., 2003; Nozari et al, 2004; Sekaran et al., 2001].

The detrimental effects associated with forced deep hypothermia reflect

the limits of the practical implementation of the (T_a—)T_b—Q relationship. It is evident that the (T_a—)T_b—Q relationship must be differentially regulated in natural hibernators compared to humans. In natural hibernators the T_b—Q effects may be integratively mediated by endogenous signaling, such as by the release of biochemical agents or by hypoxia (both addressed in detail below). Humans essentially lack such endogenous pathways and do not exhibit hypothermia-related benefits from exogenously administered pharmaceuticals or hypoxia, as a result of which Q cannot be actively adjusted downward by other pathways than through the T_b—Q relationship. The distinctive responsiveness to hypothermia between humans and natural hibernators may be due to differential neurological and biochemical regulation of T_b, both of which act via mechanisms related to thermogenesis and heat loss. Thermoregulation and the role of thermogenic and heat loss effectors is therefore addressed in the following section.

Thermoregulation following a shift in the thermoneutral zone

The chief role of thermoregulation is maintenance of T_b to support an optimal thermodynamic environment for all chemical reactions in the organism, which is around 37 °C in humans. Thermogenic control is believed to rely on several neurological pathways, which includes involvement of the preoptic anterior hypothalamus (POAH). Together, these pathways manage a thermoneutral zone (Z_{tn}) which provides a range in which the T_b is to maintain itself, and outside of which the T_b is to be adjusted towards the Z_{tn} through the use of thermogenic effectors and heat loss effectors (Figure 3). Although it is difficult to ascertain that a single location among the thermoregulatory pathways can have an effect on the Z_{tn}, it is generally accepted that the POAH exerts such an effect in hibernating and non-hibernating animals based on indirect experimental and clinical evidence [Boulant, 2000; Heller, 1979]. In humans, incidental but selective destruction of the hypothalamic region is associated with dysfunctional thermoregulation, as evidenced by passive T_b declines to as low as 29 °C [Fox et al., 1970; Lammens et al., 1989; Rudelli and Deck, 1979; Sullivan et al, 1987; White et al., 1996]. Moreover, exposure of hypothalamically impaired patients to low T_a's causes a drop

in T_b, whereas the same conditions induce a rectifying rise in T_b in 'control' subjects [Sullivan et al., 1987; Griffiths et al., 1988], attesting to impaired thermoregulatory capacity in hypothalamically afflicted patients. Altogether, these reports provide compelling evidence for a temperature integration site in the hypothalamus through which management of Z_{tn} and T_b ensures maintenance of euthermia.

On the basis of these findings it can be concluded that POAH-affected subjects exhibit a sensory defect between Z_{tn}—T_a (Figure 3A), as a result of which T_b will approximate T_a in the absence of thermoregulation.

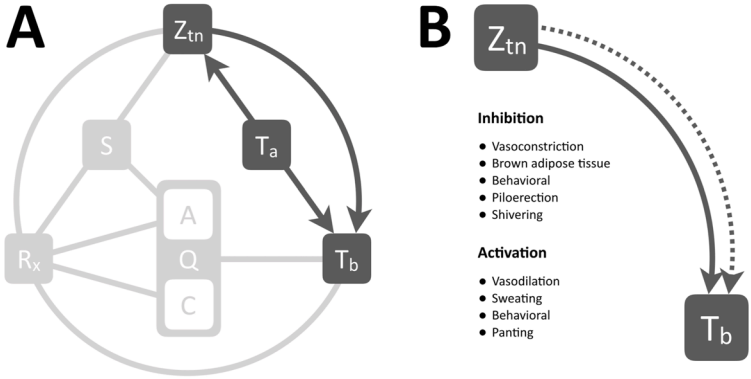

Figure 3. The relationship between the thermoneutral zone and temperature. (A) Overview of thermoregulatory processes. The T_a—T_b relationship represents heat exchange between ambient (T_a) and body temperature (T_b). Information on the T_a is processed and translated into a thermoneutral zone (Z_{tn}) through the T_a—Z_{tn} relationship, whereby the Z_{tn} maintains T_b by regulating thermal effector activity via the Z_{tn}—T_b relationship. (B) Summary of thermal effectors that are mediated by the Z_{tn}—T_b relationship. The Z_{tn} activates thermogenic processes (red) when the $T_b < Z_{tn}$ and heat loss mechanisms (blue) when the $T_b > Z_{tn}$.

Contrastingly, healthy subjects exhibit a reactive effect between Z_{tn}—T_b, whereby T_b is sustained in conformity with the Z_{tn} irrespective of the T_a via activation of thermogenic effectors (Figure 3B). Accordingly, these data imply that, under normophysiological circumstances, Q is mainly regulated by the Z_{tn} via Z_{tn}—T_b—Q such that the optimal thermodynamic conditions (37 °C) are at all times maintained. POAH-mediated thermoregulation also takes place in rodents that are capable of entering a state of torpor. Corroboratively,

selective infarction of the anterior hypothalamus in rats coincides with the inability to regulate T_b, indicating destruction of pathways that govern the Z_{tn} and abrogation of thermoregulatory function [He et al., 1999].

As opposed to humans, Z_{tn} management in smaller animals (e.g., rodents) may veer from a euthermic regime in some species due to specific changes in environmental conditions. One exemplary condition is hypoxia, which is addressed in section Hypoxia-induced hypometabolism: aligning anabolism with catabolism to illustrate the relationship between S (oxygen) and Q.

Before moving to the S—Q relationship in the context of hypoxia, however, it is imperative to address hypothermia as a function of an organism's surface:volume ratio, or the ease with which heat exchange between T_b—T_a can proceed. Small animals have a high surface:volume ratio compared to large animals, which allows for faster heat dissipation and results in subsequent lowering of T_b when exposed to cold environments. A high convective efficiency is essential for the induction of hypothermia, and is dependent on the heat loss properties such as the animal's skin phenotype, breathing pattern, the extent of skin exposure, and the animal's posture and physical activity [Luecke et al., 1971]. In addition to such effects, small animals require a higher metabolic rate than larger animals to sustain their T_b (Kleiber's law [Kleiber, 1932]), which causes small animals to become more easily affected by low T_a's. As a result, it takes considerably less time to lower the T_b and coincidentally the Q of a mouse compared to those of a human. This effect is reflected in the strong correlation between the ability and depth of hibernation and surface:volume ratio, which indicates that virtually all hibernating animals are small (i.e., high surface:volume ratio) and that increased body size is associated with a decreased depth of the T_b drop during hibernation/torpor [Geiser and Ruf, 1955]. Hence it appears that environmental/biochemical modulation of metabolism is more prevalent in small animals and subject to the effectiveness of T_b—T_a heat exchange.

Hypoxia-induced hypometabolism: aligning anabolism with catabolism

The relationship between S and Q is to an extent regulated by the intracellular oxygen tension insofar as oxygen constitutes a vital S for Q (Figure 4). During

hypoxia, Q is impaired because of insufficient oxygen availability for oxidative phosphorylation, resulting in reduced cytochrome c oxidase function [Aw and Jones, 1982] and cessation of ATP production (A). Under hypoxic but normothermic conditions, the ATP consumption rate (C) can be suppressed to match the ATP production rate, but only to a limited extent and for a short time [Hochachka et al., 1996]. In order to survive during a long period of normothermic hypoxia, an organism's metabolism must remain active to fuel metabolically vital processes, which include protein synthesis (25-30% of total ATP consumption), ion homeostasis (23-36%), gluconeogenesis (7-10%), and ureagenesis (3%) [Rolfe and Brown, 1997]. The limited production yet active consumption of ATP during normothermic hypoxia therefore forces the organism to initially switch to anaerobic respiration (Pasteur effect) – a switch that imposes limits on the maximally tolerable duration of hypoxia/anoxia due to inefficient ATP yields from glycolysis and the production of toxic metabolites such as lactic acid.

In several non-hibernating species, exposure to a prolonged period of hypoxia concurs with regulated hypothermia and hypometabolism, suggesting that hypoxia-mediated thermogenic and metabolic suppression constitutes a protective/coping mechanism for such life-threatening conditions [Gautier et al., 1985; Hayden and Lindberg, 1970; Hill, 1959; Horstman and Banderet, 1977]. This hypoxic stress response, illustrated in Figure 5, is in fact an effective survival mechanism in that the catabolic rate is realigned with the limited anabolic rate caused by hypoxia, which is in part achieved by the lowering

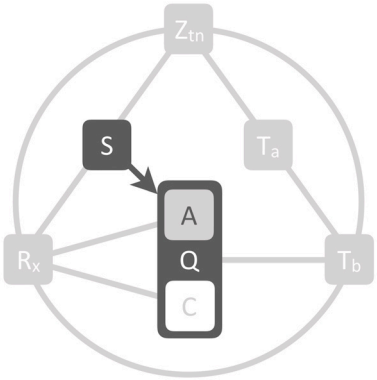

Figure 4. Effects of hypoxia on metabolism. Metabolism (Q) is controlled by substrate (S) availability. Lowering of oxygen availability (hypoxia) directly inhibits anabolism (A, i.e., ATP production) but not catabolism (C, i.e., ATP consumption). Consequently, the metabolic tolerance of hypoxia is limited by the extent to which C can be sustained in the absence of A.

of T_b through the inhibition of thermogenesis and activation of heat loss mechanisms (explained in section The effect of hypoxia-induced anapyrexia on thermoregulatory effectors). In that respect, the hypoxic stress response essentially embodies a pre-programmed manifestation of Arrhenius' law. During this process, the Z_{tn} must either shift downward or be biochemically inhibited in order to resolve the incongruity between the hypothermic T_b and the euthermically ranged Z_{tn}. A reduction in T_b (and consequently Q) resulting from a downward adjustment of the Z_{tn} is referred to as anapyrexia (Figure 6A), as opposed to pyrexia, which comprises an elevated T_b as result of an

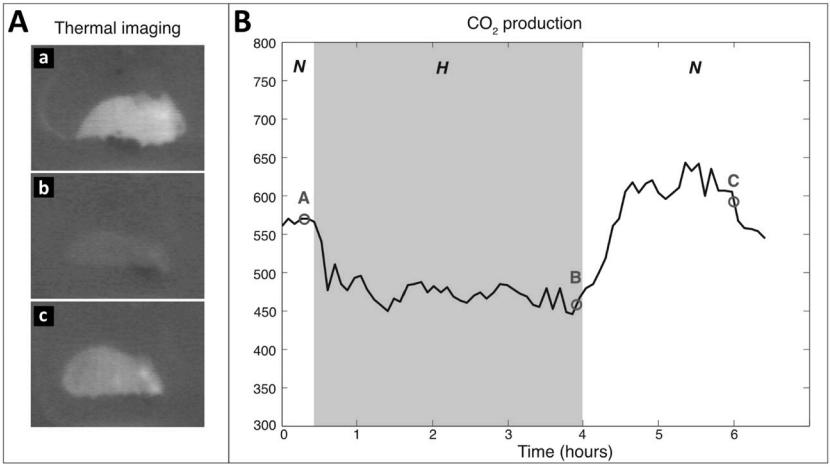

Figure 5. Induction of hypometabolism by hypoxia in mice. An experiment was conducted that exemplifies the reduction in temperature (measured with a thermal camera) and metabolism (measured by exhaled CO_2 levels) following exposure of mice (Mus musculus) to hypoxia. The mouse was placed in an air-tight container with an inlet coupled to a gas cylinder containing either an O_2:N_2 mixture of 21% O_2 (to induce normoxic conditions, N) or an O_2:N_2 mixture of 5% O_2 (to induce hypoxic conditions, H). The container was purged with the normoxic or hypoxic gas mixture at a flow rate of 1 L/min. The container also had a gas outlet that was coupled to a CO_2 sensor (model 77535 CO_2 meter, AZ Instrument, Taichung City, Taiwan). After a 30-min stabilization period under normoxic conditions, hypoxia was induced for 3.5 h, after which the container was changed back to normoxic conditions and the mouse was allowed to recover for an additional 3 h. The ambient temperature (T_a) was maintained at 23.4 ±0.3 °C. During the experiment the mouse was imaged with a thermal camera (Inframetrics, Kent, UK), whereby dark pixels indicate low temperatures and light pixels indicate high temperatures. The frame designations correspond to the lettering in the CO_2 production chart to indicate the time point and phase at which the images were acquired. Upon induction of a hypoxic environment, the body temperature (T_b) of the mouse dropped (B), as evidenced by the decreased T_b-T_a contrast between 0.5 h and 4 h. Following restoration of normoxic conditions (C), the animal's T_b gradually returned to baseline levels. The right panel shows the CO_2 profile during normoxia and hypoxia, whereby the hypoxic phase is clearly associated with reduced levels of exhaled CO_2, which constitutes a hallmark of hypometabolism.

elevated Z_{tn} (i.e., fever). How anapyrexia is mediated under hypoxic conditions in animals is elusive. The effect of anapyrexia on thermoregulatory effectors, on the other hand, is not and provides useful information on the hypoxia-anapyrexia signaling axis.

The effect of hypoxia-induced anapyrexia on thermoregulatory effectors

Hypoxia-induced anapyrexia is found in a large number of species, including mice [Hayden and Lindberg, 1970; Kottke and Phalen, 1948], hamsters [Kuhnen et al., 1987], rats [Gautier et al., 1985; Giesbrecht et al., 1985], pigeons [Barnas and Rautenberg, 1990; Gleeson et al., 1986], dogs [Kottke and Phalen, 1948; Hemingway and Nahas, 1952], primates [Kottke and Phalen, 1948], and man [Kuhnen et al., 1987], and manifests itself when the organism is concurrently exposed to low T_a. A low T_a appears to be a prerequisite for an anapyrexic response to hypoxia, as an anapyrexic response during hypoxic euthermic conditions is absent. The main question, however, is how hypoxic signaling decreases the Z_{tn} to facilitate hypothermia.

The answer may entail an effect of hypoxia on thermogenic effectors (Figure 6A), such as BAT and shivering (Figure 3B). The inhibitory effects of hypoxia on the intensity of cold- induced BAT activity include a lower afferent blood flow to BAT [Mortola, et al., 1999], reduced sympathetic nerve activity [Madden and Morrison, 2005], desensitized response to norepinephrine (a potent BAT activating agent [Cannon and Nedergaard, 2004; Hsieh and Carlson, 1957]) [Beaudry and McClelland, 2010], and can eventually lead to a reduction in BAT mass during prolonged exposure to hypoxia [Martinez et al., 2010; Mortola and Naso, 1998]. In addition, hypoxia results in the inhibition of shivering upon exposure to low T_a compared to normoxic controls in mice, dogs, and man [Kottke and Phalen, 1948]. Moreover, some species further reduce their T_b through changes in behavioral patterns, such as disengagement from cold-induced huddling [Mortola and Feher, 1998] or exhibiting an explicit preference for cooler environmental temperatures [Dupre and Owen, 1992].

Considering these effects, it can be hypothesized that hypoxia either acts directly on BAT and muscle tissue (shivering) or indirectly inhibits these

thermogenic effectors via central regulation, the Z_{tn}. The latter is a more likely mechanism of action since anapyrexic signaling controls both BAT and shivering in order to facilitate hypothermia. Poor blood oxygenation, a result of exposure to hypoxia, is relayed to the brain via the carotid bodies, which is described by a R_x—Z_{tn} relationship (Figure 6B). CBs are oxygen sensing bodies located alongside the carotid artery that contain oxygen-sensitive chemoreceptors through which they provide essential neuronal feedback on the arterial partial oxygen pressure [Prabhakar, 2000]. Excitation of the CBs by reduced oxygen levels during hypoxia possibly induces lowering of the Z_{tn} to activate heat loss effectors (Figure 3B) so as to facilitate the induction of hypothermia with the sole purpose of aligning ATP consumption rates with ATP production rates as part of the survival response to stress conditions (section Hypoxia-induced hypometabolism: aligning anabolism with catabolism). Naturally, this response prevails in species that have a sufficiently high T_a—

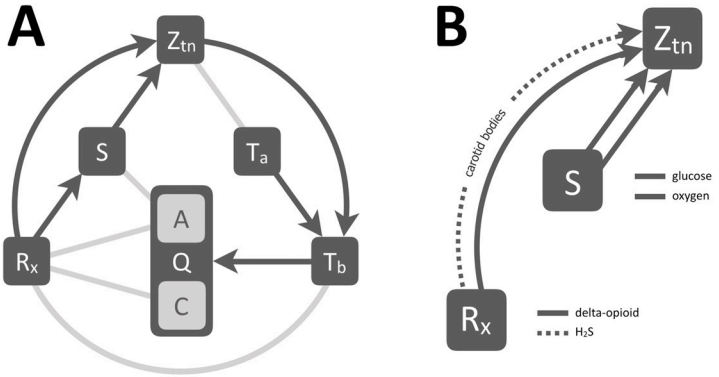

Figure 6. Hypoxia-induced hypometabolism via anapyrexic signaling. (A) The onset of hypoxia, i.e., low substrate (S = oxygen) levels, is proposed to modulate the thermoneutral zone (Z_{tn}) downward via a so-called hypoxic link. The lowering of the Z_{tn} inhibits thermogenesis and activates heat loss mechanisms through the Z_{tn}—T_b relationship, allowing heat exchange between body temperature (T_b) and ambient temperature (T_a) to occur. The consequent reduction in T_b slows down both anabolic (A) and catabolic (C) metabolism (Q) as described in Figure 2. (B) Pathways leading to anapyrexia via the R_x—Z_{tn} and S—Z_{tn} relationships. Although this relationship is exemplified for hypoxic conditions, where S comprises oxygen, it may also apply to conditions where another S is reduced, such as glucose during periods of starvation. Prolonged hypoglycemia is known to also induce hypometabolism, as addressed in section Deoxyglucose. A direct anapyrexic pathway is suggested for R_x—Z_{tn}, where a neuroactive agent such as delta-opioids directly lowers the Z_{tn} (section Delta-opioids). Alternatively, an R_x such as H_2S can also affect the Z_{tn} without affecting S availability by inducing hypoxic signaling through oxygen sensors such as carotid bodies (section *Hydrogen sulfide*).

T_b convective efficiency to allow rapid manifestation of hypothermia and corollary reduction in Q (section Thermoregulation following a shift in the thermoneutral zone), given that sustenance of life by anaerobic metabolism is time-limited. CBs are therefore an important instrumental component of the 'hypoxic link' in smaller species.

The existence of a 'hypoxic link' to the Z_{tn} (Figure 6) has been suggested [Steiner and Branco, 2002] but lacks direct evidence other than the previously mentioned changes in thermal effectors. This link implies that, under cold but normoxic conditions, the Z_{tn} enforces an array of physiological tools that coordinate a thermogenic response, such as shivering, activation of BAT, vasoconstriction, and piloerection (Figure 3B). Under hypoxic conditions, however, these thermogenic responses are dampened or even absent and coincide with activation of heat loss effectors such as vasodilation, sweating, and panting (Figure 3B) [Steiner and Branco, 2002]. Direct measurement of changes in the Z_{tn} range would be useful in substantiating the 'hypoxic link.' Unfortunately, due to incomplete knowledge of Z_{tn} functionality and technical difficulties related to reaching the neural pathways involved, it is currently very difficult to directly measure the range of the Z_{tn} or changes therein.

In summary, hypoxia (low S levels) leads to hypometabolism potentially by signaling anapyrexia through CBs, thereby allowing the body to cool via the S—Z_{tn}—(T_a—)T_b—Q relationship. The hypoxia-induced anapyrexic component provides an advantage over the T_b—Q relationship in that the anapyrexia allows the T_b to drop below normothermia, preventing the stress response that would otherwise be needed to keep the body normothermic. Nevertheless, it is unlikely that these pathways constitute all necessary conditions for the induction of natural hibernation. A closer look at (bio) chemical agents (R_x) that have the ability to induce or mimic 'anapyrexia-driven hibernation' present additional pathways, namely through their effect on S availability, the relay of S availability to the Z_{tn}, and through direct effect on Z_{tn}.

Pharmacological agents and induction of artificial hypometabolism

Induction of hypometabolism in natural hibernators normally occurs in

response to environmental triggers such as low T_a and light and/or food deprivation. The internal (bio)chemical trigger responsible for the subsequent propagation of this signal is key to understanding the hibernation process. It has been suggested that a yet to be characterized endogenous molecular compound, referred to as hibernation induction trigger (HIT), is responsible for inducing hibernation in vivo [Dawe and Spurrier, 1969; Dawe et al., 1970] via the R_x—Q(—T_b) relationship, whereby the drop in T_b is arguably a consequence of the reduced Q by the HIT (Figure 7). It should be noted that this mechanism would differ fundamentally from anapyrexic signaling, which requires Z_{tn} downmodulation and subsequent T_a—T_b equalization as a precursor event for hypometabolic induction (Figure 6). In an effort to identify the HIT, different endogenous compounds have been investigated that have potential to account for or mimic the effect of the HIT, including H_2S [Blackstone et al., 2005], 5'-adenosine monophosphate (5'-AMP) [Zhang et al., 2009], thyronamines (TAMs) [Scanlan et al., 2004], 2'-deoxyglucose (2-DG) [Dark et al., 1994], and delta-opioids (DOPs) [Horton et al., 1998, Dawe and Spurrier, 1969].

Although induction of a hypometabolic state is a shared trait of these agents, each is associated with a different pattern of physiological effects. The physiological effects related to hibernation, as summarized in Figure 8, are primarily found in small animals (Figure 8, outer ring) and not so much in large animals (Figure 8, inner ring). The high incidence of hypometabolic effects in small animals suggests that part of the R_x mechanism may rely on anapyrexia according to the R_x— (S)—Z_{tn}—T_b—Q relationship described in Figure 6, and underscores the importance of the surface:volume ratio (section Thermoregulation following a shift in the thermoneutral zone). Consequently, the currently identified hypometabolism- inducing agents are addressed in relation to their direct anapyrexic properties (R_x—Z_{tn}), their indirect anapyrexic properties (R_x—S—Z_{tn}), or their substrate affecting properties (S—A).

Hydrogen sulfide

Exposure to H_2S consistently produces a hypometabolic state in small animals such as mice and rats (Figure 8, outer ring) [Blackstone et al., 2005; Aslami

et al., 2010; Blackstone and Roth, 2007; Bos et al., 2009; Haouzi et al., 2008; Volpato et al., 2008]. However, the use of H_2S in larger animals such as pigs [Drabek et al., 2011; Li et al., 2008; Osipov et al., 2009; Sodha et al., 2009], sheep [Haouzi et al,. 2008], and heavy rats [Haouzi et al., 2009] has failed to induce a hypometabolic response (Figure 8, inner ring). The current mechanistic paradigm of the hypometabolic effect of H_2S is based on its high membrane permeability and direct inhibitory effect on cytochrome c oxidase in the electron transport chain (i.e., through the R_x—A relationship) [Beauchamp et al., 1984; Cuevasanta et al., 2012]. However, increasing evidence indicates the hypometabolic effects are the result of hypoxic signaling. For example, endogenously produced H_2S is necessary for CBs to signal hypoxia [Peng et al., 2010]. Exogenously applied H_2S, via a soluble NaSH precursor, can mimic the production of this hypoxic signal in vitro [Li et al., 2010], suggesting the

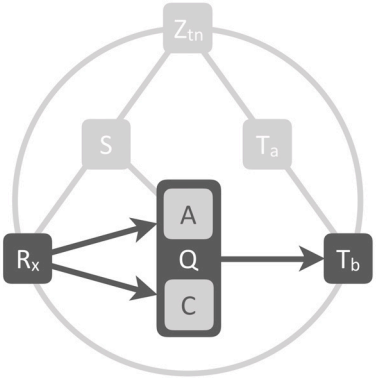

Figure 7. The effect of hibernation induction trigger on metabolic activity. It has been suggested that metabolism (Q) may be directly inhibited by pharmacological agents (R_x) such as hibernation induction trigger (HIT) via inhibition of anabolism (A) and/or catabolism (C). It should be underscored that, based on the information presented in sections Thermoregulation following a shift in the thermoneutral zone and The effect of hypoxia-induced anapyrexia and thermoregulatory effectors, this pathway is unlikely to occur in the absence of hypothermic signaling via Z_{tn} downmodulation.

utilization of the 'hypoxic link' (R_x—Z_{tn}) by H_2S (Figure 6B). This is supported by the observed dichotomy between H_2S-induced effects in small versus large species, where H_2S produces hypometabolic effects in small species but not in larger species (Figure 8). The R_x—Z_{tn}—T_b—Q relationship is dependent on a high T_a—T_b convective efficiency; a property that prevails strictly in small species due to their high surface:volume ratio (section Thermoregulation following a shift in the thermoneutral zone).

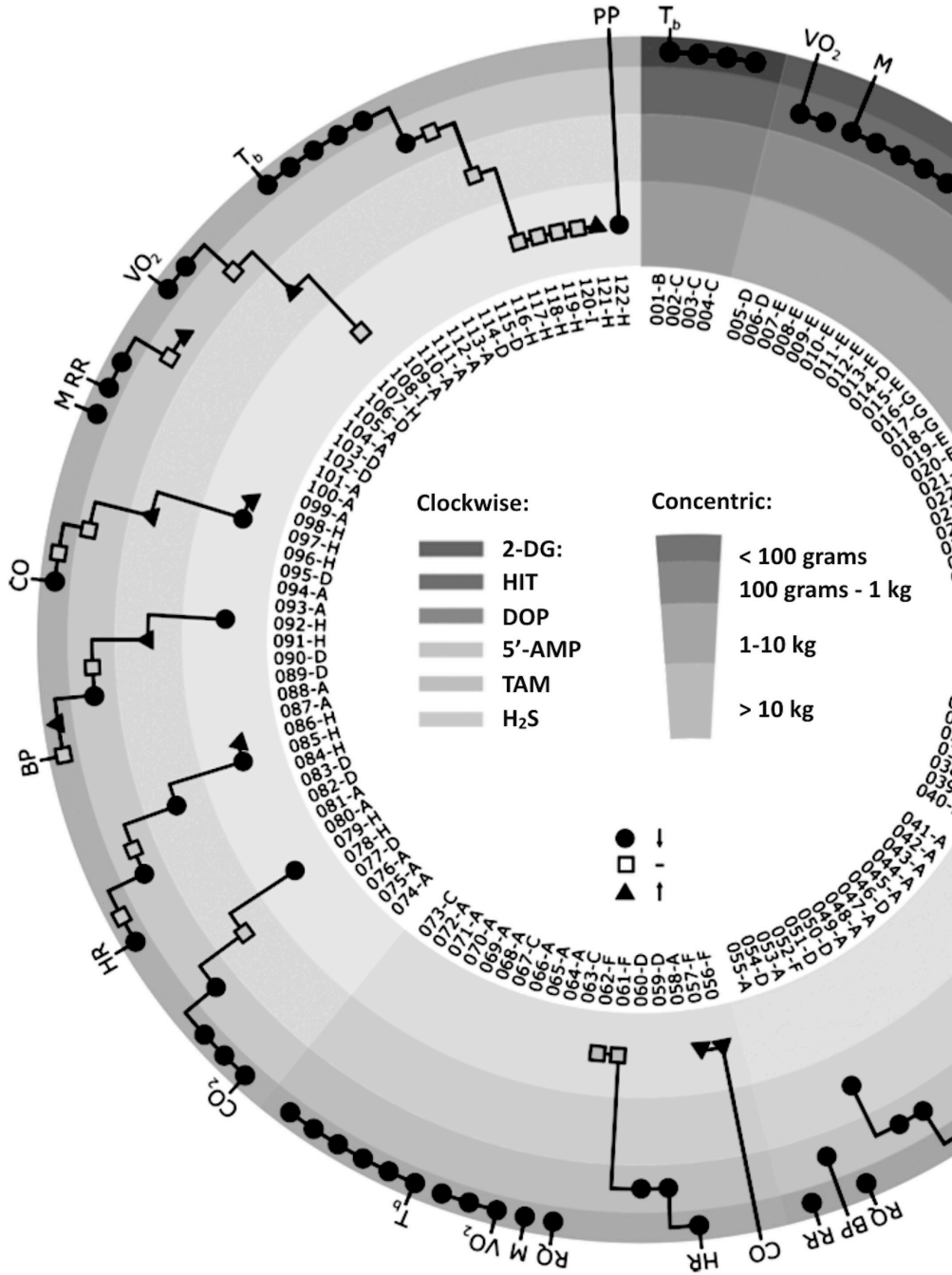
PP
T_b
VO_2
M
RR
CO
BP
HR
CO_2
RQ
T_b
VO_2
M
RR
CO
BP
HR
CO_2
RQ
Clockwise:
2-DG:
HIT
DOP
5'-AMP
TAM
H_2S
Concentric:
< 100 grams
100 grams - 1 kg
1-10 kg
> 10 kg

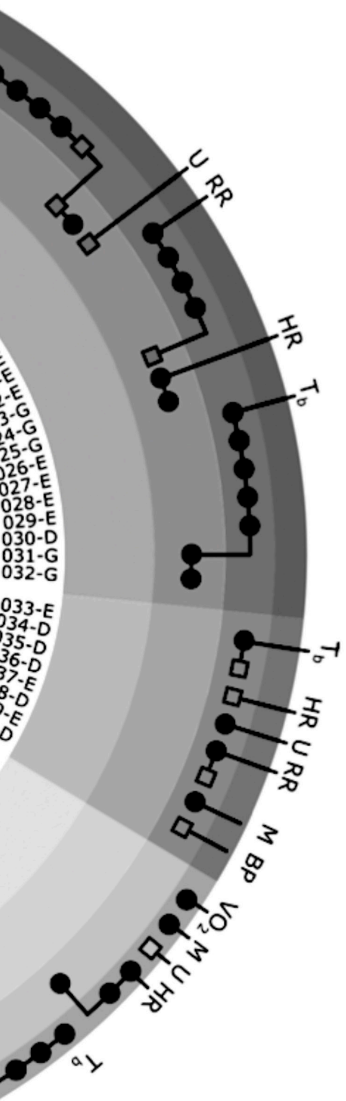

Figure 8. Physiological effects of hibernation inducing agents. Overview of physiological effects in response to 2-deoxyglucose (2-DG), 5'-adenosine monophosphate (5'-AMP), hydrogen sulfide (H_2S), hibernation induction trigger (HIT), delta-opioid (DOP), and thyronamine (TAM). Each effect is represented by a black dot (lowering of value), transparent square (equal value), or black triangle (rise of value). The effects are stratified according to the size of the animal, from outer ring to inner ring these are: < 0.1 kg (e.g., mouse), 0.1-1 kg (e.g., rat), 1-10 kg (e.g., macaque) and > 10 kg (e.g., pig). The inner white ring indicates the respective reference (number) and species (letter). Animals: A, house mouse (Mus musculus, Linnaeus), B, deer mouse (Peromyscus maniculatus, Wagner); C, djungarian hamster (Phodopus sungorus, Pallas); D, common rat (Rattus novergicus, Berkenhout); E, thirteen-lines ground squirrel (Spermophilus tridecemlineatus, Mitchill); F, domestic dog (Canis lupus familiaris, Linnaeus); G, rhesus macaque (Macaca mulatta, Zimmermann) or southern pig-tailed macaque (Macaca nemestrina, Linnaeus); H, domestic pig (Sus scrofa domesticus, Erxleben); I, sheep (Ovis aries, Linnaeus). The physiological parameters include: T_b, core body temperature; VO_2, oxygen consumption; M, motion; RR, respiratory rate; HR, heart rate; U, urine production; BP, blood pressure; RQ, respiratory quotient; CO, cardiac output; CO_2, carbon dioxide production; PP, pulmonary pressure. All parameters are expected to be reduced during hypometabolism. A full-color version can be downloaded via the QR code below.

2DG (n=4)
001-B [Stamper and Dark, 1997]
002-C [Dark et al., 1994]
003-C [Stamper et al, 1999]
004-C [Pelz et al., 2008]

HIT (n=28)
005-D [Swan et al., 1969]
006-D [Swan and Schätte, 1977]
007-E [Oeltgen et al., 1988]
008-E [Dawe et al., 1970]
009-E [Dawe and Spurrier, 1972]
010-E [Dawe and Spurrier, 1974]
011-E [Spurrier et al., 1976]
012-E [Oeltgen et al., 1978]
013-E [Oeltgen et al., 1987]
014-D [Swan et al., 1969]
015-E [Abbotts et al., 1979]
016-G [Myers et al., 1981]
017-G [Oeltgen, 1982]
018-G [Oeltgen et al.,1985]
019-E [Dawe and Spurrier, 1969]
020-E [Oeltgen et al., 1988]
021-E [Bruce et al., 1987]
022-E [Bruce et al., 1990]
023-G [Myers et al., 1981]
024-G [Myers et al., 1981]
025-G [Oeltgen et al., 1982]
026-E [Bruce et al., 1987]
027-E [Oeltgen et al., 1988]
028-E [Dawe and Spurrier, 1969]
029-E [Bruce et al., 1990]
030-D [Swan and Schätte, 1977]
031-G [Myers et al., 1981]
032-G [Oeltgen et al., 1982]

DOP (n=8)
033-E [Oeltgen et al., 1988]
034-D [Tsushima et al., 1993]
035-D [Tsushima et al., 1993]
036-D [Tsushima et al., 1993]
037-E [Oeltgen et al., 1988]
038-D [Tsushima et al., 1993]
039-E [Oeltgen et al., 1988]
040-D [Tsushima et al., 1993]

5'-AMP (n=15)
041-A [Daniels et al., 2010]
042-A [Daniels et al., 2010]
043-A [Daniels et al., 2010]
044-A [Daniels et al., 2010]
045-A [Swoap et al. 2007]
046-D [Zhang et al., 2009]
047-A [Daniels et al., 2010]
048-A [Swoap et al. 2007]
049-A [Zhang et al., 2006]
050-D [Daniels et al., 2010]
051-D [Zhang et al., 2009]
052-F [Daniels et al., 2010]
053-A [Zhang et al., 2006]
054-D [Zhang et al., 2009]
055-A [Daniels et al., 2010]

TAM (n=18)
056-F [Boissier et al., 1973]
057-F [Côté et al. 1974]
058-A [Scanlan et al., 2004]
059-D [Boissier et al., 1973]
060-D [Chiellini et al., 2007]
061-F [Côté et al., 1974]
062-F [Boissier et al., 1973]
063-C [Braulke et al., 2008]
064-A [Ju et al., 2011]
065-A [Dhillo et al., 2009]
066-A [Ju et al., 2011]
067-C [Braulke et al., 2008]
068-A [Scanlan et al., 2004]
069-A [Doyle et al., 2007]
070-A [Panas et al., 2010]
071-A [Hart et al., 2006]
072-A [Ju et al., 2011]
073-C [Braulke et al., 2008]

H_2S (n=49)
074-A [Volpato et al., 2008]
075-A [Blackstone and Roth,2007]
076-A [Blackstone et al., 2005]
077-D [Aslami et al., 2010]
078-H [Li et al., 2008a]
079-H [Simon et al., 2008]
080-A [Volpato et al., 2008]
081-A [Baumgart et al., 2010]
082-D [Aslami et al., 2010]
083-D [Ganster et al., 2010]
084-H [Li et al., 2008a]
085-H [Simon et al., 2008]
086-H [Drabek et al., 2011]
087-A [Baumgart et al., 2010]
088-A [Volpato et al., 2008]
089-D [Siebert et al., 2008]
090-D [Ganster et al., 2010]
091-H [Li et al., 2008a]
092-H [Drabek et al., 2011]
093-A [Volpato et al., 2008]
094-A [Baumgart et al., 2010]
095-D [Aslami et al., 2010]
096-H [Li et al., 2008a]
097-H [Simon et al., 2008]
098-H [Drabek et al., 2011]
099-A [Volpato et al., 2008]
100-A [Volpato et al., 2008]
101-A [Haouzi et al., 2009]
102-D [Aslami et al., 2010]
103-D [Haouzi et al., 2009]
104-A [Haouzi et al., 2008]
105-A [Haouzi et al., 2009]
106-D [Haouzi et al., 2009]
107-H [Li et al., 2008a]
108-I [Haouzi et al., 2008]
109-A [Haouzi et al., 2008]
110-A [Bos et al., 2009]
111-A [Haouzi et al., 2009]
112-A [Blackstone et al., 2005]
113-A [Volpato et al., 2008]
114-D [Aslami et al., 2010a]
115-D [Haouzi et al., 2009]
116-H [Li et al., 2008a]
117-H [Drabek et al., 2011]
118-H [Sodha et al., 2009]
119-H [Osipov et al., 2009]
120-I [Haouzi et al., 2009]
121-H [Simon et al., 2008]
122-H [Drabek et al., 2011]

Adenosine monophosphate

Intraperitoneal injections of 5'-AMP have been shown to induce an artificial hypometabolic state in mice and rats as evidenced by a profound drop in T_b (Figure 8) [Zhang et al., 2009; Daniels et al., 2010; Lee, 2008; Swoap et al., 2007]. The putative contention is that intraperitoneal administration of high 5'-AMP concentrations (e.g., 500 mg/kg) lead to extensive 5'- AMP uptake by

erythrocytes [Mathews et al., 2005], after which the high intracellular levels of 5'-AMP drive the adenylate equilibrium (ATP + AMP ↔ 2 ADP) towards production of ADP, thereby depleting erythrocyte ATP levels [Daniels et al., 2010; Lee, 2008]. As a result, erythrocyte 2,3-disphosphoglycerate is upregulated, limiting the binding of oxygen to hemoglobin's oxygen binding sites (referred to as oxygen affinity hypoxia) [Daniels et al., 2010]. In addition to the already impaired oxygen transport, the severe cardiovascular depression following 5'-AMP administration has the potential to further exacerbate this hypoxic state (referred to as circulatory hypoxia) [Swoap et al., 2007]. Although there is no conclusive evidence that these types of hypoxia have the ability to induce an anapyrexic state, the generally pervasive hypoxic state likely uses the $S—Z_{tn}—T_b(—T_a)—Q$ relationship (Figure 6A) to induce hypometabolism through CB signaling.

More recent studies have implicated a direct 5'-AMP signal transduction route to the central nervous system in seasonal hibernators, culminating in the induction of torpor [Muzzi et al., 2013; Tupone et al., 2013a; Jinka et al., 2011; Tupone et al., 2013b]. 5'- AMP signaling occurs via the A_1 adenosine receptor (A_1AR), which is ubiquitously distributed throughout all tissues, but not the A_2AR or A_3AR receptors. In the brain, A_1AR signaling leads to deceleration of metabolic rate and induction of a torpor state in arctic ground squirrels [Olson et al., 2013]. In this species, intracerebroventricular administration of the A_1AR antagonist cyclopentyltheophylline reversed spontaneous entrance into torpor during hibernation season, whereas administration of the A_1AR agonist N(6)-cyclohexyladenosine induced torpor [Jinka et al., 2011]. Later studies confirmed the manifestation of 5'-AMP-driven torpor in non-hibernators, including the mouse [Muzzi et al., 2013] and rat [Tupone et al., 2013a], suggesting that the hypothermia- and hypometabolism-inducing potential of 5'-AMP is pleiotropically applicable across species. Although the signaling is of more direct neurochemical nature compared to the hypoxic signaling, the $S—Z_{tn}—T_b(—T_a)—Q$ relationship (Figure 6A) also holds for the 5'-AMP—A_1AR signaling axis.

As indicated previously, the depth of the hypometabolic response is dependent on the $T_b—T_a$ convective efficiency (section Thermoregulation following a shift in the thermoneutral zone). This is further supported by

the extent of the drop in T_b that is observed in 5'-AMP-treated mice, which is proportional to the difference between T_b and T_a (i.e., lower T_a's induce a greater drop in T_b), demonstrating the T_b—T_a dependency [Daniels et al., 2010].

Thyronamines

TAMs are a thyroid hormone-derived group of compounds of which currently nine structural analogues have been identified [Scanlan et al., 2004]. Contrary to the structurally similar metabolism-enhancing thyronines (T_3 and T_4), exposure to TAM analogues triggers a transient T_b depression in small animals, epitomizing the induction of a hypometabolic phase (Figure 8) [Scanlan et al., 2004; Braulke et al., 2008; Doyle et al., 2007; Hart et al., 2006; Panas et al., 2010]. Although earlier studies in a canine model presented contradictory evidence with respect to metabolic effects compared to later studies (Figure 8, cardiac output), it is likely that this was a result of differences in synthesis methods and compound purity [Hart et al., 2006; Petit and Buu-Ho, 1961]. Nevertheless, the metabolic effects of TAMs remain obscure, regardless of the synthesis method.

Both in vivo and ex vivo studies have found the physiological effects of TAMs to be mainly cardiogenic in nature, producing severe hemodynamic depression, bradycardia, hypotension, and reduced cardiac output [Scanlan et al., 2004; Braulke et al., 2008; Chiellini et al., 2007]. These effects result in reduced oxygen levels (affecting the R_x—S—Z_{tn} relationship, Figure 6) by lowering the extent of blood oxygenation in accordance with Fick's principle, which describes an inverse relationship between cardiac output and oxygenation (circulatory hypoxia) [Myers et al., 2008; Selzer and Sudrann, 1958]. Although the effect of circulatory hypoxia on the Z_{tn} has not been demonstrated, the presence of hypoxia in the broader sense may support the implication of the S—Z_{tn}—T_b(— T_a)—Q relationship (Figure 6A) as a basis of the observed hypometabolism in smaller animals.

Given the magnitude of the hemodynamic collapse in small species, TAMs may additionally render the animal motionless (Figure 8, motion), which would facilitate a greater rate of thermal convection (T_b—T_a) and therefore accelerate the consequent reduction in T_b and Q (Figure 2).

Deoxyglucose

In addition to oxygen, S can also comprise glucose, as evidenced by the induction of a hypometabolic state upon glucose deprivation in hamsters and various types of mice [Dark et al., 1994; Dark et al., 1996; Stamper and Dark, 1997; Walton and Andrews, 1981]. Shortage of food, and with that the ability to use glucose as energy substrate, has the potential to induce hypometabolism or alter its depth [Stamper and Dark, 1997; Walton and Andrews, 1981; Mrosovsky and Barnes, 1974]. This principle has been demonstrated in hamsters using 2-DG, a glucose analogue that cannot undergo glycolysis as a result of the 2-hydroxyl group, which causes the animals to enter a hypometabolic state [Dark et al., 1994; Dark et al., 1996]. The hypometabolic response to 2-DG, measured by the drop in T_b, is reflective of the S—A relationship (Figure 4). Currently there is no evidence that supports the S—Z_{tn} pathway for 2-DG.

Delta-opioids

Isolation and characterization of the HIT found in serum of hibernating woodchucks and squirrels revealed a resemblance to D-Ala-D-Leu-5-enkephalin, a non-specific DOP receptor agonist [Horton et al., 1998; Oeltgen et al., 1978]. Consistent with this characterization, DOPs induce a hypometabolic state of similar depth as the HIT, whereas mu- or kappa-opioid receptor agonists show no effect [Oeltgen et al., 1978; Oeltgen et al., 1988]. The involvement of opioid receptors is further substantiated by the inability of DOP to induce hypometabolism upon exposure to naloxon, a non-specific opioid receptor antagonist [Bruce et al., 1996; Bruce et al., 1987; Margules et al., 1979; Oeltgen et al., 1982]. These findings raise the question whether DOPs make use of a direct R_x—Q relationship or act via the R_x—Z_{tn} (Figure 6). Growing evidence suggests the latter, as delta-opioids appear to be directly involved in hypoxic signaling. In mice, exposure to hypoxia has been suggested to decrease Z_{tn} via delta-1-opioid receptor agonism [Mayfield and D'Alecy, 1994a; Mayfield and D'Alecy, 1994b; Mayfield et al., 1994; Spencer et al., 1990]. Other studies have suggested that the delta-2 opioid receptor rather than a delta-1 opioid receptor is responsible for the effects on the Z_{tn} [Benamar et al., 2004; Broccardo and Improta, 1992; Salmi

et al., 2003], supported by the limited presence of delta-1-opioid receptors in the hypothalamic region [Sharif and Huges, 1989; Tempel and Zukin, 1987]. However, in both cases the preferred pathway to Z_{tn} modulation appears to involve a direct R_x—Z_{tn} relationship.

Pharmacological agent properties and the feedback loop

As demonstrated by the different mechanisms discussed in the previous section, R_x can affect Q via three potential pathways, namely via R_x—Q(—T_b) (Figure 7, suggested for HIT), via R_x—S—Z_{tn}—T_b—Q (Figure 6, suggested for H_2S, 5'-AMP, TAM, and 2-DG), and via R_x—Z_{tn}—T_b—Q (suggested for DOP). However, irrespective of the hypometabolic pathway, it is unlikely that the systemic release of a single R_x accounts for the hypothermic/hypometabolic induction process. Instead, as is the case in many biochemical pathways, it is more probable that the induction of hypometabolism is governed by a signal amplifying feedback loop (Figure 9).

With respect to the model, the ideal properties of an R_x regarding its regulatory function of the feedback loop encompass 1) endogenous production and/or release during induction of hibernation, 2) inhibitory effects on both A and C, 3) downregulatory effect on Z_{tn}, 4) equal distribution throughout the body, and 5) availability of agonists and antagonists to accelerate and abrogate R_x-mediated signaling, respectively. Although currently there is no sound evidence for the existence of an R_x feedback loop, such a mechanism is theoretically necessary to propagate a hypometabolic signal in vivo. Consequently, a mechanistic framework for such a feedback loop will be elaborated for magnesium (Mg^{2+}), which appears to play an important role in hibernation across different species.

Induction of hibernation coincides with a change in serum Mg^{2+} concentration (Figure 10). Serum Mg^{2+} levels increase by an average of 1.6-fold upon induction of hibernation in different species compared to their summer active state, which is a considerably higher increase than observed for other electrolytes. The release of Mg^{2+} into the circulation occurs from storage pools that have formed prior to induction of hibernation in cells that comprise muscle (Figure 10) and skin tissue [Platner, 1950; Platner, 1953].

The translocation of Mg^{2+} from tissue to blood and subsequent systemic distribution is in conformity with the first R_x property, i.e., the release of an endogenous agent during the induction of hibernation.

In regard to the second property, Mg^{2+} exerts an inhibitory effect on Q, affecting both A and C. Mg^{2+} acts as a necessary co-factor in over 300 enzymatic reactions [Ebel and Gunther, 1980]. When the Mg^{2+} concentration exceeds the saturating concentration required for occupying all substrate binding sites, Mg^{2+} becomes an inhibitor of enzymatic activity [Ebel and Gunther, 1980]. The inhibitory properties of Mg^{2+} are not limited to the inhibition of A, such as reduction of state III respiration (ADP-stimulated respiration) upon exposure to Mg^{2+} [Rochelle et al., 1978], but also include inhibition of C, such as reduction of Na/K-ATPase activity [Pedemonte and Beauge, 1983]. In addition, Mg^{2+} inhibits ion channels, such as the NMDA receptor ion channel and voltage gated ion channels [Frankenhaeuser and Meves, 1958; Hahin and Campbell, 1983; Mayer and Westbrook 1987]. Although inhibition of A and C are essential in sustaining a prolonged state of hypometabolism, as occurs during hibernation, this R_x property has been largely ignored in reports on conventional hibernation-inducing R_x agents (i.e., H_2S, 5'-AMP, TAM, 2-DG, and DOP).

The third property of an Rx is its downward adjusting effect on the Z_{tn}. In case of Mg_{2+} there appears to be conflicting evidence; intracerebro-ventricular perfusion with a solution containing a supraphysiological concentration of Mg^{2+} does not result in a hypothermic response in hamsters [Myers and Buckman, 1972], rats [Myers and Brophy, 1972], cats [Feldberg et al., 1970; Myers and Veale, 1971; Myers et al., 1976], and primates [Myers and Yaksh, 1971; Myers et al., 1971] but does result in a hypothermic response in pigeons [Saxena, 1976], dogs [Sadowski and Szczepanska-Sadowska, 1974], and sheep [Seoane and Baile, 1973]. However, with this perfusion approach it cannot be guaranteed that intracerebroventricular perfusion solely affected the neural pathways involved in thermoregulation. A more accurate assessment can be made on the basis of the thermal effectors, in which case Mg^{2+} exerted an inhibitory effect on shivering in cold-exposed dogs [Heagy and Burton,1948], reduced post-anesthetic shivering in patients [Kizilirmak et al., 1997; Lysakowski et al., 2007; Ryu et al., 2008], lowered the cold-induced shivering

threshold in healthy human subjects [Wadhwa et al., 2005], and promoted heat loss effectors in rats [Zweifler et al., 2004]. Essentially, these reports constitute indirect evidence for the Z_{tn} lowering property of Mg^{2+}, which is manifested through the activation of heat loss mechanisms and inhibition of thermogenic mechanisms (R_x— Z_{tn}—T_b, Figure 6).

Fourth, an R_x must distribute throughout the entire body. Although self-evident, this property is often omitted in common theories on the induction of hibernation by pharmacological agents. Heterogeneously distributed receptors of an R_x deter widespread propagation of hypometabolic signaling, and instead support hypometabolic signaling through an interposed effect such as the lowering of the Z_{tn} (e.g., DOP) or the availability of S (e.g., TAM). The systemic distribution of Mg^{2+} is unclear, but is expected to be ubiquitous given the role of this cation in many enzymatic reactions, including in the

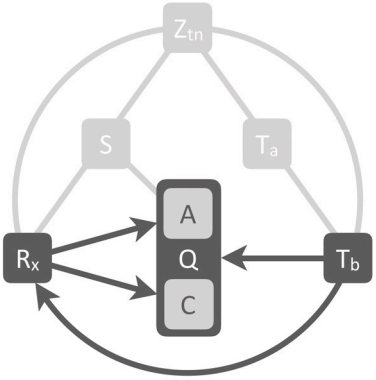

Figure 9. Signal amplifying feedback loop during hypometabolic induction. Theoretically, lowering of the body temperature (T_b) could be part of a feedback system that triggers the release of a metabolism inhibiting agent (R_x) capable of further lowering metabolism (Q) via direct inibition of anabolism (A) and/or catabolism (C). This process is embodied by the T_b—R_x— Q relationship.

hexokinase-mediated conversion of glucose to glucose 6-phosphate, which occurs in every somatic cell type as part of sugar metabolism.

Finally, it is important that an R_x is sensitive to stimulation and inhibition for the induction and abrogation of hypometabolic signaling, respectively. The natural factors that trigger hibernation include lowering of T_a and dietary change, both of which are able to increase plasma Mg^{2+} via cold-stimulated muscular and dermal release of Mg^{2+} that is stored during the pre-starvation diet period [Ros, 2009]. The subsequent rise in plasma Mg^{2+} can promote

inhibition of thermogenic activity and activation of heat loss mechanisms by lowering of the Z_{tn}, potentiating heat exchange (T_a—T_b). In addition, direct effects on shivering via Mg^{2+}-mediated inhibition of neuromuscular transmission facilitates lowering of T_b [Del and Engbaek, 1954]. The consequent cooling releases more Mg^{2+} stored in muscles and skin, further adding to the increase in serum Mg^{2+} through a positive feedback loop. As discussed in section Thermoregulation following a shift in the thermoneutral zone, a feedback loop of this type would be most efficient in small animals due to their high body surface:size ratio and result in a less profound T_b drop in larger animals.

Hypothermia and hypometabolism research and clinical implementation: important considerations

The complete model on the induction of hibernation, presented in Figure 11, is in part hypothetical and requires additional research to validate every relationship. Given the supportive experimental evidence discussed in the previous sections, the model provides a starting framework for interpreting observations made in future in vivo experiments concerning hypothermia and hypometabolism, particularly in the context of integrative physiology. There are several important considerations regarding this type of research that must be accounted for, especially when data are interpreted on the basis of the model.

As implied in sections Control of metabolism through temperature and substrate availability and Thermoregulation following a shift in the thermoneutral zone, prevention of stress signaling upon exposure to a cold stimulus is crucial to safe lowering of metabolism, underscoring the need for validation of the R_x—(S)—Z_{tn} relationship. This would require knowledge on both the location and function of the Z_{tn}, which, as alluded to previously, is currently beyond our reach. However, by investigating the impact of a stimulus such as T_a or R_x on thermogenic effectors, heat loss effectors, and behavioral thermoregulation (Z_{tn}—T_b, Figure 3B), the Z_{tn} issues can be circumvented while still gaining insight into the Z_{tn} lowering potency. Z_{tn}-related research is presently conducted in this fashion, whereby ancillary parameters (effectors

and behavior) are used as a gold standard to gauge Z_{tn} [Steiner and Branco, 2002].

Due to their high T_a—T_b convective efficiency, small animals constitute ideal subjects for screening the anapyrexic potential of an R_x or investigating the effects of hypoxia. In larger animals, the lower T_b—T_a convective efficiency necessitates the use of active cooling to accommodate induction of hypothermia and corollary hypometabolism. If active cooling in larger animal models is omitted, an anapyrexic agent or hypoxia may yield hypometabolic results in small animals but induce limited or no effect in larger animals. A totally T_b-independent R_x (i.e., R_x—Q , T_b = 37 °C) would be in contradiction to this model and in fact disprove the necessity of T_a—T_b convection. It is our opinion, however, that hypometabolism cannot occur under normothermic conditions, an opinion that is supported by extension of the Arrhenius law.

When translating these principles to a clinical setting, the use of the R_x(—S)—Z_{tn} relationship suggests that better outcomes would be achieved if hypothermic patients were pretreated with an anapyrexic agent (R_x—Z_{tn}—T_b(—T_a)) or subjected to hypoxia (S—Z_{tn}—T_b(—T_a)). The fact that clinical practice deviates from these approaches may contribute to the increased comorbidity in patients as a result of hypothermia-inflicted stress responses during trauma-induced and perioperative hypothermia [Frank et al., 1995; Stevens, 1993]. Presently, none of the strategies aimed to resolve these responses in patients encompass guidelines for Z_{tn} modulation. As a result, many patients are placed on 100% O_2 and symptomatic treatment of shivering without a clear rationale. According to our model, a more cautious approach in oxygenating hypothermic patients could be beneficial, as reflected by the S—Z_{tn}—T_b signaling axis. By subjecting a hypothermic patient to a hypoxic signal (S—Z_{tn}) or anapyrexic agent (R_x(—S)—Z_{tn}), the cold-induced stress response may be mitigated by reduction of Z_{tn} through CB signaling and alignment of T_b with T_a. As exposure to a cold stimulus readily activates thermal effectors such as shivering and BAT [van Marken, et al., 2009; Virtanen et al., 2009], such an effect would be promptly visible. However, to date no anapyrexic agents or hypoxic signaling mechanisms have been reported in a clinical setting.

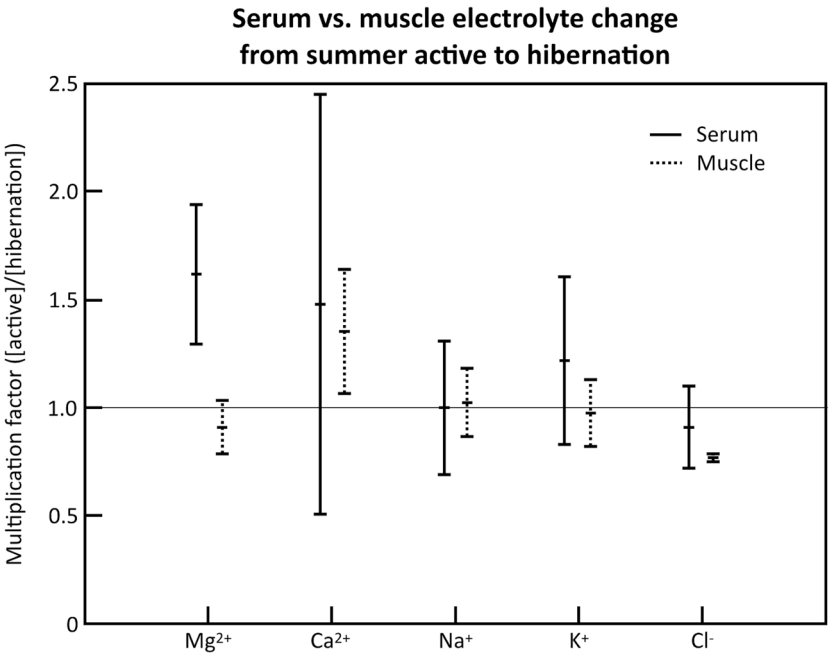

Figure 10. Electrolyte changes during induction of natural hibernation. Analysis of blood levels of magnesium (Mg^{2+}, serum n = 23, muscle n = 9), calcium (Ca^{2+}, serum n = 19, muscle n = 5), sodium (Na^{+}, serum n = 16, muscle n = 6), potassium (K^{+}, serum n = 25, muscle n = 9), and chloride (Cl^{-}, serum n = 9, muscle n = 3) from summer active state to hibernation (< 1, reduction upon induction into hibernation; 1, no change; > 1, increase in electrolyte concentration). Black bars correspond to serum electrolyte levels, grey bars indicate electrolyte levels in muscle tissue. Animals included in this figure are: European hedgehog (Erinaceus europaeus, Linnaeus) [Clausen and Storesund, 1971; Edwards and Munday, 1969; Suomalainen, 1938], long-eared hedgehog (Hemiechinus auritus, Gmelin) [Al-Badry and Taha, 1983], golden hamster (Mesocricetus auratus, Waterhouse) [Ferren et al., 1971; Tempel and Musacchia, 1975; Tempel et al., 1978, Willis et al., 1971; Riedesel and Folk, 1957b], common box turtle (Terrapene carolina, Linnaeus) [Hutton and Goodnight, 1957], pond slider (Trachemys scripta, Thunberg) [Hutton and Goodnight, 1957], painted turtle (Chrysemys picta, Schneider) [Ultsch et al., 1985; Jackson and Heisler, 1983; Reese et al., 2001; Ultsch et al., 1999], European ground squirrel (Spermophilus citellus, Linneaus) [Pengelley and Kelly, 1967], thirteen-lined ground squirrel (Spermophilus tridecemlineatus, Mitchill) [Willis et al., 1971; Riedesel and Folk, 1957; Kenny and Musacchia ,1977], groundhog (Marmota monax, Linneaus) [Bito and Roberts, 1974; McBirnie et al., 1953], yellow-bellied marmot (Marmota flaviventris, Audubon & Backman) [Zatzman and South, 1972], Asian common toad (Duttaphrynus melanostictus, Schneider) [Pratihar and Kundu, 2009], little brown bat (Myotis lucifugus, LeConte) [Riedesel and Folk, 1957; Riedesel, 1957; Riedesel and Folk, 1958], big brown bat (Eptesicus fuscus, Palisot de Beauvois) [Reidesel and Folk, 1957; Riedesel, 1957], American black bear (Ursus americanus, Pallas) [Riedesel and Folk, 1957], common musk turtle (Sternotherus odoratus, Latreille) [Ultsch, 1988], desert monitor (Varanus griseus, Daudin) [Haggag et al., 1965]. Statistical analysis was performed in MatLab R2011a. Intragroup analysis of serum versus muscle electrolyte levels (Mann-Whitney U test: p-value): Mg^{2+}, $p < 0.001$; Ca^{2+}, $p = 0.395$; Na^{+}, $p = 0.299$; K^{+}, $p = 0.067$; Cl^{-}, $p = 0.315$. Intergroup analysis of serum electrolyte levels, indicating statistical differences (Kruskal- Wallis test): Mg^{2+} versus Ca^{2+}, Na^{+}, K^{+}, and Cl^{-}, ($p < 0.05$).

CONCLUDING REMARKS

In conclusion, the lack of understanding of the induction mechanisms underlying natural hibernation stands in the way of successful application of artificial hibernation in biotechnology and medicine. Accordingly, a model was developed to assist in finding the means to translate the physiological changes observed during natural hibernation to its artificial counterpart. Summarized in Figure 11, six essential elements form the basis of our model, which were extrapolated from literature. The relationships between these elements dictate their values and collectively govern the induction and sustenance of a hypometabolic state. To illustrate the potential validity of this model, various R_x (HIT, DOP, H_2S, 5'-AMP, TAM, 2-DG, Mg^{2+}) were described in terms of their influence on the intervariable relationships and effects on Q.

Although the ultimate purpose of this hypothetical model was to help expand the paradigm regarding the mechanisms of hibernation from a physiological perspective and to assist in translating this natural phenomenon to the clinical setting, our model only comprises a part of the vastly complex biological systems that underlie anapyrexia and hypometabolism. Moreover, readers should note that concepts as 'set point' are model-based phenomena, rather than neurobiological constructs. The key to the mechanistic underpinning of anapyrexic signaling currently rests on the shoulders of neurobiology, which is slowly unveiling the neurological signaling pathways. In that respect, thermal reflexes (cold defense, fever, anapyrexia, hibernation, etc.) are mediated by changes in the discharge of neurons in neural circuits controlling thermoregulatory effectors, and understanding how and through which neuro- chemical mediators these reflexes are effected will only be accomplished through detailed neurobiological experimentation. Accordingly, basic elucidation of the neurochemistry of anapyrexia is needed for the identification of useful R_x's [Tupone et al., 2013a, Tupone et al., 2013b].

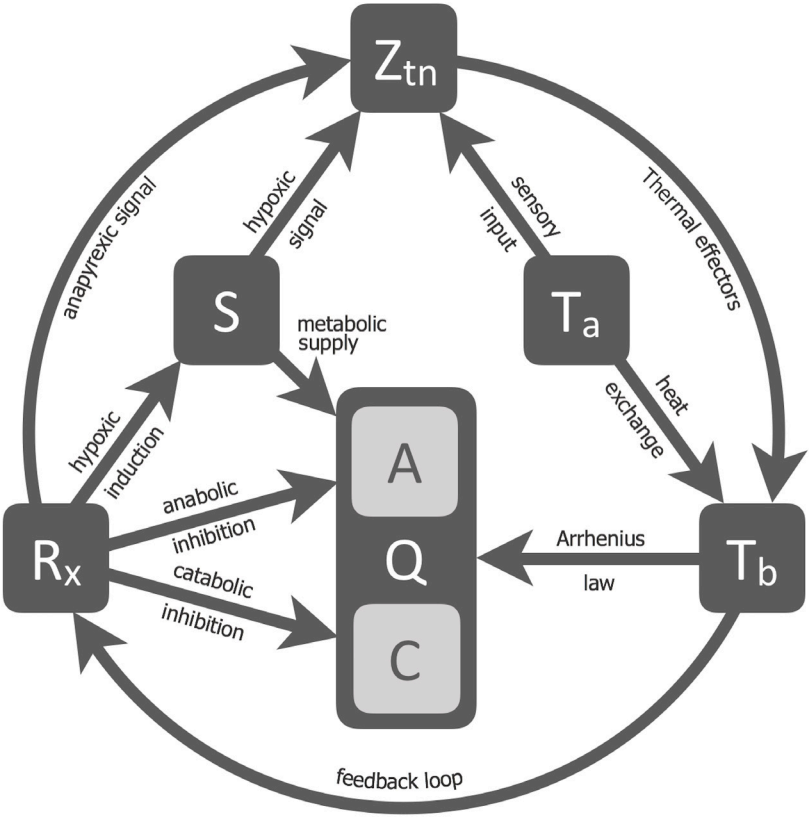

Figure 11. Model for induction of (artificial) hypometabolism. Depicted parameters: Q, overall metabolism defined as chemical reaction speed (i.e., similar to k in Equation 1); C, catabolism; A, anabolism; T_b, core body temperature; T_a, ambient temperature; Z_{tn}, thermoneutral zone; S, substrate; R_x, (bio)chemical agent able to induce hypometabolism. The relationships: T_b—Q, Arrhenius law; T_a—T_b, heat exchange; Z_{tn}—T_b, thermogenesis and heat loss mechanisms; T_a—Z_{tn}, sensory input; S—Z_{tn}, hypoxic link; R_x— S, hypoxia/hypoglycemia induction; R_x—C, catabolic modulation; R_x—A, anabolic modulation; R_x—Z_{tn}, anapyrexic signal; S—A, metabolic substrate supply; T_b—R_x, positive/negative feedback loop.

Chapter 2

(Re-)discovering pharmacological agents for the induction of artificial hibernation using data mining

Adapted from

M.C. Dirkes, T.M. van Gulik, M. Heger
J Clin Trans Res 2015(1): 6-21

ABSTRACT

A reduction in body temperature can be achieved by a downward adjustment of the thermoneutral zone, a process also described as anapyrexia. Pharmacological induction of anapyrexia could enable numerous applications in medicine. However, little is known about the potential of pharmacological agents to induce anapyrexic signaling. Therefore, a review of literature was performed and over a thousand pharmacologically active compounds were analyzed for their ability to induce anapyrexia in animals. Based on this analysis, eight agents (helium, dimethyl sulfoxide, reserpine, (oxo)tremorine, pentobarbital, (chlor)promazine, insulin, and acetaminophen) were identified as potential anapyrexia-inducing compounds and discussed in detail. The translational pitfalls were also addressed for each candidate compound. Of the agents that were discussed, reserpine, (oxo)tremorine, and (chlor)promazine may possess true anapyrexic properties based on their ability to either affect the thermoneutral zone or its effectors and facilitate hypothermic signaling. However, these properties are currently not unequivocal and warrant further examination in the context of artificially-induced hypometabolism.

INTRODUCTION

An organism's core body temperature (T_b) is of key importance to its physiological function, as reflected by the meticulous regulation of T_b. The plasticity of thermal regulation is demonstrated by numerous pathological conditions, such as the increase in T_b (pyrexia) during an infection. A lesser known, but potentially equally important thermal adaptation mechanism, is regulated decrease in T_b (anapyrexia). Anapyrexia can be described as the opposite of fever, namely a lowering of the boundaries between which the body considers itself thermoneutral (the thermoneutral zone, Z_{tn}), and concurs with the inhibition of thermogenic processes and the activation of heat loss mechanisms (Figure 1).

The ability to lower the Z_{tn} is an established feature of poikilothermic animals, one that is only starting to be recognized in homeothermic animals [Steiner and Branco, 2002]. The integration and processing of thermoregulatory signals is believed to involve several intricate neural pathways encompassing both peripheral sensory neurons and central hypothalamic neurons and nuclei [Cerri et al., 2010; Maingret et al., 2000; Crawshaw et al., 1985; Cerri et al., 2013], including the preoptic anterior hypothalamus (POAH) [Maingret et al., 2000; Crawshaw et al., 1985; Parmeggiani et al., 2000; He et al., 1999; Boulant, 2000]. Together these pathways manage the Z_{tn}, which in turn manages thermogenesis (e.g., shivering, activation of brown adipose tissue (BAT), vasoconstriction, tachycardia, tachypnea, piloerection, and behavioral accommodation) and heat loss (e.g., vasodilation, sweating, panting, and changes in behavioral patterns such as the pursuit of lower environmental temperatures (T_a)) (Figure 1) [Boulant 2000; Romanovsky et al., 2002]. Readers interested in the neuroanatomical networks that govern mammalian thermoregulation via the POAH are referred to a panel of excellent papers by Morrison and Nakamura on this subject [Morrison et al., 2008; Nakamura, 2011; Morrison and Nakamura, 2011; Nakamura and Morrison, 2011].

A method to induce anapyrexia in small animals is by subjecting the animals to hypoxia, which triggers regulated hypothermia and corollary hypometabolism in some species as a countermeasure against the hypoxic, and thus potentially lethal, conditions [Kottke and Phalen, 1948; Hayden

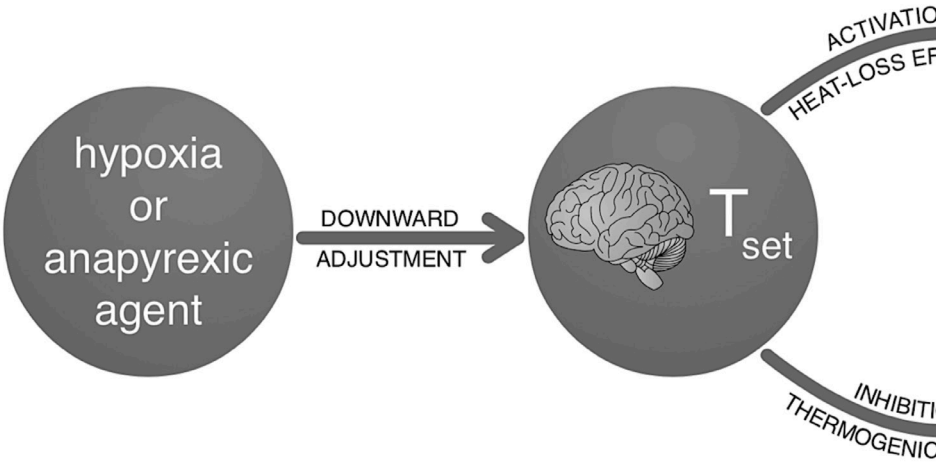

Figure 1. Regulation of body temperature (T_b) through change of the thermoneutral zone (Z_{tn}). The first sphere on the left indicates an initial external trigger, which may be an environmental stimulus such as hypoxia or a pharmacological agent with anapyrexic properties. These triggers can lead to a downward adjustment of the Z_{tn} (second sphere). In turn, the reduction of the Z_{tn} leads to activation of heat loss mechanisms (sweating, behavioral adaptation, panting, vasodilation) and inhibition of thermogenesis (shivering, activation of brown adipose tissue, behavioral adaptation, vasoconstriction, piloerection), resulting in a reduction of T_b (third sphere). The extent of T_b reduction is dependent on the rate of thermal convection, which in turn is dependent on the body surface:volume ratio (fourth sphere).

and Lindberg, 1970; Frappell et al., 1992; Gordon, 2001]. One of the putative regulatory mechanisms is centered on carotid body sensing [Peng et al., 2010; Prabhakar and Semenza, 2012]. Carotid bodies are clusters of chemoreceptors and cells near the bifurcation of the carotid artery that detect changes in oxygenation-related parameters, including partial pressure of oxygen and carbon dioxide as well as pH and temperature [Buckler et al., 2000; Gonzalez et al., 1994]. When hypoxia is sensed, anapyrexia is induced through the inhibition of thermogenic effectors and activation of cooling effectors [Steiner and Branco, 2002; Frappell et al., 1992; Gordon and Fogelson, 1991; Madden and Morrison, 2005; Hinrichsen et al., 1998], which are under control of the POAH [He et al., 1999; Boulant, 2000; Nakamura, 2011; Heller, 1979]. This protective mechanism (Figure 1) is believed to be rooted in evolution, and there is evidence that such a mechanism is

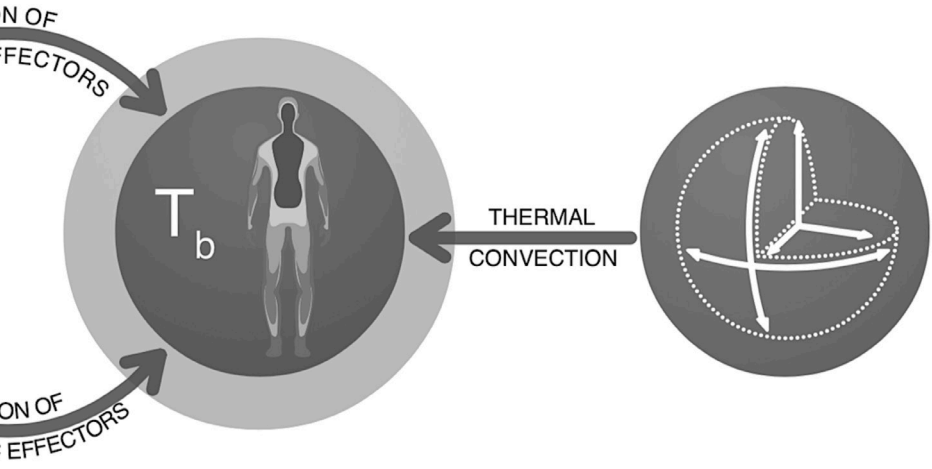

preserved in man, at least to an extent [Kottke and Phalen, 1948; Robinson and Haymes, 1990]. However, hypoxia is generally not employed in the clinical setting as a patient's already compromised state may be exacerbated at low oxygen tensions. Nevertheless, the artificial modulation of a patient's Z_{tn} is of great interest because of the protective effects that are associated with hypometabolism [Gordon, 2001].

Inasmuch as artificial (clinical) regulation of anapyrexia via the hypoxia-Z_{tn} axis does not constitute the most suitable and practical means, alternative methods have been explored. One interesting and potentially viable approach is pharmacological modulation of thermoregulatory cold receptors in the skin [Almeida et al., 2012; de Oliveira et al., 2014]. Studies published by Andrej Romanovsky's Fever Lab have demonstrated that selective inhibition of the transient receptor potential melastatin-8 (TRPM8) channel (cutaneous cold receptor) with M8-B effectively decreases the T_b in mice and rats via several thermal effectors (thermopreferential behavior, tailskin vasoconstriction, and brown adipose tissue) [Almeida et al., 2012]. Alternative strategies aimed at gaining control over the Z_{tn} by pharmacological means at intervention sites other than cutaneous cold receptors also appear promising and encompass several proposed compounds such as arginine, vasopressin, lactate, adenosine, histamine, delta- and kappa opioids, nitrogen monoxide, and

carbon monoxide [Steiner and Branco, 2002]. Although these agents harness potential for clinical application, most of the compounds are associated with undesired side-effects that have confined their use to the experimental setting.

The pharmacological induction of hypothermia through modulation of the Z_{tn} has proven quite difficult in practice, particularly since the number of reports on methods to induce anapyrexia is limited. Nevertheless, the downward adjustment of the Z_{tn} by pharmacological agents may have numerous beneficial implications for medicine and biotechnology, but also for sports and aviation/space travel. Consequently, the identification of new anapyrexic agents or re-evaluation of established compounds for their anapyrexic properties has become increasingly important. Subjecting all known pharmacological agents to specific empirical investigations, however, would be exhaustive and comprehensive.

Aim of the study

In order to provide an accessible summary of potentially useful pharmacological agents for the induction of anapyrexic signaling, we performed a review of literature and analyzed over a thousand pharmacologically active compounds for their ability to induce anapyrexia in animals. The most viable candidates were identified on the basis of the magnitude of the reported heat loss and critically appraised in the context of the Z_{tn}-mediated heat loss mechanisms (Figure 1). In this study we focused specifically on the most studied compounds that potentially harness anapyrexic properties and addressed the candidate drugs against a backdrop of empirical evidence related to mainly pharmacodynamics and toxicology. The secondary purpose of this review was to guide novel research with 'old compounds' in the context of anapyrexic signaling by elaborating on the discrepancies in reported data and knowledge gaps.

Visualizing drug-induced changes in body temperature

Between 1979 and 1986 eight extensive reviews on changes in T_b after

exposure to pharmacological agents were published by Wesley G. Clark in Neuroscience and Biobehavioral Reviews [Clark, 1979; Clark and Clack, 1980a; Clark and Clark, 1980b; Clark and Clark, 1981; Clark and Lipton, 1985a; Clark and Lipton, 1985b; Clark and Lipton, 1986; Clark, 1987]. According to the author, "this survey ... intended to provide an immediate source of information on drug-induced changes in thermoregulation" [Clark and Clark, 1980b]. Published prior to the coining of the term 'anapyrexia,' the reviews furnish relevant information on 1,295 agents in 48 mammalian species, although the size of the data compilation makes it difficult to effectively assess the anapyrexic potential of all agents. Therefore, we have created a visual tool to assist in the analysis of data by plotting the T_b change per compound and per species in a single diagram (Figure 2, see legend for methods). In short, a blue sphere indicates a reduction in T_b, which reflects the inability to maintain thermal homeostasis and hence points to potential anapyrexic properties of the agent. Contrastingly, a red sphere indicates an increase in T_b and thus pyretic properties of the agent. The size of the sphere is proportional to the magnitude of the change in T_b. Before elaborating on the most promising anapyrexia-inducing agents, it is important to outline some limitations of the analysis.

Limitations of the analytical method

The data in Figure 2 have four important limitations. Firstly, although each data point (sphere) represents the average of ≥ 10 reports, the number of animals in each report was not taken into account simply because the sample size was not indicated in every report, making a weighted analysis impossible. This may skew the data insofar as the result from one animal bears equal weight as the mean of results acquired with a larger group size.

Secondly, the change in T_b was not corrected for the T_a, which can have a considerable effect on convection and therefore the measured depth of hypothermia, particularly in small species [Dirkes et al., 2015]. Although most experiments were conducted at an average T_a that was within a normally accepted range (~18-25 °C), a few exceptions must be noted, such as for helium and DMSO, where the experiments were performed at an average

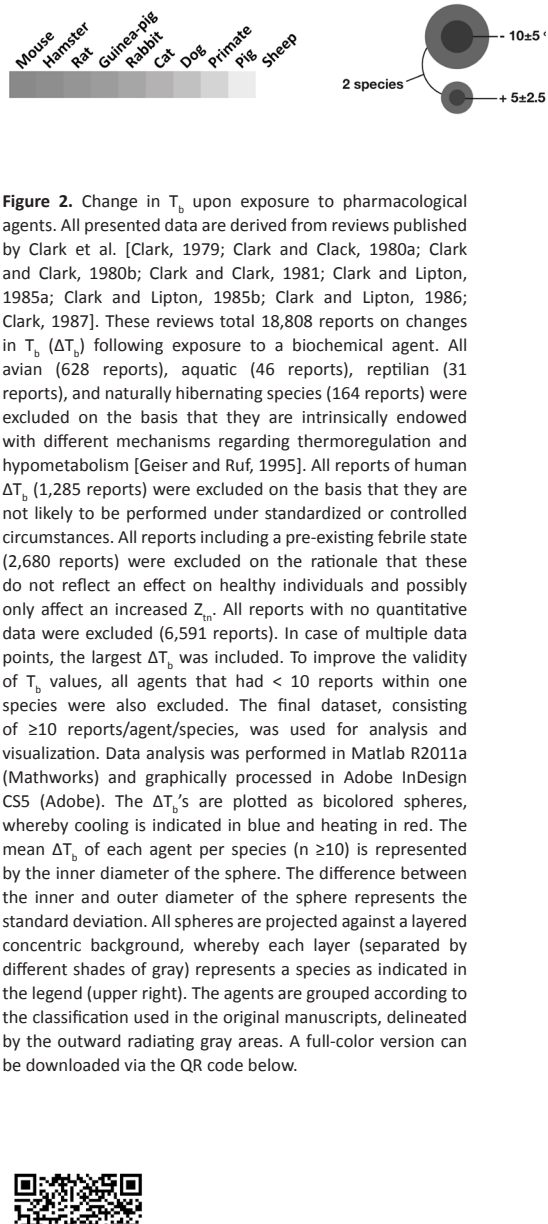

Figure 2. Change in T_b upon exposure to pharmacological agents. All presented data are derived from reviews published by Clark et al. [Clark, 1979; Clark and Clack, 1980a; Clark and Clark, 1980b; Clark and Clark, 1981; Clark and Lipton, 1985a; Clark and Lipton, 1985b; Clark and Lipton, 1986; Clark, 1987]. These reviews total 18,808 reports on changes in T_b (ΔT_b) following exposure to a biochemical agent. All avian (628 reports), aquatic (46 reports), reptilian (31 reports), and naturally hibernating species (164 reports) were excluded on the basis that they are intrinsically endowed with different mechanisms regarding thermoregulation and hypometabolism [Geiser and Ruf, 1995]. All reports of human ΔT_b (1,285 reports) were excluded on the basis that they are not likely to be performed under standardized or controlled circumstances. All reports including a pre-existing febrile state (2,680 reports) were excluded on the rationale that these do not reflect an effect on healthy individuals and possibly only affect an increased Z_{tn}. All reports with no quantitative data were excluded (6,591 reports). In case of multiple data points, the largest ΔT_b was included. To improve the validity of T_b values, all agents that had < 10 reports within one species were also excluded. The final dataset, consisting of ≥10 reports/agent/species, was used for analysis and visualization. Data analysis was performed in Matlab R2011a (Mathworks) and graphically processed in Adobe InDesign CS5 (Adobe). The ΔT_b's are plotted as bicolored spheres, whereby cooling is indicated in blue and heating in red. The mean ΔT_b of each agent per species (n ≥10) is represented by the inner diameter of the sphere. The difference between the inner and outer diameter of the sphere represents the standard deviation. All spheres are projected against a layered concentric background, whereby each layer (separated by different shades of gray) represents a species as indicated in the legend (upper right). The agents are grouped according to the classification used in the original manuscripts, delineated by the outward radiating gray areas. A full-color version can be downloaded via the QR code below.

chlorophenylalanine
arecoline
pilocarpine
carbachol
methacholine
nicotine
helium
carbon dioxide
oxygen
ergotoxine
ergotamine
atropine
methylatropine
propranolol
diethyldithiocarbamate
pentobarbital
DMSO
phenoxybenzamine
yohimbine
phentolamine
hydroxydopamine
metyrosine
reserpine
methyldopa
thyroxine
insulin
piribedil
dopamine
amantadine
apomorphine
bromocriptine
aminopyrine
indomethacin
acetominophen
sodium salicylate
phenacetin
aspirin
physostigmine
soman
isoflurophate
cannabis
delta-8-THC
delta-9-THC
lysergide
harmaline
cannabidol
aminobutyric acid
taurine
5'-hydroxytryptophan
dihydroxyphenylalanine
histidine
tryptophan
quinine
acetylstrophanthidine
histamine
succinylcholine
amitriptyline
desipramine
clomipramine
imipramine
tranylcypromine
pargyline
guanethidine
cocaine
prostaglandin D2
arachidonic acid
prostaglandin F2
prostaglandin E2
prostaglandin E1
chloroamphetamine
metamphetamine
fenfluramine
amphetamine
dinitrophenol
TRH
d-ala-2-met-enkephalinamide
muramyl-dipeptide
oxytocin
somatostatin
met-enkephalin
ACTH

T_a of 10.0 ± 13.3 °C and 12.5 ± 10.3 °C, respectively. The complete list of T_a's and the quantitative data of Figure 2 can be found in supplemental Table S1.

Thirdly, the dosage and administration route, which can affect the disposition of a pharmacological agent, were not accounted for in the analysis. An example of a dose-dependent effect on T_b can be seen with morphine (Figure 2). Morphine has the potential to both increase (cat) and decrease (dog) the T_b. These opposite findings may originate from differences in dosing since low concentrations of morphine (≤ 5 mg/kg intravenous bolus) cause a rise in T_b, whereas high concentrations (≥ 10 mg/kg intravenous bolus) cause a marked decrease in T_b [Lotti et al., 1965].

Lastly, the manner in which experiments were performed was discounted. The reports from which the data were collected were published between 1979 to 1987, i.e., just after the introduction of 'good laboratory practice' criteria in the late 1970's [Goodwin, 2008]. This may have had an impact on the accuracy of the obtained and published results.

Thermal convection: the importance of surface:volume ratio and metabolic rate

In addition to the evident thermomodulatory effects induced by some of the compounds, the data in Figure 2 is subject to two important principles that may affect anapyrexia, namely the body surface:volume ratio and Kleiber's law (discussed in [Dirkes et al., 2015]). With respect to the former, small animals cool down at a faster rate than larger animals because their relatively large surface:volume ratio facilitates more extensive heat exchange with the environment (Figure 1). Corroboratively, the largest changes in T_b are found in mice and rats (Figure 3A). Kleiber's law is an allometric law that describes an inverse relationship between metabolic rate and body size [Kleiber, 1947]. One of the pillars of this law is that smaller species need proportionally more energy than larger species to sustain their metabolism. Both principles essentially dictate that a reduction in Z_{tn} can manifest itself faster and more profoundly in small species compared to larger species. Unfortunately, the distribution of the data in Figure 2 is slightly biased towards the smaller species (supplemental Table S2), which clouds the unequivocal manifestation

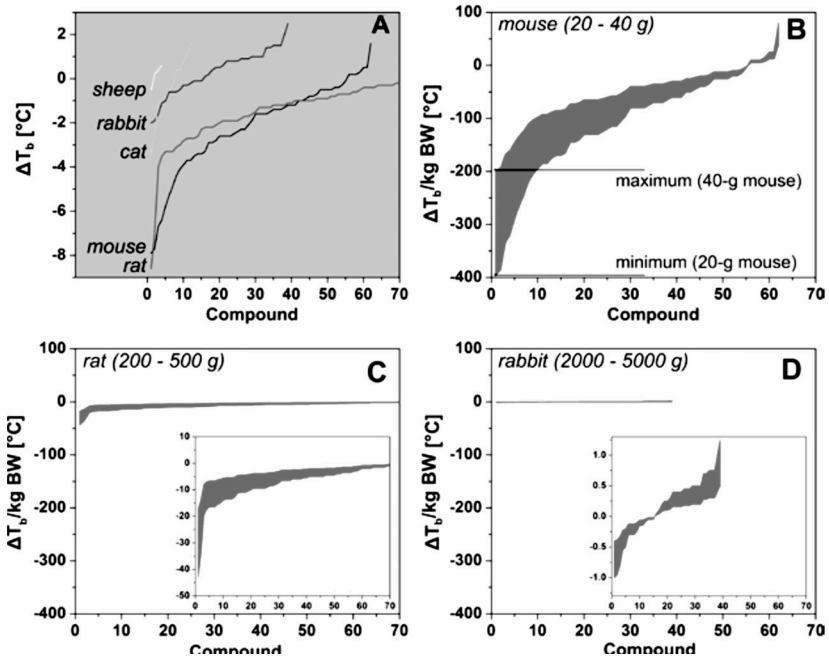

Figure 3. (A) Change in core body temperature (ΔT_b) per species plotted as a function of compound with the most profound effect on T_b (1, x-axis) to the compound with the least effect on T_b (up to 70, x-axis). The ΔT_b represents the mean of all ΔT_b's reported for the respective compound in the respective species that were included in the analysis. Research data were included on the basis of the criteria described in section 3 and the legend of Figure 2. The complete data set containing all the species is provided in Table S3. The data were normalized to the maximum and minimum common body weights (BW) of laboratory mice (B), rats (C), and rabbits (D) and should be read vertically per compound, whereby the upper limit is the minimum ΔT_b for the heaviest animals. The actual recorded values fall between the upper and lower bounds per compound. Note the different y-axis scaling of the inset plots. Common body weights were obtained from the internet (e.g., laboratory animal providers such as Harlan and Charles River).

of these principles across all species included in the analysis.

Nevertheless, a good illustration can be provided on the basis of mice (N = 62), rats (N = 96), and rabbits (N = 39) alone, as shown in Figure 3B-D, where the change in T_b was organized from greatest to lowest and plotted per compound following normalization to body weight (in kg). The upper limit and lower limit weights of these laboratory animals were used to demarcate the maximum and minimum boundaries of the T_b change per unit weight. This was done to semi-standardize the data because a considerable fraction of the articles from which the data were derived did not report the mean

body weight or weight range of the animals used in the experiments. When normalized to body weight, the heat loss per kg body weight is most sizeable in mice and smallest in rabbits, confirming the observations in Figure 2 and clearly illustrating both principles described above.

Compounds with anapyrexic potential

To identify anapyrexic agents, the data in Figure 2 were plotted according to the magnitude of T_b change, from the greatest decrease to the greatest increase in T_b (Figure 4). The magnitude of T_b decrease was used as the standard parameter to gauge anapyrexic signaling potential insofar as a downward modulation of T_b is the most important hallmark of anapyrexic signaling and does not occur in hibernators and non-hibernators in the

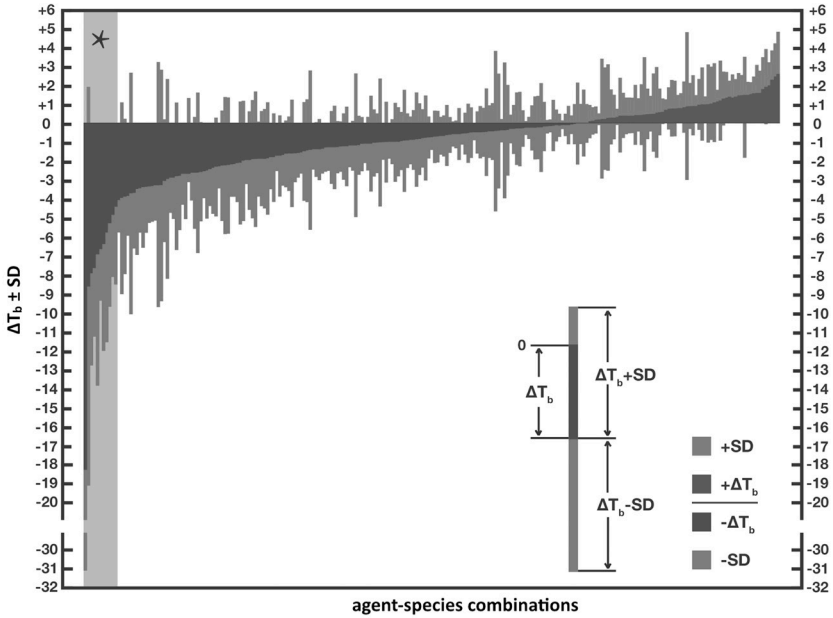

Figure 4. Ranked effect size of the change in T_b following exposure of an animal to a pharmacological agent. For the source of the data and inclusion criteria see the legend of Figure 2. All agent- species combinations (x-axis) were ranked by mean effect size (y-axis) with standard deviations (see legend within panel). The section marked with an asterix (*, top left) marks the agents that are discussed in more detail. A high-resolution full-color version can be downloaded from the Dirkes et al. [Dirkes et al., 2015].

absence of a Z_{tn} adjustment under non-stimulatory circumstances (e.g., under conditions of normoxia, abundant food supply, $T_a \approx T_b$, etc.) [Geiser and Ruf, 1995; Dirkes et al., 2015; Lotti et al., 1965; Geiser, 2004]. Based on this figure, eight agents (eleven agent-species combination) with the largest T_b decrease were selected as the most promising agents in terms of anapyrexic potential. These agents include helium (hamster, $\Delta T_b = -18.0 \pm 12.7$ °C), dimethylsulfoxide (DMSO, rat, $\Delta T_b = -8.6 \pm 10.5$ °C), reserpine (mouse, $\Delta T_b = -7.9 \pm 4.8$ °C), (oxo)tremorine (oxotremorine, mouse, $\Delta T_b = -7.7 \pm 3.6$ °C; tremorine, rat, $\Delta T_b = -6.9 \pm 6.9$ °C, mouse, $\Delta T_b = -6.7 \pm 2.7$ °C), pentobarbital (mouse, $\Delta T_b = -6.4 \pm 5.6$ °C), (chlor)promazine (chlorpromazine, mouse, $\Delta T_b = -4.4 \pm 4.1$ °C; promazine, mouse, $\Delta T_b = -5.8 \pm 5.8$ °C), insulin (mouse, $\Delta T_b = -5.3 \pm 4.4$ °C), and acetaminophen (mouse, $\Delta T_b = -4.9 \pm 3.3$ °C).

The observed reduction in T_b for these agents raises an important question: should the observed T_b reduction be diagnosed as anapyrexia or hypothermia, their sole difference being that the decrease in T_b is the result of a downward adjustment of the Z_{tn} in case of anapyrexia? A direct measurement of the Z_{tn} following administration of an agent would constitute the ultimate method to determine anapyrexic potential. However, due to the fact that we currently neither fully understand the body's temperature integration system nor have the means to monitor it, direct measurement of the boundaries that make up the Z_{tn} is impossible. Consequently, the gold standard in determination whether an organism is within the Z_{tn} boundaries is based on the activity of thermal effectors (Figure 1).

Therefore, in the next sections the eight most promising agents are addressed in the context of their effect on thermogenic and heat loss effectors such as shivering, BAT activity, sweating, vasoconstriction/ vasodilation, and behavioral accommodation (Figure 1).

Helium

Helium is a noble gas with minimal direct biological activity [Trudell et al., 1998]. Due to its biological inertness it is unlikely that helium induces cooling (Figure 2) via direct impact on the Z_{tn}. Instead, the thermoregulatory mechanism of helium may be based on its ability to augment the rate of heat convection.

The thermal conductivity of helium is 5.75 times higher than that of nitrogen [Piantadosi and Thalmann, 180]. When inhaling a gas mixture in which nitrogen is replaced by helium (e.g., Helox), the increased thermal conductivity of helium can accelerate changes in T_b in a proportional manner to T_a. The efficiency with which the pulmonary vascular bed is able to exchange heat is reflected by the clinical use of helium gas as a tool to accelerate the rewarming of hypothermic patients in combination with regular heating therapy [Danzl and Pozos, 1994]. An important prerequisite for helium-mediated reduction in T_b, as shown in Figure 2, is that it must be accompanied by a low T_a, which indeed averaged 10.0 ± 13.3 °C (supplemental Table S1).

Accelerated heat convection as the mechanism behind helium-induced hypothermia is further supported by the absence of change in behavioral thermoregulation in animals. In mice exposed to normoxic normobaric helium, there is no increase in heat avoidance, suggesting that helium does not have an effect on the Z_{tn} [Pertwee et al., 1986]. The mechanism of helium-induced hypothermia is therefore ascribable to its biophysical rather than its biochemical properties.

Dimethyl sulfoxide

DMSO has been widely exploited as an analgesic, anti-inflammatory agent, cryoprotectant, radioprotectant, transcutaneous transporter, barbiturates enhancer, and organ preservative [Armitage et al., 2005; Bradham and Sample, 1967; Kocsis, 1975; Rosenbaum et al., 1965]. However, the clinical use of DMSO was banned in 1965 by the Food and Drug Administration, restricting its applicability to experimental use. In the experimental setting the hypothermic effects of DMSO are markedly evident without inducing notable arterial and neuronal damage following systemic administration [Bakar et al., 2012], suggesting that DMSO may be an anapyrexic agent.

In rats, exposure to DMSO resulted in a decreased T_b with a simultaneous decrease in oxygen consumption and respiratory quotient, which are characteristic of a hypometabolic state [Orlando and Panuska, 1972]. The reduction in metabolism was likely triggered by a reduction in Z_{tn}, as a sustained Z_{tn} would initiate a temporary increase in oxygen consumption (a

thermogenic effector mechanism) in an attempt to bring the T_b back to a thermoneutral level.

Besides anapyrexic effects, it has been suggested that DMSO has the potential to act via the thyroid gland. Normally, the thyroid gland is under hypothalamic control to produce metabolism-promoting thyronines, which require iodine (I) for their synthesis. Upon exposure of mice to DMSO via intraperitoneal injection, the uptake of ^{131}I was shown to be attenuated, suggesting that the mechanism of DMSO-induced hypometabolism may be co-regulated by the thyroid gland [Orlando and Panuska, 1972]. However, it cannot be excluded that the observed dose-dependent reduction in ^{131}I uptake was a result of DMSO-induced reduction in T_b, or that it originated from a change in hypothalamic control (e.g., due to changes in Z_{tn}).

Nevertheless, the question remains whether the decline in T_b is anapyrexic in nature or mediated by peripheral factors. In an experiment focused on behavioral thermoregulation in rats, exposure to DMSO, which had a lowering effect on T_b, led to a 2-fold increase in the need for external heat reinforcement [Panuska, 1968]. This finding is in direct contradiction to anapyrexia, in which the lowered T_b would manifest itself by heat avoidance rather than reinforcement. In addition, the experiments performed in rats were performed in a temperature range of 0-26 °C [Clark and Clark, 1981]. The observation that DMSO caused such a large change in T_b in a small species such as a rat (Figure 3A, C) may in part be explained by the heavy cold thermal load. Finally, the interaction between DMSO and H_2O is exothermic in nature, causing erythema when applied on the skin [Bradham and Sample, 1967]. In spite of the initial warm sensation, the accompanying vasodilation can considerably augment the rate of heat loss, which may be further exacerbated by a DMSO-induced decrease in shivering [Orlando and Panuska, 1972]. It therefore appears that the physiological effects of DMSO do not completely fit the physiological response profile of an anapyrexic agent.

Reserpine

Reserpine is prescribed to patients as an antipsychotic or anti-hypertensive

drug. In the experimental setting the drug is often avoided because it induces hypothermia in small animals (Figure 2).

The mechanism of reserpine-mediated hypothermia is supposedly based on massive depletion of monoamines. Experiments in which cerebral monoamine concentrations were measured following reserpine administration revealed that reserpine depletes dopamine, norepinephrine, and serotonin levels [Somerville and Whittle, 1967; Tricklebank et al., 1984]. More specifically, reserpine was shown to decrease monoamine levels in the hypothalamus, an important part of the thermoregulatory system, suggesting anapyrexic potential [Brodie et al., 1960].

Several studies have attempted to narrow down specific monoamines that may be involved in reserpine-induced hypothermia. These demonstrated that the reduction in cerebral serotonin levels by para-chlorophynylalanine was not accompanied by hypothermia [Somerville and Whittle, 1967]. Similarly, no hypothermic response was observed following a reduction in cerebral dopamine and norepinephrine levels by α-methyl-m-tyrosine [Somerville and Whittle, 1967].

However, exposure of reserpine-induced hypothermic mice to SKF-38393, a D_1-like (dopamine) receptor agonist, led to a significant reversal of hypothermia [Duterte-Boucher et al., 1989]. Subsequent addition of SCH-23390, a D_1-like receptor antagonist, abrogated the T_b raising effects of SKF-38393, suggesting a central role for the D_1-like receptor in reserpine-induced hypothermia [Duterte-Boucher et al., 1989]. On the other hand, apomorphine, a non-specific dopamine receptor agonist, had the ability to induce hypothermia to a similar depth as reserpine, altogether indicating that the dopamine receptor plays an ambivalent but prominent role in the observed hypothermia following reserpine exposure [Lin et al., 1979].

The inconsistencies in reserpine-induced hypothermia mechanisms have been the focus of numerous reports [Cox, 1977]. However, most reports predominantly address augmentation of monoamines and their associated receptors of the central nervous system, while only a few reports describe the effects on (peripheral) thermogenic effectors. Reserpine has important inhibitory effects on thermogenic effectors such as BAT, where it has been shown to deplete norepinephrine stores [Weiner et al., 1962]. As BAT is under

adrenergic control, depleted norepinephrine stores can lead to severely impaired thermogenic activity [Cannon and Nedergaard, 2004].

Considering the current knowledge on reserpine, it could be postulated that reserpine constitutes the proverbial cannon to kill a mosquito. Generally, monoamine depletion causes many depressive effects that may encompass the POAH, and may therefore cause anapyrexia by a direct effect on the Z_{tn}. Irrespective of the central effects, reserpine's inhibitory effect on BAT will promote hypothermia indirectly by its inhibitory effect on thermogenesis through local norepinephrine depletion. These favorable properties notwithstanding, more specific knowledge on reserpine's mechanism of action is required, particularly with respect to central effects, before it can be categorized as a legitimate anapyrexic agent and clinically implemented as such.

(Oxo)tremorine

The use of tremorine and its metabolite oxotremorine are limited to the experimental setting. Exposure to tremorine does not only lead to hypothermia, but also induces generalized tremor and rigidity, owing to its muscarinic acetylcholine transport agonism [Cho et al., 1962].

Induction of hypothermia with (oxo)tremorine coincides with an important anapyrexic-like change in thermoregulatory behavior in animals, namely the active search for a cooler environment [Cox and Tha, 1975; Gordon et al., 1988]. This effect can be readily reversed by addition of atropine, a muscarinic acetylcholine receptor antagonist, suggesting involvement of cholinergic receptors in the management of Z_{tn} and T_b [Cox and Tha, 1975]. Further evidence supporting the anapyrexic effect of (oxo)tremorine is the profound hypothermia upon injection of tremorine directly into the POAH, a regulatory site involved in management of the Z_{tn}. A hypothermic response is absent when tremorine is injected into other cerebral regions [Lomax and Jenden, 1966]. Cholinergic receptors are putatively associated with T_b control. However, as they have been shown to trigger both pyretic and anapyrexic responses, their exact role in T_b control remains unclear [Avery, 1971; Myers and Yaksh, 1969; Lomax et al. 1969].

Contrary to the central anapyrexia-like effects of (oxo)tremorine, the

effects on peripheral effectors are equivocal. In larger animals, exposure to oxotremorine produces shivering, vasoconstriction, and signs of inhibited panting, altogether culminating in a T_b increase [Decima and Rand, 1965; Johnson 1975]. Although the vasoconstrictive response does not necessarily imply pyretic signaling but rather an effect of low blood pressure associated with oxotremorine exposure, the shivering can be associated with pyrexia or constitute a local effect [Dage, 1979]. The increase in T_b could possibly be supported by BAT activity, albeit the direct effects of (oxo)tremorine on BAT are largely unexplored. However, due to the limited presence of cholinergic fibers in BAT and its predominantly adrenergic control, BAT most likely plays no role in the (oxo)tremorine-induced thermogenesis [Cannon and Nedergaard, 2004; Giordano et al., 2004].

The capacity of (oxo)tremorine to induce both anapyrexia (i.e., thermoregulatory behavioral patterns, POAH-specific effects) and pyrexia (i.e., shivering, inhibition of panting) gives rise to the clinically relevant question whether its pyretic responses are centrally or peripherally regulated. The emphasis on the underlying mechanism of the pyretic responses is related to the possibility to control one of the thermogenic effectors, namely shivering, by the use of muscle relaxants. If shivering accounts for the majority of thermogenesis after (oxo)tremorine administration, anapyrexia could be effectively induced by (oxo)tremorine during hypothermic surgery on the condition it is co-administered with muscle relaxants to suppress the shivering.

Unfortunately, the amount of data on the peripheral mechanisms of (oxo)tremorine is very limited. To assess the anapyrexic potential of (oxo) tremorine, its mechanism on peripheral thermal effectors must be elucidated first.

Pentobarbital

Pentobarbital-induced hypothermia is believed to be facilitated by an increase in heat loss via dilation of cutaneous blood vessels [Lomax, 1966]. The lack of Z_{tn} involvement in pentobarbital-induced hypothermia is supported by studies in rats, where no hypothermic response was observed following injection of pentobarbital into the POAH [Lomax, 1966;

Humphreys et al., 1976]. However, intracerebro-ventricular injection of a 6-fold higher pentobarbital concentration resulted in a T_a-dependent hypothermic response that was accompanied by cutaneous vasodilation [Lin, 1981]. Accordingly, the T_a-dependent decrease in T_b and vasodilation imply that high intracerebroventricular pentobarbital concentrations produce systemic triggers that result in hypothermia, but not via the Z_{tn}. The absence of an anapyrexic effect is further supported by the lack of changes in thermoregulatory behavior in mice and rats [Strek et al., 1986].

Despite the widespread view that pentobarbital has no anapyrexic effects, more recent studies suggest that γ-amino-butyric acid (GABA) receptors, the main target of pentobarbital, may play a role in thermal homeostasis [Queva et al., 2003]. An in vitro study using hypothalamic medial preoptic slices revealed that both GABAA and GABAB receptor agonists inhibit neuronal tonic activity, implying a potential of GABA receptor agonists to modulate the Z_{tn} [Yakimova et al., 1996]. In murine GABAB knockout and partial knockdown models, hypothermic responses were observed in $GABAB^{+/-}$ and wild type ($GABAB^{+/+}$) mice but remained absent in $GABAB^{-/-}$ mice, supporting the notion that GABA receptors regulate temperature homeostasis via the Z_{tn} [Queva et al., 2003]. Despite the established pentobarbital-GABA signaling link and the apparent relationship between GABA receptor agonism and T_b control, the evidence is presently too scant to classify pentobarbital as an anapyrexic agent.

(Chlor)promazine

Both chlorpromazine and promazine are drugs with antipsychotic effects. Chlorpromazine is used to treat schizophrenia, although promazine is the major metabolite found in chlorpromazine-treated schizophrenic patients and therefore constitutes the pharmacodynamically active compound. In rats chlorpromazine does not undergo metabolism as extensively as in in humans inasmuch as dechlorination results in less than 1/20 of the promazine plasma concentration in schizophrenic patients [Sgaragli et al., 1986].

Chlorpromazine acts as an antagonist of dopamine-, serotonin-, adrenergic-, and muscarinic acetylcholine receptors. With respect to muscarinic acetylcholine receptors, chlorpromazine has an opposite effect of

that of oxotremorine, which is a muscarinic acetylcholine receptor agonist. Considering that both (oxo)tremorine and chlorpromazine can induce hypothermia, it is unlikely that the induction of hypothermia is mediated solely by muscarinic receptors.

The effects of chlorpromazine on thermal effectors are inconsistent. On the one hand, chlorpromazine injection into the POAH of primates led to hypothermia with concomitant cutaneous vasodilation and respiratory acceleration (panting), which is suggestive of anapyrexia [Chai et al., 1976]. The intraperitoneal administration of chlorpromazine in rats resulted in a T_b reduction, characterized by inhibition of thermogenic shivering and piloerection and an increase in heat loss mechanisms such as augmented blood flow in the tail [Kollias and Bullard, 1964]. On the other hand, intracerebral injection of chlorpromazine into the POAH of rats produced a T_b increase [Kirkpatrick and Lomas, 1971; Rewerski and Jori, 1968]. In mice, chlorpromazine was shown to substantially increase BAT activity [Som et al., 1983]. This observation is particularly interesting since chlorpromazine has no sympathomimetic properties, indicating possible central control.

Based on these contrasting reports, chlorpromazine does not unequivocally qualify as an anapyrexic agent. However, some of the pharmacodynamic features impart strong effects on the T_b, making them an important focus of further research.

Insulin

Hypothermia is a common response to systemic insulin exposure as an anticipatory coping mechanism for an impending hypoglycemic state [Buchanan et al., 1991]. Hypoglycemia-induced hypothermia is not only prevalent in many small animals, but is also observed in humans following e.g., insulin shock therapy [Mayer-Gross and Berliner, 1942]. Infusion of 2-deoxyglucose, a metabolically inert glucose analogue, also results in lowering of T_b in humans, implying that hypoglycemia-induced hypothermia may comprise an evolutionary conserved mechanism across different species [Thompson et al., 1980].

The main question, however, is whether hypothermia following (insulin-induced) hypoglycemia is anapyrexic in nature. In terms of anapyrexia,

insulin should exert an inhibitory effect on thermogenesis in combination with stimulation of heat loss mechanisms. In ectothermic toads, for instance, induction of hypoglycemia via both insulin and 2-deoxyglucose is associated with a behavioral drift towards lower temperatures [Branco, 1997]. This behavioral pattern ultimately causes a reduction in T_b and constitutes one of the hallmarks of Z_{tn}-mediated thermoregulation. Similarly, humans who become hypoglycemic at the expense of insulin or 2-deoxyglucose activate heat loss mechanisms such as sweating, vasodilation, and hyperventilation [Thompson et al., 1980; Molnar and Read, 1974; Passias et al., 1996].

The major thermogenic effector BAT is under control of insulin, which stimulates its anabolic (endothermic) rather than its catabolic (thermogenic) activity [Cannon and Nedergaard, 2004]. It may, however, be the hypoglycemic state itself rather than the insulin that inhibits thermogenic signaling. Hypoglycemia-mediated inhibition of thermogenesis is in agreement with the finding that shivering is attenuated in cold-exposed human subjects who have become hypoglycemic [Passias et al., 1996].

It therefore appears that hypoglycemia, and not insulin per se, has anapyrexic potential. At this stage, however, hypoglycemia-induced anapyrexia is difficult to translate to a clinical application without understanding the underlying mechanism of action in the context of thermoregulation.

Acetaminophen

Acetaminophen is a well-known and widely used analgesic and antipyretic drug. Most research on the pharmacodynamics of acetaminophen is therefore mainly focused on the antipyretic properties. However, its role as an anapyrexic agent has been proposed, but remains controversial and inconclusive. Clinical studies have demonstrated a significant reduction in T_b following acetaminophen treatment of stroke, head trauma, and subarachnoid hemorrhage [Dippel et al., 2003; Mellergard, 1992]. However, these findings are inconsistent with other reports, in which acetaminophen treatment of stroke and administration after cardiac bypass surgery showed no significant effect on T_b [Kasner et al., 2002; Stevens and Fitzsimmons, 1995]. The latter reports do not preclude the possibility that higher dosages may exhibit a thermomodulatory effect, but the amount of data on

acetaminophen-induced anapyrexic T_b reduction is too limited to draw solid conclusions at this point [Toussaint et al., 2010].

The thermoregulatory pharmacodynamics of acetaminophen remain elusive, although several advances in recent years have implicated the involvement of cyclooxygenase, peroxidase, nitric oxide synthase, cannabinoid receptors, and serotonin receptors [Toussaint et al., 2010]. In an effort to elucidate the pharmacological mechanism of acetaminophen, a study in mice revealed that acetaminophen can reduce T_b from euthermic levels, which is in support of anapyrexic properties [Li et al., 2008b]. However, the underlying mechanisms remain obscure, with data suggesting an effect on anti-glutamate and anti-oxidant capacities rather than on thermoregulatory mechanisms [Li et al., 2008b]. Moreover, the T_b-down modulatory properties of acetaminophen may have been falsely ascribed in instances where the thermoregulatory system was already activated, or functionally compromised. These instances include underlying disease or clinical trauma (e.g., cancer or stroke, such as cited in the previous paragraph [Dippel et al., 2003]) and bacterial and viral infections [Ayoub et al., 2004]. Finally, the hypothermic effect of acetaminophen has only been demonstrated in mice. Rats exposed to increasing acetaminophen dosages did not exhibit heat-avoiding behavior, indicating that no pharmacological modulation of the Z_{tn} had occurred [Vitulli et al., 1999]. Accordingly, the effect of acetaminophen on behavioral thermoregulation pleads against its classification as an anapyrexic agent, and it is unclear whether this class of drugs would induce hypothermia in a normal subject.

CONCLUDING REMARKS

Anapyrexia has yet to gain widespread acceptance as a clinically functional state. Acknowledgement of its implementation through clinical pharmacology will largely depend on three factors: the development of efficient methods to adjust the Z_{tn} downward, the ability to accurately measure the boundaries of the Z_{tn}, and the simultaneous use of external T_b control.

As indicated in the sections on the pharmacological agents above, there are various agents such as reserpine, (oxo)tremorine, and (chlor)promazine

that exhibit specific aspects suggestive of an anapyrexic potential. However, due to the primary research focus on aspects other than anapyrexia, the anapyrexic potential of these agents requires further examination. Combinational therapy and translation to larger animal models constitute important steps towards the elucidation and optimization of the anapyrexic candidate drugs.

Ultimately, for clinical application, the simultaneous use of external T_b control alongside anapyrexic agents will be essential. Due to the high body surface:volume ratio of humans, passive lowering of T_b is too inefficient to support the depth of hypothermia that is dictated by the Z_{tn} under conditions of anapyrexia. Therefore, the advantage of anapyrexic agents lies in the facilitation of hypothermic therapy by optimizing thermal effectors (i.e., inhibition of thermogenic effectors and activation of heat loss effectors), thereby preventing the manifestation of Z_{tn}—T_b mismatch-induced stressors during the induction of hypothermia.

PART II
EXPERIMENTAL STUDIES ON H_2S

Chapter 3
Induction of artificial hibernation in large mammals using H_2S

Adapted from

M.C. Dirkes, D.M.J. Milstein, M. Heger, T.M. van Gulik
Eur Surg Res 2015; 54:1 78-191

ABSTRACT

Artificially induced hypometabolism in non-hibernating mammals may have considerable clinical implications. Numerous studies in small rodent models have demonstrated that hydrogen sulfide (H_2S) induces hypometabolism, supposedly as a result of histotoxic hypoxia. However, the induction of hypometabolism is absent in large animals following H_2S administration. To determine the cause of this animal size-dependent discrepancy in H_2S pharmacodynamics, the effects of sodium H_2S (NaSH; 5 mg/kg/h, 4-hour intravenous administration) on systemic, pneumocardial, hematological, biochemical, microvascular (sublingual), and histological parameters were investigated in pigs. After 4 h, no differences were observed between the NaSH and control group with respect to systemic, pneumocardial, hematological, biochemical, and histological parameters. However, NaSH triggered significant hyperperfusion in the sublingual microcirculation, as evidenced by an increased blood vessel diameter (154 ± 16 and 85 ± 25% vs. baseline for NaSH and NaCl, respectively), total vessel density (139 ± 18 and 98 ± 13%, respectively), and perfused vessel density (139 ± 18 and 99 ± 13%, respectively). These phenomena are consistent with microvascular changes that occur during a panting response, an important heat loss mechanism (i.e., thermoregulatory effector) in pigs that is controlled by the thermoneutral zone (Z_{tn}). On the basis of our findings and the literature, a mechanistic explanation is provided for the differential manifestation of hypometabolism between small and large animals. In large animals, H_2S does not act via histotoxic hypoxia but likely triggers carotid bodies to transmit a hypoxic signal, which subsequently lowers the Z_{tn} and activates heat loss mechanisms (e.g., panting) to align ATP consumption with ATP production through hypothermia. Since large animals have a small surface:size ratio, the cooling rate is too inefficient to accommodate hypothermia and subsequent hypometabolism. This is why large animals do not exhibit hypometabolism, despite the activation of thermoregulatory effectors. This is also a reason for the poor translatability of artificial hypometabolism to the clinical setting.

INTRODUCTION

The induction of mild hypothermia in surgical patients is a relatively common perioperative procedure employed to maximally protect the organs and tissues from surgery-associated damage. At the basis of the protection lies a temperature-mediated deceleration of metabolic rate that is analogous to the principles of organ preservation by storing the organ on ice or at subnormothermic temperatures [Dirkes et al. 2013] before transplantation. However, the perioperative lowering of a patient's body temperature by a few degrees Celsius does not produce the depth of hypometabolism that is achieved during organ storage at much lower temperatures. The artificial induction of a deeper level of hypometabolism in humans would therefore constitute a revolutionary breakthrough with enormous practical implications, not only for the surgical setting but also for other fields in medicine, biotechnology, and space travel.

Hydrogen sulfide (H_2S) has long been recognized as a toxic gas that induces severe neurological and pulmonary complications [Beauchamp et al., 1984; Dorman et a., 2000]. It was therefore surprising that, in 2005, Blackstone et al. [Blackstone et al., 2005] showed that H_2S has the potential to cause a reversible state of hypometabolism in mice without harmful side effects. Since this discovery, the hypometabolic effects of H_2S have been reproduced in various small animal models [Baumgart et al., 2010; Volpato et al., 2008], sparking renewed interest in the clinical applicability of artificial hypometabolism.

Despite several successful experiments in small animals (i.e., mouse, rat) [Blackstone et al., 2005; Baumgart et al., 2010; Volpato et al., 2008], the exposure to H_2S has produced conflicting results in large animals (i.e., sheep, pig) [Simon et al., 2008; Derwall et al., 2011; Drabek et al., 2010] with respect to the induction of hypometabolism. A reduction in core body temperature (T_b), which epitomizes a reduction in metabolism, is repeatedly found in small animals treated with H_2S or sodium SH (NaSH), an established soluble H_2S precursor [Blackstone et al., 2005; Aslami et al., 2010]. However, when larger animals are exposed to either SH or NaSH, a reduction in T_b fails to manifest itself [Drabek et al., 2010; Li et al., 2008a].

The lacking hypometabolic response in large animals adds to the overall elusive nature of H_2S-mediated physiological mechanisms. The putative mechanism of H_2S is based on its potential to reversibly inhibit cytochrome c oxidase (CcO, complex IV) of the mitochondrial electron transport chain [Nicholls and Kim, 1982]. It has been suggested that the consequent cessation of oxidative phosphorylation is responsible for the lowering of T_b and the reduction in CO_2 production [Blackstone et al., 2005; Aslami et al., 2009]. However, the link between electron transport chain inhibition and H_2S-induced hypometabolism remains hypothetical for the in vivo setting. In order to explain the animal size-related discrepancies observed in vivo after H_2S exposure, the induction of hypometabolism must depend on additional mechanisms that extend beyond the current mechanistic paradigm and reported experimental evidence.

Here we postulate that the physiological responses resulting from exposure to H_2S can be explained by an additional mechanism that is also capable of inducing hypometabolism. This mechanism deviates from local (i.e., cellular) effects of H_2S and approaches hypometabolic signaling from an integrated systems physiology angle with a central role for T_b-regulating systems. The rationale behind this mechanism is supported by a series of experiments in which we subjected pigs to a sublethal dose of NaSH (5 mg/kg/h). Our experiments confirm the inability of H_2S to induce hypometabolism/hypothermia in pigs, whereas these effects have been observed in H_2S-exposed small animals. However, these experiments revealed effects of H_2S on sublingual microvasculature that are suggestive of a T_b regulatory change in the absence of hypothermia.

As a consequence of the proposed T_b-regulating mechanisms, we suggest that the hypo-metabolic effects of H_2S are strongly dependent on body size and that the hypometabolic capacity decreases with increasing body size. The body size dependence of hypometabolism in non-hibernating mammals may therefore comprise a significant hurdle in translating artificial hypometabolism into the clinical setting, unless effective and safe means are found to modulate thermoregulatory mechanisms and rapidly cool the human body.

MATERIAL AND METHODS

Ethical Approval

The animal experiments were approved by our institute's animal ethics committee (BEX102342). Animals were handled and cared for in accordance with the European Institutional Animal Care and Use Committee Guidelines and the National Institute of Health Guidelines for the Care and Use of Laboratory Animals. It should be noted that the original experiments were planned to be performed in alert animals. However, due to the manifestation of severe H_2S-induced pulmonary edema in pilot experiments, the animal ethics committee obliged us to conduct the study under general anesthesia.

Experimental Design

Fourteen female specific pathogen-free Landrace pigs (Sus scrofa domestica, 49 ± 2 kg; Van Beek SPF Varkens, Lelystad, The Netherlands) were used. All animals were housed under standard laboratory conditions (12-hour light/ dark cycle) and acclimatized for 7 days with ad libitum access to water and food. Prior to the experiments, the animals were fasted for 2 h with free access to water.

Animals were randomly allocated to either the NaSH or the NaCl group (n = 7 per group). After stabilization, baseline measurements were acquired as listed in table 1. Next, the thermal blanket was removed and infusion of NaSH or NaCl was started. The NaSH solution (Sigma Aldrich, St. Louis, Mo., USA) was freshly prepared before each experiment to a NaSH total [in milligrams, calculated as body weight (kg) × 4 h × 5] in 40 ml of 0.9% NaCl solution. The solution was loaded into a syringe and placed into a syringe pump (Harvard Apparatus, Holliston, Mass., USA). The pump volume was set to 10 ml/h, resulting in an infusion rate of 5 mg/ kg/h and a cumulative systemic NaSH concentration of 5.4 mM (assuming a blood volume of 65 ml/kg and using a NaSH molecular weight of 56.06). In the case of the control group, only 0.9% NaCl solution was loaded into the syringe and infused at the same rate (10 ml/h). Both solutions were administered via the cephalic vein.

During the experiment, sample and data collection were performed as listed in table 1. After 4 h, the animals were terminated by exsanguination.

Anesthesia Protocol

All investigations were performed in the same operating room. Premedication consisted of an intramuscular injection of 10–15 mg/kg ketamine (Eurovet Animal Health, Bladel, The Netherlands), 1–1.5 mg/kg midazolam (Actavis, Parsippany, N.J., USA), and 0.1 mg/kg atropine (Centrafarm, Etten-Leur, The Netherlands). After inhalation of a mixture of O_2 and isoflurane (2–3%, O_2:air ratio 1.5:3 liters/min; Forene, Abott Laboratories, Queensborough, UK), the animals were placed in the supine position, and the left ear vein was cannulated (18G Vasofix; B. Braun, Melsungen, Germany) for the administration of anesthesia. Animals were intubated with an 8-mm endotracheal tube (Covidien, Athlone, Ireland) and ventilated using a Datex-Ohmeda Aestiva/5 ventilator (GE Healthcare, Madison, Wisc., USA).

Maintenance anesthesia consisted of 5–10 µg/kg/h sufentanil (Hameln Pharmaceuticals, Hameln, Germany), 10–15 mg/kg/h ketamine (Eurovet Animal Health), 1–2 mg/kg/h dormicum (Actavis), and 2–2.25 mg/kg/h rocuronium bromide (Sandoz, Holzkirchen, Germany). Fluid management consisted of 0.9% NaCl (Baxter Healthcare, Deerfield, Ill., USA) infused at 15 ml/kg/h via the ear vein. Due to the pigs' high basal glucose metabolism, plasma glucose concentration was maintained by infusion of 20% glucose at 100 ml/h (Baxter Healthcare) via the cephalic vein through a BD Connecta cannula (Becton Dickinson Medical, Franklin Lakes, N.J., USA). All incision sites for the placement of catheters were pretreated locally with xylazine injections (total 0.3 mg/kg; Eurovet Animal Health). The right brachial artery was cannulated for blood pressure monitoring and collection of arterial blood samples using a 6-Fr enteral feeding catheter (Vygon, Ecouen, France). The bladder was approached transabdominally via a microlaparotomy and cannulated with a 20-Fr silicone bladder catheter (Bard Medical, Covington, Ga., USA). The right jugular vein was cannulated with a Swan- Ganz thermodilution catheter (5 Fr; Edward Lifesciences, Irvine, Calif., USA) and placed intrapulmonary according to the manufacturer's instructions.

The pigs were stabilized for at least 30 min after placement of the catheters. During the stabilization phase, the animals were covered with a thermal blanket (Travel Safe Healthcare, Mijdrecht, The Netherlands) to maintain body temperature, and pressure-controlled ventilation was set to

Parameter	Sample time (min)	Figure
Mean arterial presure[a] Systolic pressure[a] Diastolic pressure[a] Heart rate (HR)[a] Cardiac output (CO)[b] Pulmonary wedge pressure[b]	-30, 0, 60, 120, 180, 240	Figure 1c
T_b[b] T_a[c]	-30, 0, 60, 120, 180, 240	Figure 1a
Breathing frequency[d] End-tidal CO_2[d] Fractional inspiratory O_2[d] Respiratory volume[d] Pulmonary artery pressure[b] Saturation[e]	-30, 0, 60, 120, 180, 240	Figure 1b
PPV[f] TVD[f] PVD[f] BVd[f] MFI[f]	0, 60, 120, 180, 240	Figure 2a Figure 2b Figure 2c Figure 2d N.A.
pCO_2[g] pO_2[g] ABE[g] $HCO3^-$[g] Ht[g] Hb[g] O_2Hb[g] p50[g] pH[g] Gucose[h]	-30, 0, 60, 120, 180, 240	Figure 1d

Table 1. Summary of determined physiological parameters. The parameters measured in this study were obtained from the following devices: a pressure transducer; b Swan-Ganz thermodilution catheter; c external temperature sensor; d mechanical ventilator; e pulse oximeter on tail; f sublingually positioned MicroScan; g blood gas analyzer; h glucose meter.

18 mm Hg with a F_iO_2 of 41.2 ± 1.7%, which was kept at these levels for the remainder of the experiment.

Parameters

Ambient temperature (T_a) was measured with a 51–54 Series II thermometer (Fluke, Everett, Wash., USA). T_b was measured with the Swan-Ganz catheter. Arterial blood gas analysis was performed using an ABL80 Flex gas analyzer

(Radiometer, Brønshøj, Denmark).

The microcirculation of the sublingual mucosa was examined using sidestream dark field (SDF) video microscopy (MicroScan Video Microscope System; MicroVision Medical, Amsterdam, The Netherlands) as described previously [Goedhart et al., 2007; Milstein et al., 2012]. Briefly, the SDF technique operates by epi-illuminating the tissue of interest with 530-nm light, resulting in images of intraluminally circulating erythrocytes (appearing as dark globules) contrasted by a pale background. The SDF instrument was mounted on the operating table, and after a stabilization period, a 2-min video recording was captured prior to infusion for baseline analysis and subsequently repeated at a 1-hour interval during infusion. Microvascular monitoring was unsuccessful in 2 experiments in the NaCl group and in 2 experiments in the NaSH group due to unavailability of the equipment. The microvascular data used for analysis was therefore based on n = 5 per group. Microvascular (vessels <25 μm) parameters representing total vessel density (TVD; mm vessel/mm2), perfused vessel density (PVD; mm perfused vessel/mm2), proportion of perfused vessels (PPV; %), and microvascular flow index [MFI; score based on identifying the predominant flow type in four quadrants, defined as being either absent (0), intermittent (1), sluggish (2), or normal (3)] were analyzed using Auto- mated Vascular Analysis software (AVA v3.02; MicroVision Medical). The analysis of blood vessel diameter (BVd) was performed by randomly selecting 5 blood vessels in each of the 4 image quadrants (i.e., 20 in total) in the AVA software (Figure 3). By selecting a specific location on a vessel segment (e.g., a bifurcation or vascular crossing) as a landmark, reproducible (sequential) BVd measurements for the same 20 blood vessels could be analyzed in continuous mode (Figure 3).

Statistical Analysis

Data were analyzed in Matlab R2011a (MathWorks, Natick, Mass., USA). Differences between ordinal variables were tested with a Student's t test in case of a normally distributed data set and with a Wilcoxon rank sum test for data sets that did not pass the normality test (i.e., the data related to microvascular dynamics). A Kolmogorov-Smirnov test was used as a normality test. A p-value <0.05 was considered statistically significant. The interval

estimate is given by a 95% confidence interval (CI). Data are presented as mean ± SD.

RESULTS

The data discussed in this section were either found to be significantly different between the NaSH and NaCl group and/or to have implications for metabolic parameters.

Temperature

Over the course of 4 h, the T_b of animals in the NaCl and NaSH group declined from 37.4 ± 0.3 and 37.7 ± 0.4°C to 33.5 ± 1.5 and 33.2 ± 0.3°C, respectively (NaCl, $p < 0.001$, 95% CI = 2.73–5.10, and NaSH, $p < 0.001$, 95% CI = 4.01–4.99; Figure 1a). Between these groups there were no significant differences at any of the time points ($p \geq 0.097$). During the experimental period, the T_a was 20.9 ± 0.6°C for the NaCl group and 20.5 ± 0.3°C for the NaSH group over all time points, with no significant differences between these groups at any time point ($p \geq 0.059$).

Respiratory and Cardiovascular Parameters

During the experiment, the respiratory volume remained stable from 477 ± 46 and 458 ± 31 ml at t = 0 h (between groups: p = 0.472, 95% CI = –42.8 to 81.9) to 416 ± 50 and 382 ± 27 ml at t = 4 h (between groups: p = 0.249, 95% CI = –30.82 to 97.96) for NaCl and NaSH, respectively.

The mean end-expiratory CO_2 level was 38.7 ± 2.3 and 38.3 ± 4.0 mmHg at t=0 h (p= 0.726, 95% CI = –4.9 to 3.6) and 33.6 ± 5.8 and 34.1 ± 3.6 mm Hg at t = 4 h (p = 0.823, 95% CI = –6.2 to 5.1) in the NaCl and NaSH groups, respectively (Figure 1b).

The mean arterial pressure was 75 ± 10 and 77 ± 6 mm Hg at t = 0 h (p = 0.603, 95% CI = –11.7 to 7.4) and 71 ± 22 and 61 ± 9 mm Hg at t = 4 h (p = 0.220, 95% CI = –8.5 to 30.2) in the NaCl and NaSH groups, respectively (Figure 1c). During the experimental period the heart rate remained constant from 82 ± 10 and 78 ± 9 beats/min at t = 0 h (p = 0.352, 95% CI = –6.1 to 14.7) to 61 ± 4 and 62 ± 9 beats/min after 4 h (p = 0.742, 95% CI = –11.6 to

8.7) in the NaCl and NaSH groups, respectively. Similarly, the cardiac output remained unaltered from 4.6 ± 0.4 and 4.5 ± 0.8 liters/min at t = 0 h (p = 0.702, 95% CI = –0.7 to 1.0) and 4.3 ± 0.7 and 4.6 ± 1.0 liters/min at t = 4 h (p = 0.429, 95% CI = –1.3 to 0.6) in the NaCl and NaSH groups, respectively. Pulmonary artery pressure remained stable in both groups and did not exhibit differences between animals in the NaCl and NaSH group. The same applies to wedge pressure.

Bloodgas analysis yielded a pO_2 of 215±22 and 209±14 mmHg at t=0h (p=0.607, 95% CI = –22.7 to 35.6) that remained unaltered at 227 ± 25 and 217 ± 20 mm Hg at t = 4 h (p = 0.522, 95% CI = –26.7 to 47.2) in the NaCl and NaSH groups, respectively. The arterial partial CO_2 pressure (pCO_2) was constant at 41 ± 3 and 39 ± 3 mmHg at t=0h (p=0.322, 95% CI = –2.5 to 6.4)

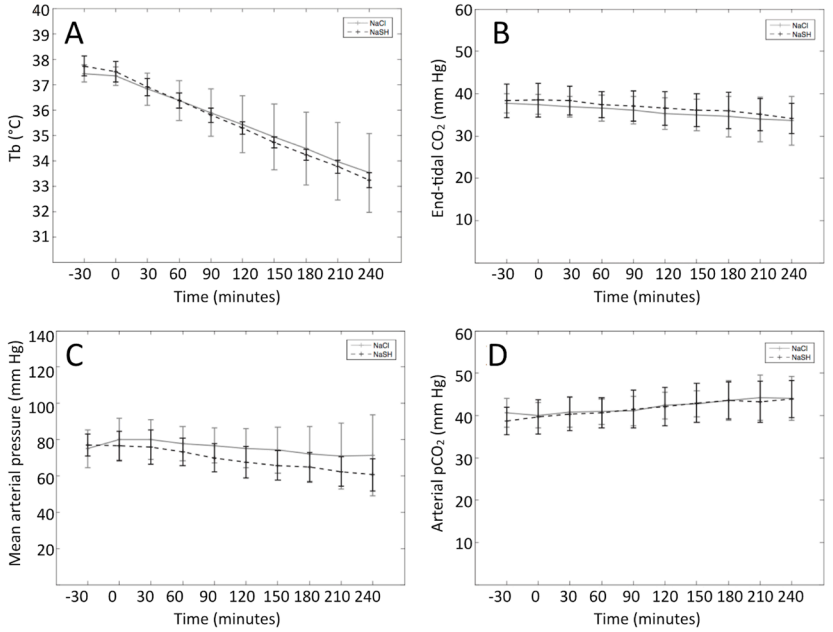

Figure 1. Physiological and metabolic parameters as a function of time. a T_b (°C). b End-tidal expiratory CO_2 (mm Hg). c Mean arterial pressure (mm Hg). d Arterial pCO_2 (mm Hg). Statistically significant differences between the NaSH group (black dotted line) and NaCl group (grey continuous line) are indicated with an asterisk ($p < 0.05$).

and 44 ± 5 and 44 ± 4 mm Hg at t = 4 h (p = 0.946, 95% CI = –5.2 to 5.6) in the NaCl and NaSH groups, respectively (Figure 1d).

No significant differences in end values were found between the NaCl and NaSH groups with respect to ABE, HCO_3^-, Ht, Hb, O_2Hb, p50, pH, and blood glucose.

Biochemical Parameters

At t = 4 h, no statistically significant differences were observed between the NaCl and the NaSH group with respect to plasma AST, ALT, LDH, and creatinine.

Microvascular Dynamics

A representative time series analysis is presented in figure 3, and the quantification results are presented in figure 2. The PPV remained above

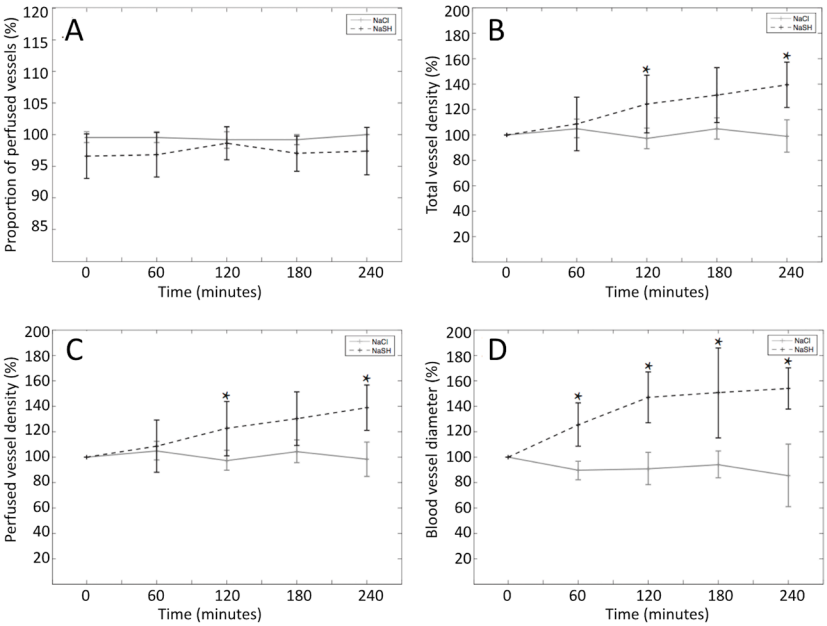

Figure 2. Microvascular parameters. a PPV (%). b TVD (%). c PVD (%). d BVd (%). Statistically significant differences between the NaSH group (black dotted line) and NaCl group (grey continuous line) are indicated with an asterisk (p < 0.05).

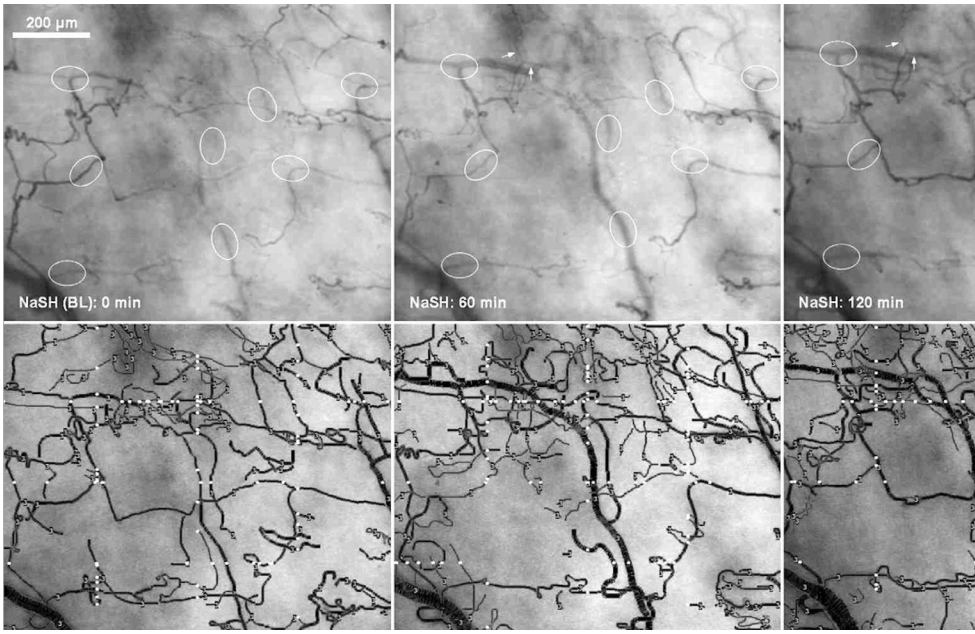

Figure 3. Intraoperative SDF video microscopy images of porcine sublingual microcirculation before (baseline, BL) and 60, 120, 180, and 240 min after NaSH infusion. The images in the top panels illustrate the consistency with which microcirculatory anchor points (ovals) could be retrieved for image analysis over time throughout the entire experimental procedure. The progressive evolution of microvascular vasodilation (see e.g., the centrally positioned, vertically coursing blood vessel) with subsequent recruitment of microvessels (arrows) can be clearly observed during NaSH infusion. The overall darker shade of gray observed at 120, 180, and 240 min indicates an increase in the amount of red blood cells and blood flow into the imaged tissue segment. The bottom panels coincide with the top microcirculation images and illustrate the completed processing of each video sequence for microcirculatory measurements.

96.6% in the both groups, indicating homogeneous microcirculatory perfusion in the region of interest (Figure 2a). Over the course of 4 h, the TVD in the NaSH group increased to 139 ± 18% of baseline ($p = 0.008$). No changes in TVD were observed in the NaCl group, comprising 98 ± 13% of baseline ($p = 0.016$ between groups at $t = 4$ h; Figure 2b). A similar trend was observed with respect to the PVD at $t = 4$ h, namely a 139 ± 18% increase versus baseline in the NaSH group, compared to no change (99 ± 13%) in the NaCl group (between groups at $t = 4$ h, $p = 0.016$; Figure 2c).

In the course of 4 h, the BVd increased to 154 ± 16% of baseline in the

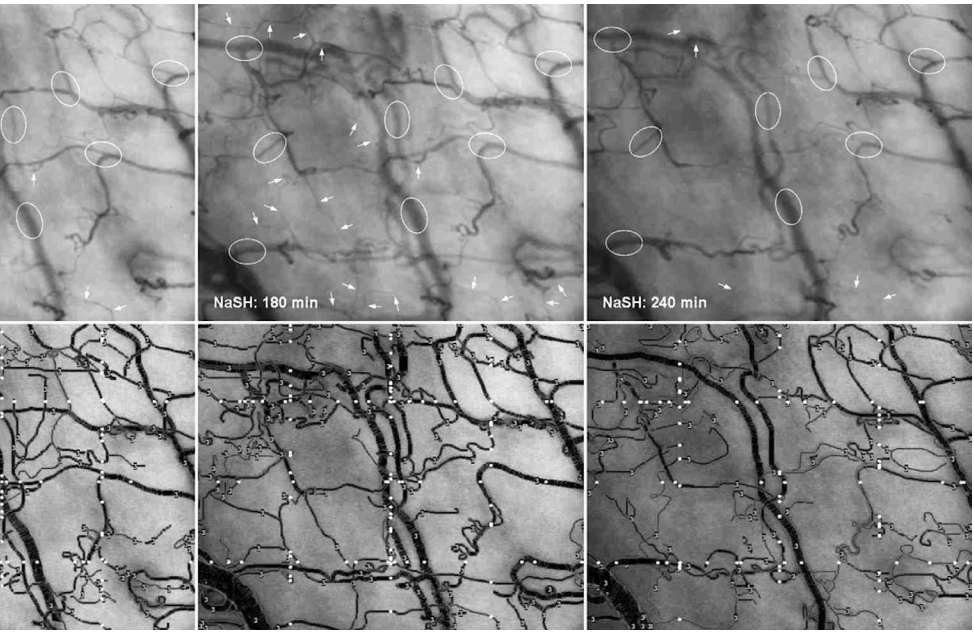

NaSH group (p = 0.008) and decreased to 85 ± 25% of baseline in the NaCl group (p = 0.127). A difference in BVd between animals in the NaCl and NaSH group was already observed after 1 h (p = 0.016) and remained until the end of the experiment (t = 4 h, p = 0.008; Figure 2d). The mean MFI score over all time points was 2.9 ± 0.3 in the NaSH group and 3.0 ± 0 in the NaCl group, indicating adequate continuous microvascular perfusion throughout the experiment.

Histology

No histological aberrations or signs of damage were observed in biopsies obtained from the heart, intestine, kidney, liver, lung, muscle, and spleen in either group. Any signs of pulmonary edema associated with exposure to H_2S (via its soluble precursor NaSH, see Discussion) were absent.

DISCUSSION

These experiments confirm that, over the course of 4 h, exposure to a low

dose of NaSH (5 mg/kg/h) does not produce a hypometabolic response in pigs based on T_b and expiratory CO_2, nor does it induce significant changes in cardiovascular or pulmonary parameters. This NaSH dose does, however, trigger significant vasodilation of the sublingual vasculature, as evidenced by the increase in BVd, and it significantly increases sublingual blood flow, as evidenced by the augmented PVD and TVD.

It should be noted that intravenously administered NaSH, which is converted to H_2S in the circulation and cells [Lee et al., 2011], was associated with pulmonotoxicity, despite the fact that the administered dose was lower than that used in mice [Han et al., 2011] and rats [Aslami et al., 2010].

Gaseous H_2S and solubilized NaSH did not lead to pulmonotoxicity in these species [Aslami et al., 2010; Han, et al., 2011]. The reasons behind the interspecies differences in the response to NaSH/H_2S are currently elusive. We deliberately chose to continue the research despite these phenomena because the pulmonary dysfunction was expected to impair gas exchange in the lung microcirculation and hence promote a state of circulatory hypoxia and corollary hypoxic signaling. As explained below, hypoxic signaling is considered one of the mechanisms underlying hypothermia. The consequences of pulmonotoxicity would therefore constitute instrumental support for the hypothesis.

In the following sections, the two mechanisms that may play a role in H_2S-mediated hypometabolism (Figure 4) are outlined in light of our findings. The first mechanism constitutes the current paradigm and is based on the histotoxic hypoxia-inducing properties of H_2S (Figure 4; No. 1). The second mechanism proposed in this paper is hypoxic signaling (Figure 4; No. 2), with support of a body size dependence (Figure 4; No. 3). Although both mechanisms can coexist in H_2S-subjected animals, our findings primarily support involvement of the second mechanism as the main modus operandi of H_2S induced hypometabolism.

Mechanism 1: Histotoxic Hypoxia

The current mechanistic paradigm of H_2S-induced hypometabolism (Figure 4; histotoxic hypoxia) is based on the noncompetitive binding of H_2S to

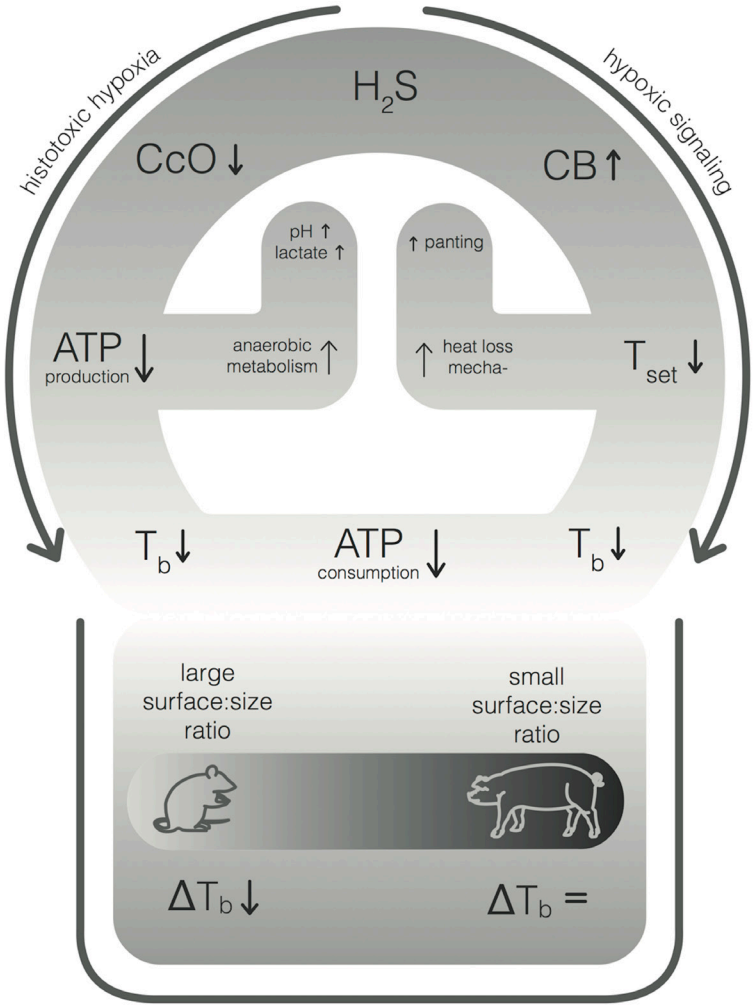

Figure 4. The mechanisms proposed to be involved in H_2S-induced hypometabolism. Each mechanism is elaborated in the corresponding paragraph of the Discussion. Mechanism 1 (Histotoxic hypoxia): inhibition of CcO by H_2S, resulting in lowered ATP production and subsequent lowering of T_b. Inhibition ATP production stimulates anaerobic metabolism, which concurs with elevated serum lactate levels and acidosis. Mechanism 2 (hypoxic signaling): H_2S-induced hypoxic signaling via CBs, leading to a downward adjustment of the Z_{tn} in the preoptic anterior hypothalamus and con- sequent reduction in T_b. The lowered Z_{tn} activates heat loss mechanisms such as panting to facilitate cooling. Mechanism 3 (body size dependence): the efficiency of T_b reduction via either the CcO or CB pathway is dependent on body size. Consequently, the reduction of T_b takes place in small animals but is impaired in large animals.

mitochondrial CcO, which results in the inhibition of aerobic respiration and leads to reduced ATP production [Beauchamp et al., 1984; Nicholls and Kim, 1982; Collman et al., 2009]. This process is referred to as histotoxic hypoxia and occurs irrespective of the oxygen tension. Histotoxic hypoxia has been suggested to cause the hypometabolic effects found in H_2S-exposed small animals, although currently there is no direct in vivo evidence linking the observed hypometabolism to CcO inhibition.

The inhibition of CcO is caused by the binding of H_2S to oxidized heme a3 and CuB sites, similar to what is observed during exposure to cyanide, a well-known histotoxic agent [Hill et al., 1984; Cooper and Brown, 2008; Scott et al., 1985]. As a result, the mitochondrial proton gradient required for ATP synthase functionality is abrogated, which leads to the cessation of ATP production. When assumed that the ATP-consuming processes are not blocked by H_2S, the inhibition of CcO would ultimately culminate in intracellular ATP depletion. However, before intracellular ATP depletion takes place, ATP production is temporarily maximized via anaerobic respiration. Therefore, when H_2S-induced histotoxic hypoxia manifests itself in the absence of hypothermia (hypothermia leads to hypometabolism and a reduced ATP consumption rate, precluding a switch to anaerobic respiration), an increase in anaerobic metabolism is expected.

The outcomes in this study are not suggestive of a shift to anaerobic respiration, at least not on the basis of the pH data, which showed no difference between groups. Corroboratively, Drabek et al. [Drabek et al., 2010] used a similar porcine model and also did not observe increased lactate production or decreased pH levels between animals that had received 5 mg/kg/h NaSH and controls, indicating that anaerobic metabolism had not been activated following NaSH infusion.

Presuming that the (bio-)chemical effects of H_2S are species independent, the lacking increase in anaerobic respiration in larger animals indicates that the employed H_2S concentration is either too low or entails an additional or different pathway. With respect to the former, the NaSH concentration employed in our experiments is relatively high compared to most studies in small animals, and higher H_2S concentrations (10 and 15 mg/kg/h) led

to significantly augmented mortality rates in our model [unpublished data, Blackstone et al., 2005], essentially refuting the concentration argument [Aslami et al, 2009]. Although a concentration-dependent effect cannot be unequivocally ruled out, our findings regarding the microvascular parameters provide a compelling avenue for interpreting the data via additional mechanisms.

Mechanism 2: Hypoxic Signaling

The alignment of ATP production with consumption is paramount to survival and constitutes a hallmark of hypometabolism. Numerous small animal species take advantage of their ability to lower the T_b as a means to synchronize energy metabolism with energy needs [Frappell et al., 1992; Hayden and Lindberg, 1970; Kottke and Phalen, 1948; Steiner and Branco, 2002]. This synchronization strategy is based on two principles: the downward adjustment of T_b (hypothermia) by hypoxia, for example, and the consequent induction of hypometabolism (i.e., reduced energy consumption) as a result of hypothermia (described by the Arrhenius equation).

Changes in T_b, or thermoregulation, are thought to be governed by the thermoneutral zone (Z_{tn}), which acts as an internal reference to the ideal T_b [Boulant, 2000]. Although the span of the Z_{tn} in thermoregulation cannot be measured directly, it can be extrapolated from the activity of its thermogenic effectors (e.g., shivering, piloerection, activation of brown adipose tissue) and heat-loss effectors (e.g., sweating, panting). In pigs, the number of heat loss effectors is limited due to the lack of cutaneous sweat glands, shifting the thermoregulatory processes to panting as the main heat loss mechanism [Ingram, 1967].

Our experiments indicate that a change in panting behavior may take place upon exposure to NaSH. Over the course of 4 h, the flow and diameter of the sublingual microvasculature increased significantly in the NaSH group compared to the control group (Figure 2), which is consistent with the microvascular changes that occur during a panting response [Kindermann and Pleschka, 1973; Rönert and Pleschka, 1976]. If these microvascular changes had been a generalized microvascular response, it would have impacted

blood pressure, heart rate, and cardiac output [Steiner and Branco, 2002]. Instead, all systemic cardiovascular parameters remained stable and did not differ from the control group, indicating that NaSH affected a restricted and specific region of microcirculation. The microvascular changes therefore imply that NaSH invokes a panting response, which in turn strongly suggests that NaSH exerts an effect on the Z_{tn}, given that this specific heat loss effector (i.e., panting) is controlled by the preoptic anterior hypothalamus [Hammel et al., 1960]. Although the underlying mechanism of this response cannot be definitively deduced from our experiments, it can be theorized to involve hypoxic signaling (in the absence of hypoxia, which is addressed in the next paragraph) based on the well-established link between hypoxia and heat loss effectors [Steiner and Branco, 2002]. In support of this argument, H_2S has been shown to exert a direct effect on thermoregulatory parameters in the brain. A T_b-modulatory effect of exogenously administered H_2S proceeded via the anteroventral preoptic region, albeit the decrease in T_b occurred only under hypoxic conditions and not under normoxia [Kwiatkoski et al., 2012]. This thermoregulation was mediated by cystathionine β-synthase, an enzyme that endogenously produces H_2S in the brain.

In light of our findings, it is unlikely that poor blood oxygenation was responsible for a hypoxic signal, given that there were no differences between the NaSH and control group with respect to the arterial pO_2. In the absence of anaerobic metabolism, as discussed in the previous section, it is also unlikely that histotoxic hypoxia was extensive enough to produce a hypoxic signal. So, in sum, we observed a H_2S-mediated panting response (heat loss effector) that constitutes an inherent part of Z_{tn}-directed thermoregulation. This type of thermoregulation is innately triggered by hypoxia as part of a protective hypometabolism-inducing mechanism but, in the case of our experiments, occurred in the absence of hypoxia (i.e., no direct effect of H_2S on the Z_{tn}). Accordingly, it can be speculated that the hypoxic signaling action of H_2S is more specific and circumventive, whereby H_2S induces hypoxic signaling under normoxic conditions. One such signaling mechanism may be through carotid body (CB) sensing, via which H_2S could mediate a decrease in the Z_{tn} and subsequent activation of a panting response (Figure 4; hypoxic signaling) while 'fooling' the body into 'thinking' that it is experiencing

hypoxia. Corroboratively, the link between H_2S and CB sensing has been well established in the last few years [Telezhkin et al., 2009; Prabhakar, 2012; Kemp and Telezhkin, 2014].

CBs are oxygen-sensing bodies located alongside the carotid artery, which contain chemoreceptors that provide essential neuronal feedback on arterial pO_2 [Prabhakar, 2000]. In CB cells, it was demonstrated that exposure to NaSH produced a comparable excitatory effect as hypoxia [Li et al., 2010]. Moreover, endogenously produced H_2S was shown to transmit a potent hypoxic signal in CBs [Peng et al., 2010]. Accordingly, these findings suggest that the hypoxia-mimicking properties of H_2S on CBs may account for the hypoxic signal theorized to affect the Z_{tn} and initiate the observed panting response, even at normophysiological pO_2.

However, even if CB signaling in general contributes to H_2S-induced lowering of the T_b through lowering of the Z_{tn} and subsequent hypometabolism, as is expected to be the case in small animals, it fails to account for the absence of cooling in pigs without the support of a body size-dependent element.

Body Size Dependence

Given the general unanimity of the published data, it can be concluded that H_2S exposure in small animals produces a different metabolic response than in large animals. In light of figure 4, this raises an important question, namely whether the proposed mechanisms of histotoxic hypoxia and hypoxic signaling can explain both the induction of hypometabolism in small animals (e.g., mouse, rat) and an absence of these effects in large animals (e.g., pig, sheep).

Both histotoxic hypoxia and (CB-emanating) hypoxic signaling must be accompanied by the lowering of T_b and metabolic rate in order to attune ATP consumption with production and thereby prevent excessive intracellular ATP depletion. The efficiency with which the T_b is lowered is not only affected by the activity and extent of heat loss mechanisms, but also depends highly on the body surface:size ratio. Small animals cool down at a faster rate than larger animals because their relatively large surface:size ratio facilitates more extensive heat exchange with the environment. Consequently, the

underdeveloped heat loss mechanisms in pigs, in combination with a small body surface:size ratio, deters the manifestation of a hypometabolic state during H_2S exposure simply because cooling in these animals is too inefficient to properly accommodate the thermoregulated hypometabolic induction. This is why panting is observed in the absence of hypothermia; the pig's body essentially wants to enter a hypometabolic state but cannot because it lacks the capacity to efficiently get rid of heat.

Study Limitations

There are several limitations to this study that need to be pointed out. First, additional control experiments were not performed to experimentally corroborate the panting response as well as the CB sensing hypothesis. With respect to experimental validation of the panting response, the vascular dynamics could have been measured by SDF microscopy in a different vascular bed to confirm that the microvascular hyperdilation was regional (i.e., confined to the sublingual microcirculation), as would be expected for panting. There is a possibility that the hyperdilation may have resulted from the vasodilatory properties of H_2S [Pozsgai et al., 2012], despite the cardiovascular and pulmonary parameters that indicate the contrary. Also, the panting response encompasses other heat loss mechanisms than only increased sublingual blood flow, such as changes in the ventilation of alveolar versus dead space and evaporation from the upper airway. These parameters were not measured. In regard to CB sensing, the experiments could have been repeated following surgical severance of the respective CB-hypothalamus neural networks, for example Hering's nerve.

Second, the panting response in the pigs in our experiments was characterized by a ~40–70% increase in microvascular parameters (TVD, PVD, BVd). In panting dogs, the average sublingual blood flow increased from 11 to 60 ml/min, with a maximum of 74.7 ml/ min [Rönert and Pleschka, 1976]. This represents a ~445% increase in blood flow, suggesting that the panting response was weak in pigs, notwithstanding any interspecies differences in panting behavior.

Concluding remarks

As the most important biochemical effect of H_2S-induced hypometabolism, the long-standing paradigm of CcO inhibition does not hold for larger animals and therefore requires reconciliation. We propose an additional mechanism that can help consolidate H_2S-mediated hypometabolic pathways across a wider variety of species. It was hypothesized that H_2S acts on CBs, producing a hypoxic signal that lowers the Z_{tn} and allows the activation of heat loss mechanisms through a panting response. This would make H_2S a Z_{tn}-modulatory rather than a hypometabolic agent.

Our experimental findings provide only partial support for this mechanism and are confined to pigs. Unfortunately, thermal effector changes upon H_2S exposure are relatively poorly reported in the literature and could therefore not be included as supporting material. The proposed mechanism therefore warrants further research and the results should be reproduced in other large animal species.

If H_2S-mediated hypometabolic signaling is indeed predicated on the rate of heat loss, the effectiveness of H_2S to induce hypometabolism is expected to be inversely related to body size. As a result, H_2S in large animals could reach an equal hypometabolic depth as in small animals, provided that they are actively cooled to facilitate sufficient heat loss.

Chapter 4

Induction of artificial hibernation in small mammals using H_2S

Adapted from

S.D. Hemelrijk*, M.C. Dirkes*, M.H.N. van Velzen,
R. Bezemer, T.M. van Gulik, M. Heger

Si Rep 2018 Mar 1; 8(1): 3855

* Both authors contributed equally to this work

ABSTRACT

Hydrogen sulfide (H_2S, 80 ppm) gas in an atmosphere of 17.5% oxygen reportedly induces suspended animation in mice; a state analogous to hibernation that entails hypothermia and hypometabolism. However, exogenous H_2S in combination with 17.5% oxygen is able to induce hypoxia, which in itself is a trigger of hypometabolism/hypothermia. Using non-invasive thermographic imaging, we demonstrated that mice exposed to hypoxia (5% oxygen) reduce their body temperature to ambient temperature. In contrast, animals exposed to 80 ppm H_2S under normoxic conditions did not exhibit a reduction in body temperature compared to normoxic controls. In conclusion, mice induce hypothermia in response to hypoxia but not H_2S gas, which contradicts the reported findings and putative contentions.

INTRODUCTION

Hibernation is a hypometabolic state characterized by a regulated decrease in core body temperature (T_b) (i.e., hypothermia) towards ambient temperature (T_a) and consequent reduction in oxygen (O_2) consumption and carbon dioxide (CO_2) production. It is engaged by several mammalian species [Heldmaier et al., 2004] to protect the organism from (environmental) stressors such as extreme cold, hypoxia [Gordon and Fogelson, 1991; Steiner and Branco, 2002], and starvation [Dark et al., 1994; Planel et al., 2004] and ultimately death.

The regulated decrease in T_b, which is termed anapyrexia, encompasses the downmodulation of the 'internal thermostat' outside of the thermoneutral zone [Heller and Colliver, 1974; Heller et al., 1977; Song et al., 1995; Song et al., 1997; Cannon and Nedergaard, 2004]. The thermoneutral zone constitutes a temperature range in which heat production (from basal metabolism) is in equilibrium with heat loss to the environment. The organism functions best when the T_b resides in the thermoneutral zone, but engages anapyrexia as a coping mechanism. How the anapyrexic signaling is biochemically and physiologically regulated and how the 'internal thermostat' is circumvented is largely elusive and hypothetical, but the ultimate outcome is unequivocally a state of hypometabolism. The natural purpose of the hypometabolism is to temporarily realign energy needs with reduced energy/O_2 supply under conditions of stress in order to sustain life under circumstances that could otherwise have lethal consequences.

The state of cold hypometabolism is believed to be a result of systematic deviation from homeothermy, which in turn is caused by a reduction in or cessation of metabolism. The resulting hypothermia assists, or propagates, the hypometabolic state in accordance with Arrhenius' law. This law states that the rate of chemical reactions (i.e., metabolism) decreases when the temperature decreases [Arrhenius, 1889; Peleg et al., 2012]. Consequently, both the consumption of substrate (in this case O_2) and the formation of product (in this case CO_2, toxic metabolites such as lactate, and reactive O_2 species) are reduced during hypothermia, as has been confirmed in natural hibernators during hibernation in terms of expired CO_2 [Heldmaier

et al., 2004] The alignment of metabolic demand with supply as well as the decreased formation of cytotoxic metabolites confer sustenance of life and cytoprotection in the stress-exposed organism.

In line with the above, mimicking these natural phenomena in non-hibernators such as humans by artificially inducing hypometabolism holds tremendous potential in medicine, aviation and space travel, and sports. An artificially induced hypometabolic state has been hypothesized to impart similar protective effects on otherwise stressed cells. Accordingly, numerous studies have focused on identifying agents that are capable of inducing hypometabolism in non-hibernating mammals (i.e., anapyrexic agents), which have yielded 5'-AMP [Zhang et al., 2006; Daniels et al., 2010], DADLE [Dawe and Spurrier, 1969, Horton et al., 1998], 2-deoxyglucose [Planel et al., 2004; Bechtold et al., 2012], thyronamines [Scanlan et al., 2004; Braulke et al., 2008], and exogenous hydrogen sulfide (H2S) [Blackstone et al., 2005] as potential anapyrexic agents. Of these, exogenous H_2S has received the most attention in the last few years in response to the Science publication by Blackstone et al. [Blackstone et al., 2005]. However, our experiments in mice, which duplicated the experiments by Blackstone et al. [Blackstone et al., 2005], revealed that exogenous H_2S does not induce hypothermia at normoxic conditions. Instead, the hypothermia observed in the experiments emanates from a hypoxia-induced anapyrexic response, which is a natural response in mice to hypoxic stress [Gordon and Fogelson, 1991; Steiner and Branco, 2002]. The results are described in this paper and addressed in the context of artificial hypometabolism.

Exogenous H_2S has been proposed to induce hypometabolism that is associated with a state of suspended animation [Blackstone et al., 2005]. Mice that were subjected to a gas mixture composed of 17.5% O_2, 80% nitrogen (N_2), and 80 ppm H_2S exhibited a 22 °C reduction in T_b (Figure 1A) after 4 h of exposure, yielding a T_b that was slightly above the T_a of 13 °C. At this point CO_2 production and O_2 consumption had decreased by approximately 90%, suggesting that the animals had reached a state of hypometabolism by anapyrexia. Moreover, this state was reversible inasmuch as all metabolic parameters reverted to baseline within 4 h after the exposure to H_2S was abrogated. During this recovery period the T_b also gradually restored to

baseline at a T_a of 24 °C. In another study by Volpato et al., inhalation of air containing 17.5% O_2 and 80 ppm H_2S induced similar anapyrexic effects in mice at a T_a of 27 °C as well as 35 °C (Figure 1B) [Volpato et al., 2008], altogether suggesting that inhaled H_2S reduces the T_b to T_a levels.

The mechanism behind exogenous H_2S-induced suspended animation [Blackstone et al., 2005; Volpato et al., 2008] is generally ascribed to the direct inhibition of oxidative phosphorylation [Beauchamp et al., 1984] and consequent histotoxic hypoxia. Because of is its high membrane permeability, H_2S is readily delivered to tissues via the circulation where it transgresses cell membranes and localizes to various intracellular organelles, including mitochondria [Cuevasanta et al., 2012]. H_2S binds cytochrome c oxidase (complex IV) in the electron transport chain in a reversible and noncompetitive fashion. As a result, H_2S prevents O_2 binding to cytochrome c oxidase and thereby interferes with the reduction of O_2 to water.

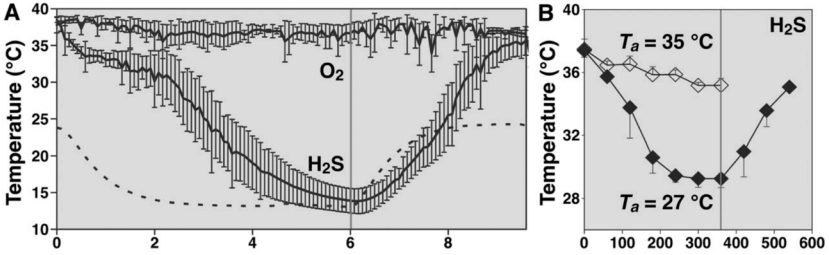

Figure 1. Previously reported temperature effects of H_2S. Temperature effects of inhaled H_2S gas (80 ppm) on the T_b of mice as a function of exposure time as reported by Blackstone [Blackstone et al., 2005] (A) and Volpato [Volpato et al., 2008]. (B). In (A) mice were exposed to 80 ppm H_2S and 17.5% O_2 (n=7) or 17.5% O_2 (n=4) for 6h, followed by a recovery phase at 17.5% O_2 in both groups (6–10 h, right part of red vertical line). The T_a was decreased during the exposure phase (dotted line). In (B) similar experiments were performed as in (A) but at fixed T_a's of 27 °C (closed diamonds, n = 3) or 35 °C (open diamonds, n = 4). The 6-h H_2S exposure phase was followed by a 3-h recovery phase in air at a T_a of 27 °C (6–9 h, right part of red vertical line). Data modified from [Blackstone et al., 2005; Volpato et al., 2008].

Concurrently, H_2S interferes with the production of adenosine triphosphate (ATP) by ATPase due to H_2S-induced perturbation of electron transfer and proton gradient over the mitochondrial inner membrane [Cooper and Brown, 2008; Nicholls et al., 2013]. It should be noted, however, that H_2S-mediated histotoxic hypoxia has never been proven to directly translate to H_2S-induced

hypothermia. Similarly, experimental evidence that H_2S triggers a downward shift of the thermoneutral zone directly remains at large.

Although the hypometabolic effects of exogenous H_2S seem convincing, the putative mechanism for the hypometabolic state induced by exogenous H_2S, i.e., cytochrome c oxidase inhibition [Beauchamp et al., 1984], may not account for the observed effects. As H_2S is a toxic, irritant gas [Beauchamp et al., 1984], inhalation is known to provoke epithelial damage in the upper [Lopez et al., 1987] and lower respiratory tract [Prior et al., 1988; Stein et al., 2012] in rats and pulmonary edema in pigs [Simon et al., 2008; Althaus et al., 2012]. The pulmonotoxicity of exogenous H_2S may therefore be associated with hypoxemic hypoxia.

Hypoxia, on the other hand, is a very potent inducer of anapyrexia, hypothermia, and hypometabolism and, thereby, of suspended animation [Steiner and Branco, 2002]. Several hibernating and non-hibernating mammalian species, including mice, exposed to different degrees of hypoxic atmospheres (i.e., F_iO_2 5–10%) immediately drop their T_b to enter a reversible state of hypometabolism [Frappell et al., 1992; Gautier, 1996; Branco et al., 1997; Hinrichsen et al., 1998]. The hypothermic effects of hypoxia are known to be caused by downward adjustment of the 'internal thermostat,' and involve the preoptic anterior hypothalamus (POAH), as has been demonstrated in thermobehavioral experiments in rodents [Gordon and Fogelson, 1991]. Consequently, we proposed that the hypothermia in exogenous H_2S-exposed mice, which constitutes a hallmark feature of hypometabolism, emanated from the combination of mild hypoxia (17.5% O_2) and inhalation of H_2S gas, and not the exogenous H_2S gas per se.

MATERIALS AND METHODS

Animals

Forty-eight female C57Bl/6 mice (Charles River, L'Arbresle, France; 10–12 weeks of age) were acclimated for 2 weeks under standardized laboratory conditions with a 12 h light/dark cycle, a constant ambient temperature (T_a) of approximately 21 °C, and ad libitum access to standard chow and drinking water. The experimental protocol was evaluated and approved by the animal

ethics and welfare committee of the Academic Medical Center, University of Amsterdam under protocol number BEX102753. Animals were treated in compliance with institutional guidelines and the National Institute of Health Guidelines for the Care and Use of Laboratory Animals (NIH publication No. 86–23, revised 2011).

Experimental setup and gas mixtures

The hydrogen sulfide (H_2S) and 17% oxygen (O_2) gas mixtures were obtained from Westfalen (Münster, Germany) and consisted of (1) 80 ppm H_2S, 21% O_2, and 79% nitrogen (N_2); (2) 80 ppm H_2S, 17% O_2, and 83% N_2; or (3) 17% O_2, and 83% N_2. The 5% O_2 gas mixture was obtained from Linde Gas (The Linde Group, Munich, Germany) and consisted of 5% O_2 and 95% N_2. Normoatmospheric air (21% O_2 and 79% N_2) was used as control.

An experimental setup was custom-built to allow controlled gas exposure while unobtrusively assessing body temperature (T_b) with a thermographic camera (ThermaCAM SC2000, FLIR Systems, Wilsonville, OR) in non-anesthetized mice. The setup consisted of gas-tight polypropylene chambers, length × depth × height of 109 mm × 109 mm × 61 mm) that were sealed at the imaging end with a thin, infrared light-permeable polyethylene sheet to permit thermal imaging from outside metal wires were secured longitudinally so that the animals could not reach the polyethylene sheet. Gas inflow and outflow tubes were connected to each box at the posterior end for modulation of experimental conditions. The gas permeability of the chambers was tested by air pressure decline experiments. Also, a thermistor (Fluke 51 II, Fluke Corporation, Everett, WA) was secured in the posterior wall to facilitate the measurement of the temperature in the chamber. The thermistor was used as a calibrator for the thermographic camera images, as the thermographic images display the temperature of the copper bolt retaining the thermistor. The experimental setup can be found in more detail in Hemelrijk et al. [Hemelrijk et al., 2018].

To ascertain sufficient inflow of gas in all experiments and prevent CO_2 accumulation, the flow rates were controlled on the basis of CO_2 outflow concentrations (<600 ppm, CO_2 Meter, Ormond Beach, FL). The system was also connected to an O_2 and H_2S meter (model OdaLog 7000, App-

Tek International, Brendale, Australia), which was calibrated by a certified company prior to the experiments (Carltech, Maarheeze, the Netherlands). The O_2 and H_2S meter was post hoc tested for measurement accuracy. The experiments were performed at a mean ± SD T_a of 21.2 ± 0.6 °C.

Experimental procedure

To test the hypothesis that H_2S-induced hypothermia emanates from hypoxia and not H_2S, all 48 animals were randomly divided among 5 experimental groups. Group A was exposed to 80 ppm H_2S in 21% O_2 and 79% N_2 (H_2S in 21% O_2 group, N=12), group B was exposed to 80 ppm H_2S in 17% O_2 and 83% N_2 (H_2S in 17% O_2 group, N=6), group C was exposed to 5% O_2 and 95% N_2 (5% O_2 group, N=12), group D was exposed to 17% O_2 and 83% N_2 (17% O_2 group, N = 6), and group E was exposed to 21% O_2 and 79% N_2 (normoxia group, N = 12).

Mice were placed in the chambers individually. After 1 h of exposure to normoxia (21% O_2 and 79% N_2), the mice were exposed to one of the gas mixtures (A – E) for 6 h, after which 6 of the animals per group were allowed to recover at normoxic conditions for 3 h before being terminated. The other 6 animals of group A, C and E were terminated immediately after the 6 h of exposure for another study. No anesthetics were used before or during the experimental procedure.

Thermal imaging and data processing

Animals were filmed every hour for 10 min with a thermographic camera (ThermaCAM SC2000, FLIR Systems, Wilsonville, OR) (Figure 2). Thermographic camera images (3 images per second) were processed and analyzed in ThermaCAM Researcher 2001 (FLIR Systems). The mean maximum superficial temperature was calculated per time point per group.

The tail temperatures of animals in group A (N = 3), C (N = 3), and E (N = 1) were obtained from the thermographic camera images at 0 h, just before the start of exposure, and approximately 4 min after the start of exposure. We noticed the intergroup differences in tail temperature during the experiments, as a result of which the tail temperature was measured in only 7 animals. The mean difference in tail temperature between both time points

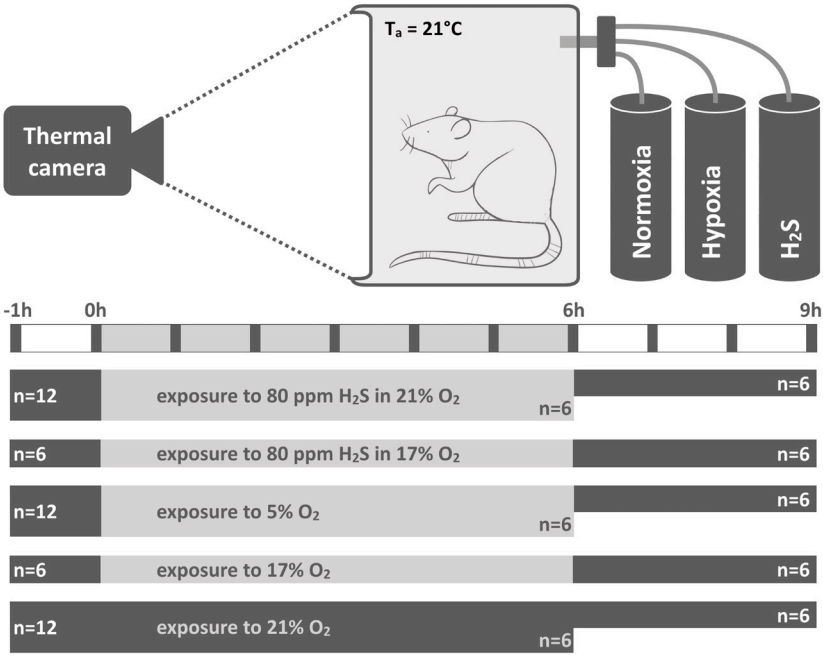

Figure 2. Schematic illustration of the experimental setup and design. The animals were allocated to one of the following experimental groups: (A) 80 ppm H_2S in 21% O_2 and 79% N_2 (H_2S in 21% O_2 group, N = 12); (B) 80 ppm H_2S in 17% O_2 and 83% N_2 (H_2S in 17% O_2 group, N=6); (C) 5% O_2 and 95% N_2 (5% O_2 group, N=12); (D) 17% O_2 and 83% N_2 (17% O_2 group, N = 6); and (E) 21% O_2 and 79% N_2 (normoxia group, N = 12). The experiments were performed at a mean ± SD T_a of 21.2 ± 0.6 °C, measured with a thermistor. During the whole experiment the mice were solitarily housed in a custom-built airtight cage and recorded with a thermographic camera (CAM) for 10 min every hour (red markers) for skin temperature- and locomotor activity analysis. After 1 h of baseline 21:79% O_2:N_2 exposure, each mouse was exposed to a gas mixture (A–E) for 6 h that was passed through the airtight cage, after which 6 of the animals in each group were allowed to recover at 21:79% O_2:N_2 for 3 h. The other 6 animals of group (A,C and E) were sacrificed for another study.

was calculated and compared for group A and C.

Locomotor activity was assessed per time point using the same thermal images as were used for the calculation of superficial temperature. An analytics program was written in LabVIEW (LabVIEW, National Instruments, Austin, TX). The thermographic camera images were converted to grayscale images and loaded into LabVIEW. Locomotor activity was calculated per animal per time point (−1 up to 9 h) on the basis of fluctuations in pixel intensity. A pixel was considered to reflect 'motion' when the grayscale intensity difference between direct temporally consecutive pixels exceeded

7 on a scale of 0 to 255. The intensity difference of at least 7 was based on the disappearance of background scatter present as intensity differences between 1 and 6. Values were expressed as the mean ± SEM amount of pixels with 'motion' per group per time point.

Statistical analysis

Statistical analyses were performed using MatLab 2013a (MathWorks, Natick, MA). Homogeneity of variance in each group was tested using the Bartlett's test. Based on equality of variances, either a one-way ANOVA or a Kruskal-Wallis test was performed, followed by a Tukey's range test or Dunn's test, respectively, to compare ordinal variables related to maximum superficial temperature and locomotor activity between groups. Tail temperature values were compared using an unpaired student's t-test. P-values less than 0.05 were considered significant. All values were presented as mean ± SEM, unless otherwise mentioned.

RESULTS

To test the hypothesis that exogenous H_2S-induced hypothermia emanates from hypoxia and not H_2S, we performed experiments in 48 female C57BL/6 mice using a similar approach as was employed by Blackstone et al. [Blackstone et al., 2005]. The experiments, which are outlined in Figure 2 and the Materials & Methods section of this paper, encompassed the following groups: (A) 80 ppm H_2S in 21% O_2 and 79% N_2 (H_2S in 21% O_2 group; N = 12 mice); (B) 80 ppm H_2S in 17% O_2 and 83% N_2 (H_2S in 17% O_2 group; N=6 mice); (C) 5% O_2 and 95% N_2 (5% O_2 group; N=12 mice); (D) 17% O_2 and 83% N_2 (17% O_2 group; N = 6 mice); and (E) 21% O_2 and 79% N_2 (normoxia group; N = 12 mice). The effects of exogenous H_2S and a hypoxic atmosphere on T_b at a T_a of ~21 °C were measured non-invasively with a thermographic camera and the locomotor activity of the animals was quantitated with dedicated motion analysis software.

As shown in Figure 3, hypothermia and reduction in locomotor activity only occurred in mice subjected to hypoxic conditions. 5% O_2-exposed animals immediately dropped their T_b to approximately 2 °C above the T_a (Figure 3B, P

< 0.0001) and reduced their locomotor activity to nearly nil compared to the H_2S in F_iO_2 21% and normoxia groups (Figure 3C, $P < 0.0001$) during the entire exposure period. The exogenous H_2S in 21% F_iO_2 group did not differ from the normoxia group during 6 h of 80 ppm H_2S gas exposure in neither superficial temperature nor locomotor activity. At 3 h of exposure, however, animals in the H_2S in 17% F_iO_2 group started to drop their T_b to approximately 4 °C above T_a, in contrast to F_iO_2 17%-exposed control animals (Figure 3B, $P < 0.0001$). Alleviation of the hypoxic conditions during the restoration phase resulted in complete reversal of the superficial temperature to baseline levels within 1 h in the F_iO_2 5% group, which is in agreement with previous reports [Blackstone et al., 2005; Volpato et al., 2008] (Figure 1). During the 3 h of restoration at normoxic atmosphere, the H_2S in F_iO_2 17%-exposed animals remained hypothermic and only restored T_b to the level of the F_iO_2 17% and 21% control groups at 9 h (Figure 3B, $P < 0.01$). Mice in the H_2S groups exhibited some discomfort during H_2S exposure, as evidenced by the cringed posture, which occasionally concurred with vigorous locomotion.

Peripheral vasodilation is one of the cooling mechanisms that is autonomically regulated in response to a mismatch between the T_b and the internal thermostat (i.e., T_b > thermoneutral zone) [Steiner and Branco, 2002; Nakamura, 2011; Kanosue et al., 1994]. Peripheral vasodilation is integral to anapyrexia [Steiner and Branco, 2002], which enables cooling. The cooling process is in turn facilitated by the blockade of thermogenic effectors and the enabling of peripheral vasodilation [Kanosue et al., 1994; Owens et al., 2002; Rudaya et al., 2012]. Therefore, the extent of peripheral vasodilation was determined by measuring the change in tail temperature at baseline and at approximately 4 min after initiation of H_2S - or hypoxia exposure.

The tail of 5% O_2-exposed animals warmed up right after the start of exposure (+2.1 ± 0.5 °C, N = 3, $P < 0.05$ versus the H_2S group, unpaired student's t-test), while the tail of H_2S in 21% O_2-exposed animals (−1.3 ± 1.1 °C, N = 3) and normoxia-exposed animals (+0.1 °C, N = 1) did not exhibit changes in temperature ($P > 0.05$, unpaired student's t-test) (Figure 4). These results provide compelling evidence for the induction of peripheral vasodilation by hypoxia but not exogenous H_2S, and hence for hypoxia-mediated anapyrexic signaling. The absence of a vasodilatory response in the exogenous H_2S group

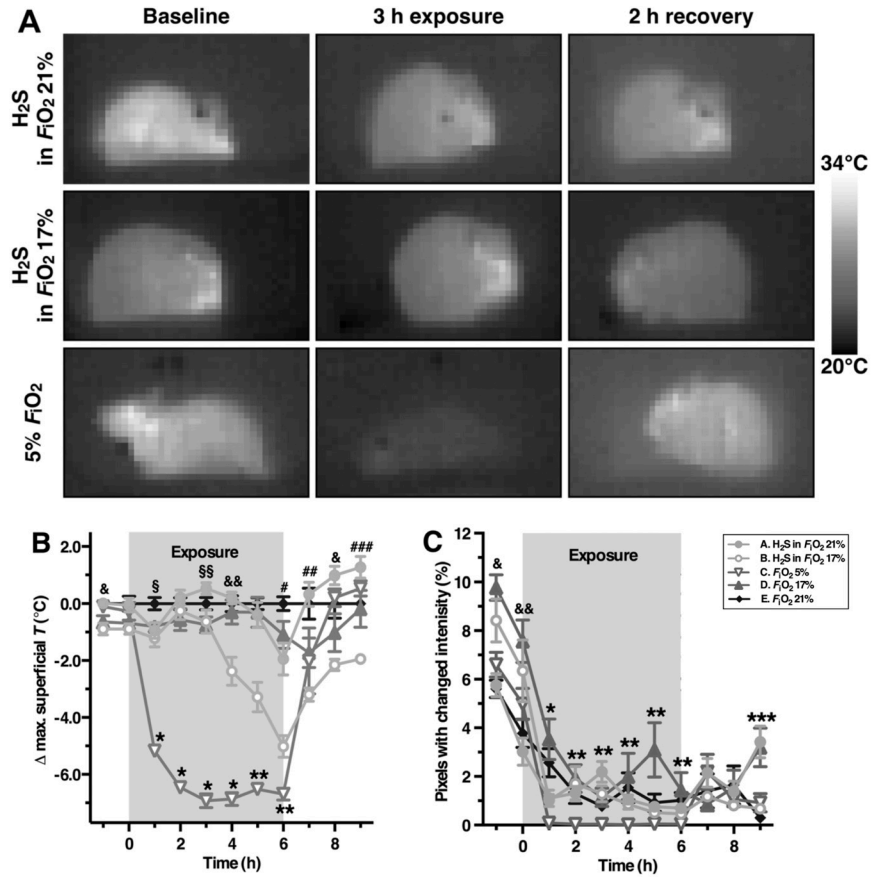

Figure 3. Temperature and locomotor effects of H_2S compared to hypoxia. (A) Thermal images of H_2S-exposed mice in 21% O_2 (top row), in 17% O_2 (middle row), and hypoxia-subjected mice (bottom row) before (baseline), during, and after (recovery) exposure. The color of the animals reflects their temperature (scale bar). (B) The difference between the maximum superficial temperature (Δ max. superficial T) of the hypoxia (F_iO_2 5% and 17%) and H_2S (F_iO_2 17% and 21%) groups versus the normoxia group (F_iO_2 21%) was plotted as a function of time before exposure (up to 0 h), during exposure (0–6 h), and after exposure (6–9 h). (C) Mouse mean locomotor activity per time point per group plotted as a function of time before exposure (up to 0 h), during exposure (0–6 h), and after exposure (6–9 h). Locomotor activity was derived from temporal changes in pixel grayscale intensity as described in the online supplemental information. In (B) and (C) the means ± SEM are plotted for N=12/group (group A, C and E) or N=6/group (group B and D) up to 6 h, and for N=6/group from 6 to 9 h. Statistical significant intergroup differences: (A) * C vs. all, P<0.0001; ** C vs. A, D, E, P<0.0001; & B vs. A, C, E, p<0.01; && B vs. all, P<0.0001; § E vs. A, B, P<0.0001; §§ D vs. A, P<0.0001; # B vs. E, P<0.001; ## B vs. A, P<0.05; ### B vs. A, C, P<0.01. (B) * C vs. A, D, E, P<0.0001; **C vs. all, P<0.0001; *** E vs. A, D, P<0.01; & D vs. A, C, E and B vs. A, E, P<0.0001; && D vs. E, A, and B vs. A, P<0.001.

is in agreement with the surface temperature data, which encompassed an absence of hypothermia (Figure 3).

DISCUSSION

Based on the experimental evidence, namely T_b, tail temperature, and locomotion, it can be concluded that inhalation of H_2S gas at 80 ppm in a native atmosphere of 21% O_2 and 79% N_2 does not induce hypothermia in mice, which contradicts what has been reported previously [Blackstone et al., 2005; Volpato et al., 2008]. Hypoxia, on the other hand, is a very potent inducer of hypothermia that, given the peripheral vasodilation observed in the tail vasculature, may comprise part of an anapyrexic response [Gordon and Fogelson, 1991; Steiner and Branco, 2002]. The subclinical thermal effects of mild hypoxia, however, are potentiated by combined 80 ppm H_2S gas exposure.

One consistent finding in mouse studies on the pharmacological induction of hypothermia is that the animal's T_b or surface temperature approximates the T_a and subsequently enters a plateau phase that is sustained in the vicinity of T_a. Regardless of what actually caused the hypothermic signaling in the experiments by Blackstone et al. [Blackstone et al., 2005] and Volpato et al. [Volpato et al., 2008], the T_b was in all instances downmodulated to a depth at which the T_b was more or less in equilibrium with the T_a, irrespective of the magnitude of the T_a (i.e., 13 °C, 27 °C, or 35 °C). The same pattern was observed in our experiments (T_a = 21 °C), suggesting that the hypothermia may have been mediated via a common mechanism. Moreover, this decline-plateau pattern suggests that the cooling process is passive once the thermogenic effectors have been shut off. The cooling is halted upon reaching a thermodynamic equilibrium where $T_b = T_a$, i.e., a point at which the organism is not equipped to cool further. Unlike under normophysiological circumstances, where T_b is tightly regulated via engagement of cooling effectors or thermogenic effectors [Nakamura, 2011; Clapham, 2012], the hypothermic state seems to sustain itself through passive heat transfer only.

The main differences between the results of Blackstone et al., Volpato et al., and our results are the rate of cooling and subsequently the time required

to reach the plateau phase ($T_b = T_a$). The cooling rate was approximately 1.3 °C/h and 4.0 °C/h in the experiments of Volpato et al. and Blackstone et al., respectively, whereas in our experiments the cooling rate was approximately 5.3 °C/h. The convergence of T_b with T_a required ~6 h in the study of Blackstone

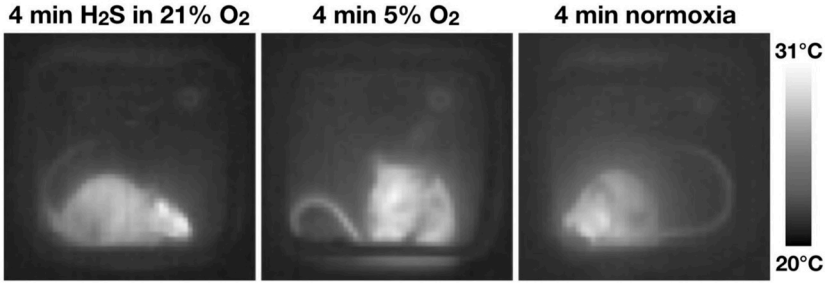

Figure 4. Tail temperatures in H_2S and hypoxia-exposed mice. Representative thermographic camera images of mice approximately 4 min after initiation of exposure to H_2S in 21% O_2 (left), 5% O_2 (middle), or normoxia (right). Yellow indicates a high surface temperature (31 °C), blue indicates a low surface temperature (20 °C) as indicated by the scale bar. Note the difference in tail temperature (on the basis of yellow intensity) of the hypoxic animal versus the H_2S gas-exposed and normoxic animals. The warmer tail in the hypoxic mouse is indicative of peripheral vasodilation; a cooling effector that is induced by anapyrexia.

et al., ~4 h in the study of Volpato et al., and 2 h in our study (Figure 3). The same animal species with similar animal weights were employed in all studies. Hence, it is unlikely that these discrepancies arose from differences related to physical laws such as Galilei's square-cube law, the implication of which is that animals with a large body surface:mass ratio (i.e., small animals) cool faster than animals with a small body surface:mass ratio (i.e., large animals) [Heldmaier et al., 2004]. The discrepancies in cooling rate also did not emanate from differences in metabolism in accordance with Kleiber's law, which states that small animals exhibit a relatively higher metabolic rate to maintain euthermia compared to larger animals [Heldmaier et al., 2004; Kleiber, 1947].

In light of the finding that exogenous H_2S is not an inducer of hypothermia, the question that remains to be answered is "why did Blackstone et al. and Volpato et al. observe hypothermia in H_2S-exposed mice?" Volpato et al. was able to reproduce the hypothermic effects of 80 ppm H_2S of Blackstone et al. Consequently, we do not question the methodology and validity of their results. In our opinion, the answer lies in the hypoxic conditions that

were induced by the combination of subatmospheric F_iO_2 and the various mild forms of exogenous H_2S-induced hypoxia. The 3.5% lower F_iO_2 versus native atmospheric F_iO_2 (17.5% versus 21%, respectively) is, in itself, not sufficient to trigger anapyrexia in mice, unless such mild hypoxic conditions are exacerbated by exogenous H_2S. In line with our results obtained in the 17% F_iO_2 groups, the exacerbation likely occurred in the experiments by Blackstone et al. and Volpato et al. for four possible reasons. First, as explained in the Introduction section, H_2S can induce histotoxic hypoxia by inhibiting cytochrome c oxidase and corollary ATP production, resulting in reduced metabolic supply (energy). Consequently, the organism is forced to adapt its metabolic demand to survive by means of e.g., hypothermia (Arrhenius' law). Secondly, H_2S can limit the binding of O_2 to hemoglobin's O_2 binding sites [Ríos-González et al., 2014], thereby causing O_2 affinity hypoxia [Daniels et al., 2010]. Thirdly, H_2S reduces cardiac output through its deregulatory and negative chronotropic effects on cardiac rhythm [Volpato et al., 2008; Stein et al., 2012], which leads to circulatory hypoxia [Myers et al, 2008]. Fourthly, H_2S is pulmonotoxic [Lopez et al., 1987; Prior et al., 1988; Stein et al., 2012] and may impair pulmonary O_2/CO_2 exchange and the extent of O_2 saturation, which in turn may aggravate the circulatory hypoxia caused by the cardiovascular effects. In addition, based on ex vivo experiments, H_2S seems to play an essential role in hypoxic pulmonary vasoconstriction [Madden et al., 2012]. Therefore, administration of exogenous H_2S to the lungs may further compromise pulmonary blood flow during hypoxic conditions, which can augment hypoxemic hypoxia. Accordingly, all these forms of H_2S-mediated hypoxia may add to the mild hypoxia caused by subatmospheric F_iO_2 levels and culminate in a hypoxic state that is considerable enough to trigger anapyrexia. As addressed in Dirkes et al. [Dirkes et al., 2015], circulatory hypoxia is sensed through carotid bodies located in the carotid artery [Milson and Burleson, 2007; Prabhakar and Semenza, 2012] that, under non-hypometabolism-inducing, hypoxic conditions, relay arterial O_2 tension (P_aO_2)-related information to the brain. The brain subsequently (hyper)activates certain physiological functions to remediate the hypoxia [Marshall, 1994], which include panting [Izumizaki et al., 2004; Peng et al., 2010; Li et al., 2010; Teppema and Dahan, 2010; Sugimura et al., 2010] and

tachycardia [Sugimura et al., 2010; Lifson et al., 1977]. How this is blocked during the induction of anapyrexia is currently unclear.

Endogenous H_2S as well as intracerebrally administered exogenous H_2S analogues inhibit the ventilatory and thermal response to hypoxia in the hypothalamus and brain stem. Contrastingly, microinjection of Na_2S (H_2S precursor) in the anteroventral preoptic hypothalamus of rats potentiates hypothermic signaling by hypoxia, but does not alter T_b under normoxic conditions [Kwiatkoski et al., 2012]. Microinjection of the endogenous H_2S production inhibitor amino-oxyacetate in the sympathetic excitatory rostral ventrolateral medulla of rats attenuates hypoxia-induced hypothermia [Donatti et al., 2014]. As H_2S passes the blood-brain barrier freely, central effects of inhaled H_2S could have contributed to hypoxia-induced anapyrexia via the hypothalamus or brain stem [Beauchamp et al., 1984], albeit an unequivocal mechanistic explanation remains warranted in light of the contrasting results.

In the experiments of Blackstone et al. and Volpato et al., T_b was determined by telemetry devices that record the core temperature (i.e., intra-abdominal temperature). In our experiments, the superficial temperature was determined. We believe that this approach is valid for the purpose of this study inasmuch as we were interested in temperature trends as a function of exposure time and gas composition, and not the real T_b per se. Since all groups were thermographically analyzed in the same manner, the resulting data yield credence to our conclusions. Moreover, the use of thermographic imaging has some benefits over intra-abdominal temperature determination, such as the determination of thermoregulatory vasoactivity by tail temperature measurement (Figure 4).

Although this paper focused on the hypometabolic properties of H_2S gas, several animal studies on the effects of liquid H_2S analogues NaHS and Na_2S have been published. After inhalation, H_2S gas diffuses freely across the alveolar membrane and enters the blood as predominantly HS^- and H_2S [Beauchamp et al., 1984]. Accordingly, intravenous administration of solubilized H_2S precursors/analogues is believed to follow the same pharmacodynamics as administration through inhalation, only without the detrimental effects on local pulmonary physiology and toxicity. The

hypothermic effects of NaHS and Na_2S in small as well as in large animals have been reviewed before [Asfar et al., 2014]. Continuous administration of NaHS is assumed to induce hypothermia in anesthetized rats, although these studies lack essential control groups [Aslami et al., 2010; Aslami et al., 2013]. The evidence considering the hypothermic and hypometabolic effects of NaHS in large animals has been conflicting: in a pig study a small hypothermic effect was observed following 8 continuous hours of NaHS administration [Simon et al., 2008], whereas in several other studies in pigs [Dirkes et al., 2015; Drabek et al., 2011] and sheep [Haouzi et al., 2008] such hypothermic effects were not reproducible. The differences between the effects of H_2S in small and large animals have been contemplated by Dirkes et al. and are explained by the inability of large animals to lose heat sufficiently due to the low body surface:mass ratio [Dirkes et al., 2015].

In this paper, the tail temperature was used as a measure of central activation of peripheral cooling mechanisms (i.e., peripheral vasodilation), as has been used before in the determination of thermoregulatory peripheral vasoactivity in pyrexic mice [Rudaya et al., 2005]. However, as reviewed by Lim et al., H_2S has biphasic effects on the vascular tone: at low concentrations H_2S induces vasoconstriction and at higher doses vasodilation is induced, as evidenced in mouse and rat aortic tissue [Kubo et al., 2007; Ali et al., 2006; Lim et al., 2008]. Consequently, the absence of thermoregulatory vasodilation and a consequent increase in the tail temperature of three animals (Figure 4) could also be a direct vasoconstrictive effect of low-dose H_2S. Nevertheless, H_2S-induced vasoconstriction is unlikely to be responsible for the absence of H_2S-induced hypothermia in our experiments. A 'masked' thermoregulatory vasodilative response would be accompanied by deactivation of brown adipose tissue (BAT) and shivering thermogenesis (i.e., major source of heat in mice at a T_a of 21 °C) [Heldmaier et al., 2004; Clapham et al., 2012]. Subsequently, the cessation of thermogenesis would be reflected in the T_b/superficial temperature of H_2S-exposed animals, which was not observed (Figure 3).

Concluding remarks

In conclusion, exogenous H_2S is not a hypometabolism-inducing agent. The

hypometabolism induced in mice that were subjected to exogenous H_2S was caused by hypoxia. At subatmospheric F_iO_2 levels, exogenous H_2S exacerbates the hypoxic conditions to such a degree that anapyrexia and hypothermia are triggered. Accordingly, exogenous H_2S is a hypometabolic adjuvant rather than a hypometabolism-inducing agent.

PART III
SINGLE ORGAN APPLICATION

Chapter 5
Preparing the liver for artificial control of hepatic physiology

Adapted from

I.C.J.H. Post, M.C. Dirkes, M. Heger, J. Verheij, K.M. de Bruin,
D. de Korte, R.J. Bennink, T.M. van Gulik.
Liver Transpl 2013 Aug; 19(8): 843-51

ABSTRACT

Donor graft washout can be impaired by colloids in organ preservation solutions that increase the viscosity and agglutinative propensity of red blood cells (RBCs) and potentially decrease organ function. The colloid-induced agglutinative effects on RBCs and RBC retention after liver washout with Ringer's lactate (RL), histidine tryptophan ketoglutarate solution, University of Wisconsin solution, and Polysol were determined as a function of the washout pressure (15 or 100 mm Hg) and temperature (4 or 37°C) in a rat liver washout model with ^{99m}Tc-pertechnetate–labeled RBCs. Colloids (polyethylene glycol in Polysol and hydroxyethyl starch in University of Wisconsin) induced RBC agglutination, regardless of the solution's composition. RL was associated with the lowest degree of ^{99m}Tc-pertechnetate–labeled RBC retention after simultaneous arterial and portal washout at 37°C and 100 mm Hg. RL washout was also associated with the shortest washout time. A single portal washout with any of the solutions did not result in differences in the degree of RBC retention, regardless of the temperature or pressure. In conclusion, no differences were found in portal washout efficacy between colloidal solutions, histidine tryptophan ketoglutarate, and RL. Simultaneous arterial and portal washout with RL at 37°C and 100 mm Hg resulted in the least RBC retention and the shortest washout time.

INTRODUCTION

The procurement of a liver graft is preceded by organ washout with a preservation solution (perfusate) under hypothermic (4°C) conditions to prepare the organ for storage [Pegg et al., 1982]. The completeness of the washout has been proposed to be an important determinant for liver graft function [‘t Hart et al., 2004; Tojimbara et al., 1997]. During washout, perfusates prevent acidosis by providing a high buffer capacity, and they counteract cell swelling or hypo-osmotic extravasation of fluids because of added impermeants and/or colloids. Histidine tryptophan ketoglutarate solution contains mannitol as an impermeant.

Although mannitol may not strictly act as an impermeant in the liver [Cereijo-Santalo, 1972; Klöppel et al., 1994], it yields similar or improved washout results in comparison with hydroxyethyl starch–containing University of Wisconsin (UW+) solution [Guerrara and Karim, 2008; Feng et al., 2007]. UW+ and polyethylene glycol–containing Polysol (PS+), which is an experimental perfusate, contain hydroxyethyl starch (HES) [Hessheimer et al., 2012] and polyethylene glycol (PEG) [Pegg et al., 1982], respectively, as colloids.

The addition of colloids to a perfusate increases the viscosity of the solution, which is exacerbated by the low temperatures at which a perfusate is used to cool an organ [Post et al., 2012]. In addition, colloids have a hyper-aggregatory effect on red blood cells (RBCs) that results in rouleaux formation [Zhao et al., 2011]. Consequently, the use of colloidal perfusates during a washout procedure may induce endothelial damage and lead to occlusion of the microvasculature and corollary no-reflow phenomena [Brodsky et al., 2002]. Furthermore, the washout procedure is regarded as an important part of the organ preservation protocol inasmuch as the primary goals of the initial washout are to clear the organ of blood and to reduce its core temperature when hypothermic storage follows. Higher washout pressures (100 mm Hg) or normothermic temperatures (37°C) might prevent microcirculatory RBC entrapment and ensure proper distribution of the perfusate through the liver [‘t Hart et al., 2004; Tojimbara et al., 1996; Bishop et al., 2001; Yamauchi et al., 2000; Ong et al., 2011; Pirenne et al., 2001]. However, high pressures are

associated with increased shear stress, which can lead to endothelial lining perturbations or even affect cellular energy metabolism [Tisone et al., 1997; Tokunaga et al., 1988]. These potential complications during washout have been successfully circumvented by the application of Ringer's lactate (RL) as a washout and short-term preservation solution [Tan et al., 2007; Kawashima et al., 1999].

Because the aforementioned effects of the perfusate temperature and colloid-induced RBC agglutination during liver washout had not been clarified, this study was designed to quantify RBC retention after liver washout at different temperatures and pressures. First, the agglutination of RBCs was assessed microscopically in perfusates in the presence or absence of colloids. Second, a rat liver washout model was employed to determine the washout efficacy of several perfusates through scintigraphic analysis of intrahepatically retained, ^{99m}Tc-labeled RBCs after hypothermic or normothermic washout at a low or high washout pressure. This study revealed that the extent of intrahepatic RBC retention was not affected by the applied pressure, solution, colloidal content or type, temperature, or washout time during liver washout via the portal vein. Simultaneous arterial and portal washout with RL at 37°C and 100 mm Hg resulted in the least RBC retention and the shortest washout time.

MATERIALS AND METHODS

Perfusates

Two types of perfusates were used: colloid-containing perfusates and colloid-free perfusates. The colloid-free perfusates included RL (Baxter, Deerfield, IL); polyethylene glycol-free histidine tryptophan ketoglutarate (HTK-; Dr F Köhller-Chemie, Bensheim, Germany); and a custom-produced batch of polyethylene glycol-free Polysol (PS-; Organoflush, Amsterdam, the Netherlands), which is an experimental perfusate. The colloid-containing perfusates were polyethylene glycol-containing histidine tryptophan ketoglutarate (HTK+) enriched with PEG-35 (20 g/L; Sigma-Aldrich), UW+ solution (Fresenius Hemocare, Emmer -Compascuum, the Netherlands), and standard PS+ (containing PEG-35).

Assessment of RBC Agglutination With Brightfield Microscopy

The RBCs that were used were prepared from fresh platelet- and leukocyte-poor human RBC concentrates (packed cells; Sanquin, Amsterdam, the Netherlands) suspended in saline-adenine-glucose-mannitol medium in conformity with the blood bank's donor protocol. The packed cells contained a mix of RBCs from at least 2 donors. RBCs were added to solutions approximately 5 minutes before imaging. A 2-µL RBC suspension was prepared 5 minutes before imaging in RL, HTK-, PS+, or UW+ with a hematocrit of 20% (Advia 2120, Siemens, Munich, Germany) and transferred to a microscope slide for imaging. Additionally, RBCs were added to HTK+ and PS- to demonstrate colloid-dependent RBC agglutination. The preparations were visualized through a 100x oil immersion objective on a Leica DMBL microscope (Leica Microsystems, Wetzlar, Germany) equipped with a Leica DC200 charged coupled device camera that was controlled with QWin software (Leica Microsystems).

In Vivo Radioactive Labeling of RBCs

The institute's animal ethics committee approved all animal experiments (BEX102507), and animals were treated in accordance with the Guide for the Care and Use of Laboratory Animals (National Institutes of Health). Male Wistar rats weighing 254 ± 627 g were anesthetized with an intraperitoneal injection (0.27 mL/100 g of body weight) of Hypnorm (10 mg/mL fluanisone and 0.515 mg/mL fentanyl citrate; Veta-Pharma, Leeds, United Kingdom), Dormicum (5 mg/ mL; Actavis Group, Zug, Switzerland), and water in a 1:1:2 ratio. RBCs were labeled in vivo with the ^{99m}Tc-pertechnetate procedure adapted for small laboratory animals [Hascalik et al., 2008]. Briefly, 50 µg of freshly prepared pyrophosphate (PYP; Technescan, Covidien, Petten, the Netherlands) in a 0.2-mL saline solution was injected intravenously into the tail vein, and this was followed by 40 MBq of ^{99m}Tc-pertechnetate (Ultra-Technekow, Covidien) in a 0.2-mL saline solution after 30 minutes.

Liver Washout

After 10 minutes of ^{99m}Tc-pertechnetate circulation, washout was performed according to a previously described procedure [Bessems et al., 2005]. After

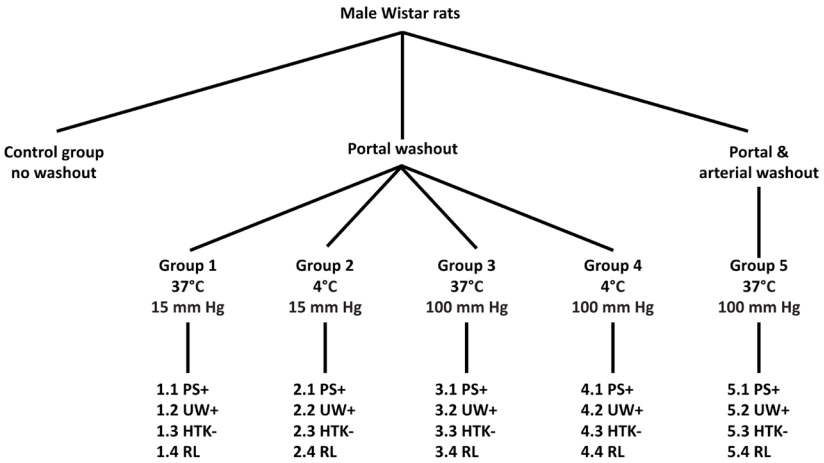

Figure 1. Diagram of the experimental setup and group sizes. n=6 per solution.

mobilization of the liver and intestines, a blood sample was obtained from the inferior caval vein (radioactive RBC reference) and weighed on a precision scale (AB204, Mettler Toledo, Greifensee, Switzerland). Next, heparin (1000 U/animal; Leo Pharma, Breda, the Netherlands) was administered via the tail vein. After 5 minutes, the aorta was ligated cranially of the celiac trunk and at the level of the iliacal bifurcation, and cannulated with a 4-Fr enteral feeding tube (Vygon, Ecouen, France) in case of arterial washout. All groups underwent a portal washout procedure for which the portal vein was ligated proximally, dissected, and cannulated with a 6-Fr enteral feeding tube (Vygon). The inferior caval vein was ligated just above the renal vein and thereafter cut at the level of the iliac bifurcation and suprahepatically to prevent congestion. Subsequently, the liver was washed out with 50 mL of PS+, UW+, HTK-, or RL (n=6 per solution) at 4 or 37°C (n=6 per temperature) and at a pressure of 15 (standard) or 100 mm Hg (n=6 per pressure) [‘t Hart et al., 2004] through aortic and portal catheters while washout times were recorded with a stopwatch (Figure 1). The washout pressure was calibrated before each experiment with a pressure transducer used in intravenous lines (Edward Life- sciences, Irvine, CA) that was positioned proximally to the portal vein and/or hepatic artery. After the 50-mL washout, the liver was removed and weighed. In the control group (no washout), the suprahepatic and

infrahepatic caval vein, portal vein, and hepatic artery were simultaneously ligated, which trapped all the blood in the liver before removal. Rats were sacrificed by heart dissection during the wash-out or excision of the liver.

RBC Retention and ^{99m}Tc-Pertechnetate Distribution After Washout

Analysis of radioactive RBCs in blood samples and livers was performed with a γ-counter (Auto-Gamma 5530, Packard Instruments, Downers Grove, IL). The intrahepatic blood content was calculated as the weight percentage of radioactive RBCs in the liver by the total liver γ-count divided by the liver weight and corrected for the reference blood sample ((total liver γ-count/liver weight)/(blood γ-count/blood weight)x100%). The amount of residual radioactive RBCs was expressed as a percentage difference from control livers.

On the basis of the high residual RBC retention after portal vein washout (discussed later), the RBC labeling dynamics of ^{99m}Tc-pertechnetate/PYP were verified with a dynamic γ-scan in four rats. Two rats underwent standard in vivo RBC labeling (as discussed previously), whereas PYP was omitted for the other two rats and was replaced with a physiological saline solution that does not interact with ^{99m}Tc-pertechnetate [Dewanjee, 1974]. Images were acquired on a dual-head γ-camera (E.cam with 180 frames/5 seconds at 128 x 128 pixel resolution, Siemens, Erlangen, Germany) to study the distribution and excretion of ^{99m}Tc-pertechnetate and ^{99m}Tc-pertechnetate/PYP. Furthermore, a pinhole collimator (3-mm insert, 128 x 128 pixel resolution)–equipped γ-camera (ADAC ARC 3000, Philips, Amsterdam, the Netherlands) was used to magnify the duodenal region to assess the possibility of radioactive duodenal excretion via the biliary system in the absence of a gallbladder in rats. The scintigraphic images were processed with Hermes image software (Hermes Medical Solutions, Stockholm, Sweden).

Histology

Livers after washout were sectioned into 3 parts and placed in a 10% (vol/vol) buffered formalin solution at 4°C for 5 days to allow radioactive decay. Subsequently, the parts were embedded in paraffin, cut into 5-µm sections, deparaffinized, and stained with hematoxylin and eosin. An experienced liver

pathologist who was blinded to the experimental procedure assessed the liver sections for washout-induced injury according to the scoring method presented in Post et al. [Post et al., 2013]. Images were acquired on an Olympus BX41 microscope equipped with a UC30 charged coupled device camera (Olympus, Tokyo, Japan).

Statistical Analysis

Data were processed in GraphPad (GraphPad Software, La Jolla, CA), and arterial liver washout times were analyzed with the Kruskal-Wallis test with Dunn's post hoc test. All other liver washout and histological scoring data were tested for intragroup and intergroup differences via a 2-way analysis of variance with the Bonferroni post hoc test. Results are expressed as means and standard deviations, and a P-value < 0.05 was considered statistically significant.

RESULTS

Agglutination of RBCs

Brightfield microscopy revealed extensive agglutination of RBCs suspended in colloid-containing perfusates; this was evidenced by rouleaux formation and morphological alterations of cells in HTK+, PS+, and UW+ (Figure 2C, D, F). RBC agglutination was not observed in solutions not containing colloids; as shown for RL, HTK-, and PS- (Figure 2A, B, E).

HTK+ and PS- confirmed that the RBC agglutination was colloid-induced and not attributable to other perfusate constituents. Furthermore, impermeant- and colloid-free RL led to extensive RBC blebbing (shedding of bullae from the cell surface), as shown in Figure 2A.

Liver Washout

When RBC retention was averaged over all perfusate groups, portal washout was found to have reduced the mean RBC retention to 44.5% ± 1.7% ($P < 0.05$) of the liver weight (8.1 ± 2.5 g), whereas the retention in the control group (no washout) was 91.2% ± 17.5%. In contrast to the controls, simultaneous arterial and portal washout at 37°C and 100 mm Hg further reduced the

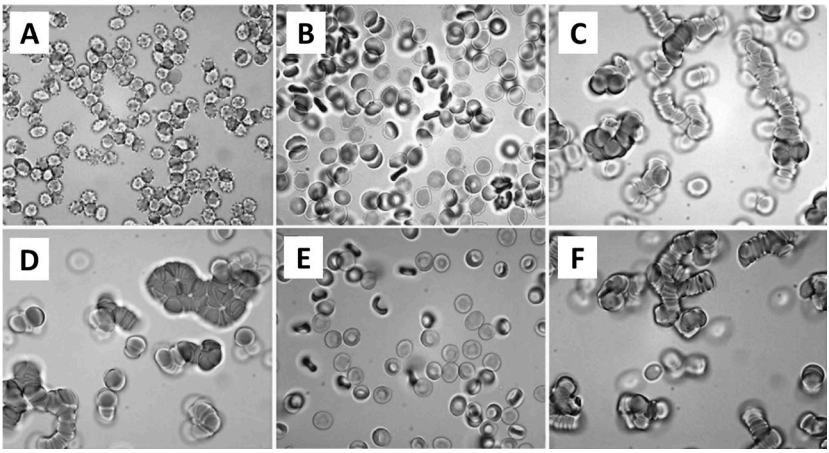

Figure 2. Brightfield micrographs of RBC-containing suspensions diluted with different solutions to a hematocrit of 20%: (A) RL; illustrating blebbing of RBCs without agglutinative effects, (B) HTK-; illustrating no agglutination, (C) HTK+; illustrating extensive rouleaux formation, (D) PS+; illustrating extensive rouleaux formation, (E) PS-; illustrating no agglutinative effects, and (F) UW+; illustrating agglutinative effects microscopically comparable to those shown in panels C and D.

retention (averaged over all perfusates) to 29.3% ± 7.9% ($P < 0.001$; Figure 3A).

A perfusate-dependent reduction in RBC retention was achieved when RL was used for simultaneous arterial and portal washout at 37°C and 100 mm Hg (18.7% ± 9.4%) versus portal washout with RL at 4°C and 15 mm Hg (45.6% ± 5.1%, $P < 0.01$) and at 4°C and 100 mm Hg (50.5% ± 24.1%, $P < 0.001$). Also, portal washout with RL at 37°C and 15 mm Hg resulted in higher RBC retention (45.7% ± 30.5%, $P < 0.01$) than simultaneous arterial and portal wash-out with RL at 37°C and 100 mm Hg. However, simultaneous arterial and portal washout with RL at 37°C and 100 mm Hg was significantly different only from simultaneous arterial and portal washout with UW+ (37.4% ± 6.6%, $P < 0.01$).

A significant portal washout time reduction ($P < 0.001$) was achieved through washout with UW+ and PS+ at 4°C and 100 mm Hg (18.3 ± 8.0 and 15.1 ± 1.8 seconds, respectively) versus washout at 4°C and 15 mm Hg (84.4 ± 23.8 and 71.4 ± 35.3 seconds, respectively), as shown in Figure 3B. Also, portal washout with HTK-, UW+, and PS+ at 37°C and 100 mm Hg significantly reduced washout times (7.0 ± 2.0, 13.3 ± 2.7, and 22.6 ± 28.3 seconds,

respectively) in comparison with washout at 37°C and 15 mm Hg (49.7 ± 38.2, 106.0 ± 20.2, and 79.3 ± 6.5 seconds, respectively; P < 0.001). The influence of pressure instead of temperature on the washout time was evidenced by the significant reduction (P < 0.001) in the washout times at 4°C and 100 mm Hg with HTK-, UW+, and PS+ (10.5 ± 8.1, 18.3 ± 8.0, and 15.1 ± 1.8 seconds, respectively) versus the washout times at 37°C and 15 mm Hg. The arterial washout time was reduced with HTK- (29.7 ± 3.8 seconds, P < 0.05) and RL (21.6 ± 7.7 seconds, P < 0.001) at 37°C and 100 mm Hg versus UW+ at 37°C and 100 mm Hg (96.3 ± 7.2 seconds).

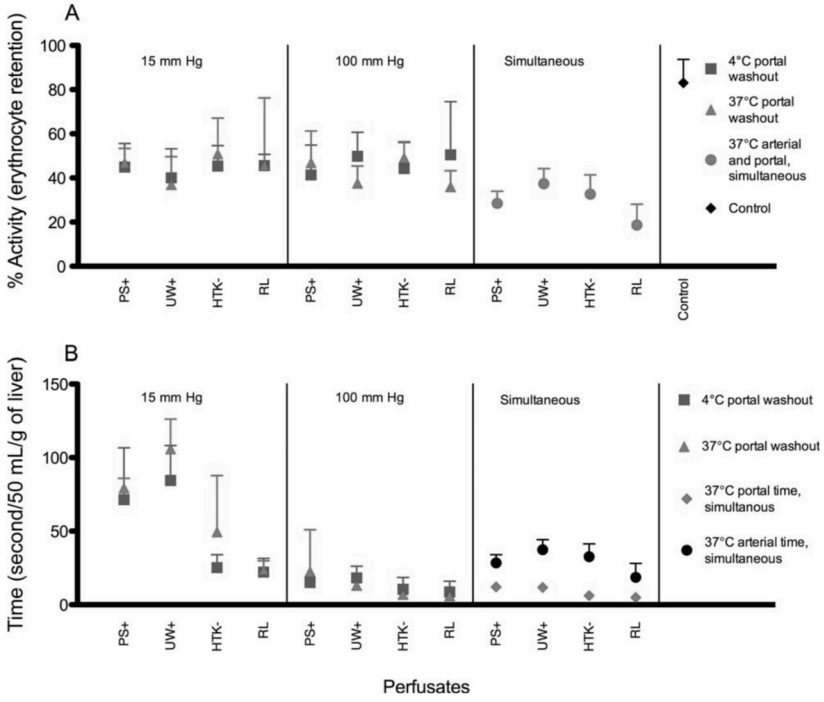

Figure 3. (A) Residual ^{99m}Tc-pertechnetate–labeled RBC content in the liver categorized by the washout pressure group. The 4°C group is shown in blue, the 37°C group is shown in red, and the control group (no washout) is shown in black. Simultaneous arterial and portal washout with RL at 37°C and 100 mm Hg showed significantly less retention than the other washout modalities (P<0.001). (B) Times needed for 50-mL washout via the portal vein are depicted in blue (4°C) and red (37°C), with black used for the arterial washout time of simultaneous arterial and portal washout at 37°C and 100 mm Hg. The use of noncolloidal solutions or the application of a washout pressure of 100 mm Hg significantly reduced the washout times (P < 0.001).

^{99m}Tc-Pertechnetate Distribution in Rats

Intravenously injected PYP, bound to the β-chain of hemoglobin, chemically reduces intracellular pertechnetate and causes ^{99m}Tc to become trapped in RBCs after intravenous administration. Renal accumulation of radioactivity and subsequent excretion into the bladder were seen in rats that received PYP and ^{99m}Tc-pertechnetate (Figure 4A,C). The thyroid and salivary glands could be distinguished with low-level radioactivity because of the small fraction of ^{99m}Tc-pertechnetate unbound to PYP. In rats receiving ^{99m}Tc-pertechnetate without PYP, the accumulation of ^{99m}Tc-pertechnetate in the thyroid and salivary glands was slightly higher than that in PYP-receiving rats, and excretion was predominantly visualized in the gastric mucous membrane in the absence of renal excretion (Figure 4B,D). With intrahepatic RBC retention after arterial and portal washout with RL at 37°C and 100 mm Hg, questions arose about whether the RBCs were hepatically cleared. Low-level radioactive biliary excretion into the duodenal loop was observed after approximately 20 minutes of circulation of ^{99m}Tc-per-technetate/PYP, and this potentially accounted for or contributed to the residual radioactivity (18.7%).

Histology

A histological assessment of the livers did not show differences between the washout groups or perfusates. Furthermore, injury scores were very low with a mean of 6.5 ± 0.5 out of a 40-point maximum score. The obtained histological scores were 6.3 ± 1.1 for 37°C and 15 mm Hg, 6.5 ± 0.2 for 37°C and 100 mm Hg, 6.6 ± 0.8 for 4°C and 15 mm Hg, 6.6 ± 0.6 for 4°C and 100 mm Hg, and 6.6 ± 0.6 for combined washout.

DISCUSSION

This study has shown that PEG and HES cause agglutination of RBCs, regardless of the preservation solution used, whereas simultaneous arterial and portal washout with RL at 37°C and 100 mm Hg significantly reduces RBC retention and washout times. In light of this colloid-induced RBC agglutination, the need for colloids in washout solutions has been questioned [Bessems et al., 2006; Mosbah et al., 2006]. Moreover, liver washout with solely RL has been

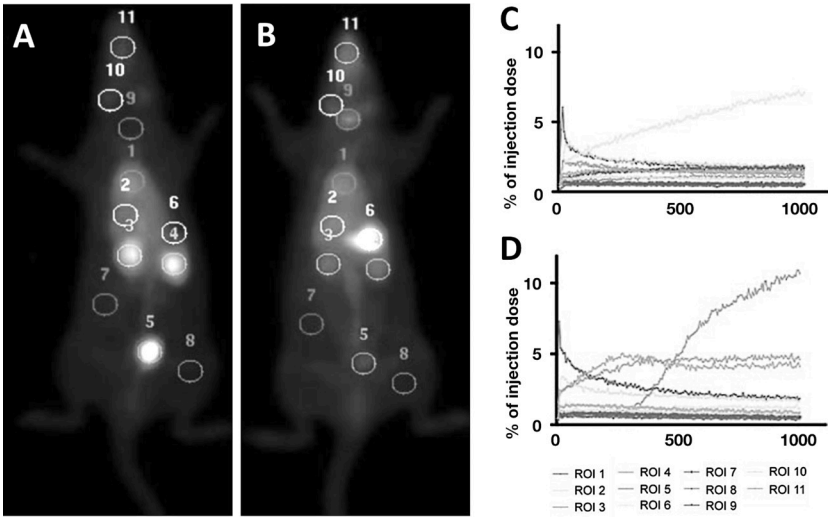

Figure 4. Biodistribution of ^{99m}Tc-pertechnetate in rats. (A) In the presence of PYP, ^{99m}Tc-pertechnetate/PYP was excreted via the urinary tract, whereas (B) in the absence of PYP, ^{99m}Tc-pertechnetate was taken up by the salivary and thyroid glands as well as the gastric mucosa. (C,D) The percentages of the administered radioactive dose that accumulated or excreted over time per ROI are depicted for conditions A and B, respectively. The ROIs were located over (1) the heart, (2) liver, (3) right kidney, (4) left kidney, (5) urinary bladder, (6) stomach, (7) abdominal background, (8) peripheral background, (9) thyroid gland, (10) parotid gland, and (11) submandibular gland.

shown to yield good functional results, even though RL is not suitable for preservation that encompasses prolonged storage [Kawashima et al., 1999; Dinant et al., 2009]. Our study has confirmed that RL is best at reducing RBC retention after simultaneous arterial and portal washout at 37°C and 100 mm Hg. Although RL is equally as viscous as HTK- at 37°C [Post et al,. 2012], HTK- did not lead to reduced RBC retention. Any potential coagulation-related side effects of RL during intravenous infusions, as reported previously [Levac et al., 2010], can be overcome by full heparinization.

Although perfusate compositions with respect to colloidal solutions versus non-colloidal solutions are the basis of the ongoing washout debate, the perfusates in this study did not differ in RBC retention after portal washout. Thus, colloid-induced agglutination does not appear to cause solution- and corollary viscosity-dependent changes in washout efficacy in rat livers as previously suggested [Zhao et al,. 2011]. The viscosities of the solutions applied here were determined previously by our group and were found to be equal with respect to HES- and PEG-containing solutions [Post

et al,. 2012]. However, colloid-lacking solutions were 2.5-fold less viscous, regardless of the temperature. Despite these differences in viscosity, no acute histological damage that might affect liver function was observed in livers washed out with colloid-containing solutions, despite the pressure of 100 mm Hg and the relatively high shear stresses imparted by these solutions [Morariu et al., 2003].

A potential difference in perfusates when they are employed under hypothermic and normothermic conditions is the pH. Higher temperatures will result in a slightly lower pH [Gómez et al., 2001; Bonventre and Cheung, 1985]. However, adjusting the pH with sodium hydroxide to correct for temperature-induced differences would alter the osmolarity and Na^{2+}/K^{+} ratio of perfusates [Bessems et al., 2005; Pegg et al., 1982]. Because an acidic milieu may exert a protective effect on parenchymal cells [Gómez et al., 2001; Bonventre and Cheung, 1985] and we did not anticipate significant effects from minor differences in the pH on liver washout outcomes, we chose not to alter the pH. This consideration was also made in light of the short exposure times during normothermic washout.

Interestingly, a remnant RBC fraction of 18.7% was present after simultaneous arterial and portal wash-out with RL at 37°C and 100 mm Hg, and this led to the question whether RBCs were cleared hepatically. Despite the comparable ^{99m}Tc-pertechnetate kinetics in rats and humans, more rapid elimination in the rat biliary system was found. Radioactive biliary excretion in the gallbladder or ileal loop after RBC labeling in humans is a rare finding, but it has been observed 24 hours after the administration of ^{99m}Tc-pertechnetate [Wood and Hennigan, 1984; Brill, 1985; Kotlyarov et al., 1988; Sato et al., 1988; Abello et al., 1991]. Although rats do not have a gallbladder, a pinhole collimator–equipped camera revealed radioactive bile being excreted into the duodenum after approximately 20 minutes in our experiments. With a mean bile flow of 0.6 µL/g of liver/minute in rats [Spiegel et al., 1998], accumulation in the intrahepatic biliary tract occurred before visualization by the pinhole camera; as a result, higher residual radioactivity could be found in the liver after washout.

The livers were washed out via the portal vein (as in the rat model described by ’t Hart [‘t Hart et al., 2004]) or simultaneously via the portal

vein and hepatic artery. If a colloidal solution were used for arterial washout during hypothermia, a time up to 10 times the time of portal vein washout would be needed. In that scenario, the times needed for portal washout and arterial washout would differ greatly, and this would result in a nonperfused portal vein for the extra duration of the arterial washout.

Prolonged washout times were predominantly observed with colloidal solutions, but in the case of portal washout only, they were shortened by the application of 100 mm Hg washout pressure. However, a high pressure is associated with increased shear stress and has previously been reported to induce endothelial damage [Tisone et al., 1997]. Endothelial damage, in turn, may lead to graft dysfunction as a result of per- fusion defects [Basile et al., 2011; Kliche et al, 2011]. Contrastingly, increased washout pressure and thus shear stress have been shown to result in improved early organ function [‘t Hart et al., 2004; Tisone et al., 1997; Tokunaga et al., 1988]. Increased shear stress with higher washout pressures actually reduced endothelial damage by 20% in kidney grafts in comparison with standard-pressure washout with colloidal and noncolloidal perfusates [‘t Hart et al., 2004]. In the latter study by ’t Hart, the presence of a colloid in the perfusate did result in small and large venule injury, whereas large venule injury was observed only in the noncolloidal group. The histological analysis performed in this study did not reveal any differences between the perfusate groups with respect to these types of vascular injury.

In the final analysis, RL at 37°C and 100 mm Hg appeared to be the most optimal washout solution in an organ retrieval setting [Bessems et al, 2006; Thuillier et al., 2011; Hughes et al., 1996; Gastaca et al., 2012; Treckmann et al., 2012]. Accordingly, this study evinced that simultaneous arterial and portal vein washout with RL at 37°C and 100 mm Hg resulted in the least RBC retention in the liver. These results suggest that our long-held concept of cold washout with an organ preservation solution as the first step in effective organ storage should be reconsidered. However, further combined analysis of improved washout, the contributory role of arterial washout [Gastaca et al., 2012], different solutions [Treckmann et al., 2012; Wilson et al., 2012], and subsequent graft outcomes after transplantation should first confirm these findings.

Chapter 6
Artificial control of hepatic physiology using machine perfusion

Adapted from

M.C. Dirkes, I.C.J.H. Post, M. Heger, T.M. van Gulik
Artif Organs 2013 Aug; 37(8)

ABSTRACT

Machine perfusion (MP) is a potential method to increase the donor pool for organ transplantation. However, MP systems for liver grafts remain difficult to use because of organ-specific demands. Our aim was to test a novel, portable MP system for hypothermic preservation of the liver. A portable, pressure-regulated, oxygenated MP system designed for kidney preservation was adapted to perfuse liver grafts via the portal vein (PV). Three porcine livers underwent 20 h of hypothermic perfusion using Belzer MP solution. The MP system was assessed for perfusate flow, temperature, venous pressure, and pO_2/pCO_2 during the preservation period. Biochemical and histological parameters were analyzed to determine post-preservation organ damage. Perfusate flow through the PV increased over time from 157 ± 25 mL/min at start to 177 ± 25 mL/min after 20 h. PV pressure remained stable at 13 ± 1 mm Hg. Perfusate temperature increased from 9.7 ± 0.6°C at the start to 11.0 ± 0.0°C after 20 h. Aspartate aminotransferase and lactate dehydrogenase increased from 281 ± 158 and 308 ± 171 U/L after 1h to 524 ± 163 and 537 ± 168 U/L after 20 h, respectively. Blood gas analysis showed a stable pO_2 of 338 ± 20 mm Hg before perfusion of the liver and 125 ± 14 mm Hg after 1 h perfusion. The pCO_2 increased from 15 ± 5 mm Hg after 1 h to 53 ± 4 mm Hg after 20 h. No histological changes were found after 20 h of MP. This study demonstrated the feasibility of a portable MP system for preservation of the liver and showed that continuous perfusion via the PV can be maintained with an oxygen-driven pump system without notable preservation damage of the organ.

INTRODUCTION

Organs that meet extended criteria for donors (ECD), such as those from the elderly and nonheart-beating donors as well as steatotic livers, are known to be more prone to preservation-induced damage than healthy donor organs [Desphande and heaton, 2006]. Continuous artificial circulation through an organ during machine perfusion (MP) has the potential to keep ECD organs in a better functional condition.

For decades, MP of the liver was primarily confined to the experimental setting and thus far only one clinical (phase 1) series has been reported [Guarrera et al., 2010]. Although this trial has presented encouraging results for MP of liver grafts, widespread implementation tends to be constrained by the difficulty to practically implement the technology necessary for the preservation of livers. Currently, the major obstacle preventing large-scale clinical application of MP for liver grafts is the lack of portable, oxygenated hypothermic (4°C) MP systems that are compatible with the size of liver grafts and the associated perfusion demands [Schreinemachers et al., 2007].

We have developed a disposable oxygenated MP system (Airdrive, Portable Organ Perfusion, Amsterdam, The Netherlands) that has demonstrated its value in experimental hypothermic kidney preservation [Schreinemachers et al., 2010]. The system is based on an oxygen-driven, positive displacement pump that allows pressure-controlled pulsatile perfusion and oxygenation of the perfusion medium. In this study, the settings, perfusion dynamics, and peri- and post-transplantation organ quality were assessed in the Airdrive MP system during 20-h hypothermic preservation of porcine liver grafts.

MATERIALS AND METHODS

Airdrive system

The Airdrive system (Portable Organ Perfusion) is based on pressurized oxygen as the driving force, which is used for three purposes: (I) to drive a positive displacement pump; (II) to supply the oxygenator; and (III) to induce overpressure in the organ chamber to support sterility. The oxygen is provided by a standard onboard 2-L pressurized cylinder containing

medical grade oxygen (Medidis, Lelystad, The Netherlands). A 12-V, non-rechargeable battery powers the gas valves and pressure feedback systems via a proportional-integral-derivative controller.

The pump design is based on a low-energy, reciprocating positive displacement membrane pump (Figure 1). The pump contains an embedded filter (15 micron, DEHP-free PVC) and has a maximum output of 13.9 mL perfusate per cycle. During the pump cycle, a software-embedded maximum pressure limit prevents overshoot of pressure and flow to the organ. Transducer P_2 (Figure 2) can limit the pressure to 6.0 kPa (45 mm Hg). When P_2 exceeds the maximum pressure, the system switches to a burst of short pump actions to relieve the oxygen in the system, lowering P_2 to within the designated limits. Once baseline levels are reached, normal operation is resumed. Excess usage of the oxygen supply and batteries are prevented by flow limitation. The flow rate is limited to 250 mL/min for portal vein (PV) perfusion. A temperature sensor is embedded in the pump design, which, during normal pump action, provides an identical temperature to the afferent organ tube temperature (unpublished data).

The oxygenator is comprised of a coil of porous silicone tubing that is placed inside a pressurized oxygen container prior to an expansion chamber and a bubble trap. The oxygen used for the pump and oxygenator dissipates into the chamber to induce overpressure. This pressure is limited by two outlets in the lid covered with breathable fabric (Porex, Aachen, Germany), maintaining an overpressure in the organ chamber during perfusion.

During preservation, the flow, pressure, intra-organ vascular resistance (VR), temperature, and preservation time are continuously displayed and stored. All components are embedded in polystyrene (Neopor, Medisize, Hillegom, The Netherlands) to provide optimal isolation. Four pre-cooled packs (stored at -20°C) are placed underneath the organ chamber inside the transporter box for temperature control.

Experimental procedure

All animal experiments were approved by the institute's animal ethics committee and animals were treated in accordance with the National Institute of Health Guidelines for the Care and Use of Laboratory Animals. Three

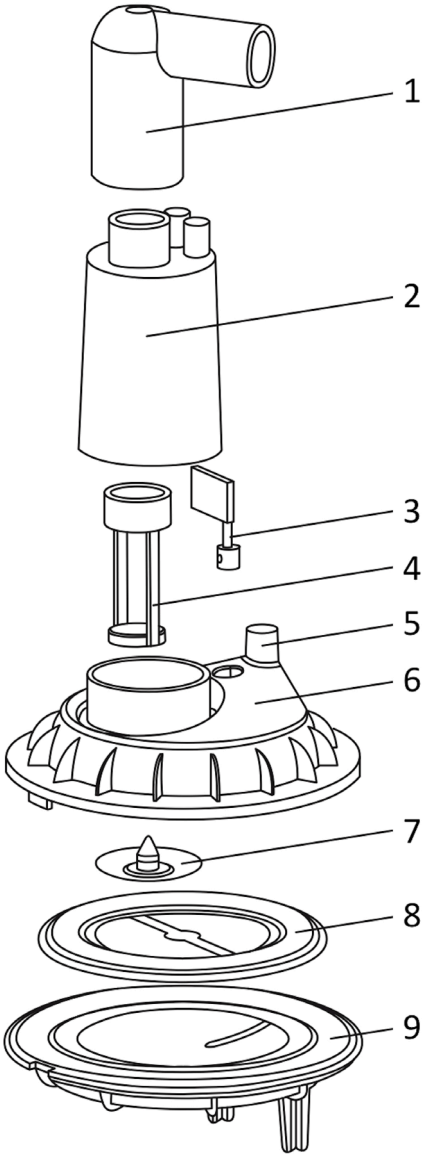

Figure 1. Airdrive pump mechanism. 1 Pump inlet, 2 body for erythrocyte filter, 3 temperature sensor, 4 erythrocyte filter, 5 perfusion liquid output connector, 6 upper pump body, 7 valve, 8 membrane with central weight, 9 lower pump body.

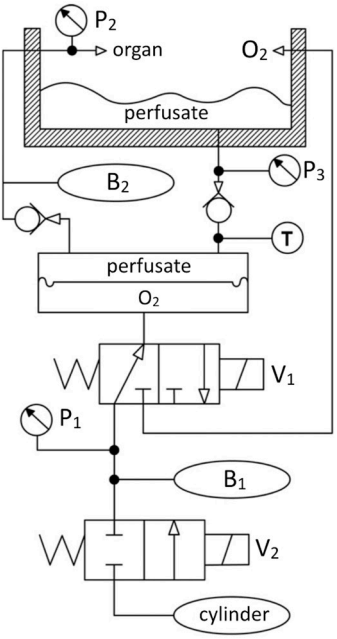

Figure. 2. Schematic view of oxygen and perfusate flow in the Airdrive system. A. Oxygen pressure is reduced to 12.5 (±2.5) kPa from the oxygen cylinder (160 kPa). Gas valves V1 and V2 are controlled by a proportional-integral-derivative controller. Expansion chambers are denoted as B1 (10–15 kPa) and B2 (1.6 kPa). Transducers P1 and T are monitored, and their data stored during the preservation period, whereas P2 and P3 are used for feedback control.

female landrace pigs weighing 50.3 ± 3.1 kg underwent a liver procurement procedure under general anesthesia according to a previously described anesthesia protocol [Schreinemachers et al., 2010].

The celiac trunk and PV were cannulated using a 9-Fr (3-mm) polyamide luer lock cannula (VBM Medizintechnik, Sulz am Neckar, Germany) after administration of 25.000 IU of heparin (Leo Pharma BV, Breda, The Netherlands). The common bile duct was ligated. A washout system with 4 L cold (4°C) histidine-tryptophan-ketogluterate solution (Custodiol, Dr. Franz Köhler Chemie, Bensheim, Germany) was used at 100-cm hydrostatic pressure for both hepatic artery (HA) and PV. Ice slush was placed in the abdomen to facilitate cooling of the organ. After 2 L of washout solution had passed through the liver, the organ was removed and the washout continued on the back-table with an additional 2 L, during which a peripheral biopsy was obtained and the gallbladder was flushed with saline solution via a puncture. The gall bladder was cannulated and left in place in this experimental setup to serve as a bile collection reservoir.

The Airdrive system was primed with 1 L of Belzer MPS (Bridge to Life, Columbia, SC, USA) according to the manufacturer's instructions. One gram of ceftriaxone (Fresenius Kabi, Bad Homburg, Germany) was added to the perfusion medium. The liver was placed in a suspended polyurethane hammock (Inoac USA, Bardstown, KY, USA) inside of the organ chamber of the

Airdrive and, the PV was connected to the pump tubing. After connecting the organ, the liver software program was initiated and perfusion of the organ was commenced.

Blood gas analysis (pO_2 and pCO_2) was performed on the circulating perfusate using an ABL80 Flex gas analyzer (Radiometer, Brønshøj, Denmark) before placement of the liver in the Airdrive (t = 0 h) and at 1, 3, 5, 10, and 20 h of perfusion. Perfusate samples for biochemical assessment (lactate dehydrogenase (LDH), aspartate aminotransferase (AST), and total bilirubin) were obtained at similar time intervals as the blood gas analysis. The flow (number of pumpstrokes x 13.9 mL), pressure (P_2), VR (flow/ pressure), and temperature were recorded hourly from the display.

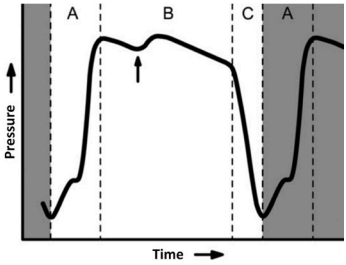

Figure 3. Pressure profile of a pump cycle. The cycle is comprised of three phases indicated by A, B, and C, where the white plane demarcates one cycle. The arrow designates closure of V_2 coinciding with maximum O_2 pressure build-up in B_2 (Figure 2)

Biopsies for histological examination were obtained at two time points: a peripheral biopsy after the flush but before placement in the Airdrive (control sample) and a peripheral and core biopsy after 20 h of perfusion in the Airdrive. Biopsies were fixed and imaged as described previously [Heger et al., 2011].

The sections were scored (10 fields per section) in a randomized blinded fashion by a liver pathologist, according to a modified liver scoring system. The data were analyzed using Matlab (Mathworks, Natick, MA, USA) and presented as mean ± standard deviation.

RESULTS

PV flow exhibited a gradual increase over time from 157 ± 25 mL/min at start to 177 ± 25 mL/min after 20 h of perfusion (Figure 4A). The mean PV pressure remained constant throughout the entire preservation period (13 ± 1 mm Hg) (Figure 4C). VR remained constant with 0.08 ± 0.02 mm Hg/min/L at start of perfusion and 0.07 ± 0.02 mm Hg/min/L after 20 h (Figure 4C). Perfusate temperature showed an increase from 9.7 ± 0.6°C at start to 11.0 ± 0.0°C

after 20 h of perfusion (Figure 2A). Mean liver weight was 1.3 ± 0.3 kg. Bile, probably residual, had accumulated in the gallbladder after 20 h of perfusion, totaling 7 ± 2 mL.

Biochemical parameters showed an increase in AST and LDH from, respectively, 281 ± 158 and 308 ± 171 U/L after the first hour, to, respectively, 524 ± 163 and 537 ± 168 U/L after 20h (Figure 4F). The bilirubin concentration remained below detection levels at all times (<1 μmol/L), indicating no bile leakage. Blood gas analysis before placement of the liver yielded a pO_2 of 338 ± 20 mm Hg and a pCO_2 of <1 mm Hg (Figure 4E). After organ placement in the Airdrive, the pO_2 dropped to 125 ± 14 mm Hg and the pCO_2 increased to 15 ± 5 mm Hg. After 20 h of perfusion, the pO_2 remained stable at 124 ± 14 mm Hg and the pCO_2 increased further to 53 ± 4 mm Hg. Histological scoring is shown in Figure 4B. None of the biopsies showed evidence of portal edema, parenchymal necrosis, or mitosis (score = 0). All biopsies showed signs of sinusoidal dilation (mean score 2 ± 0.7 on 1 to 3 scale), with no apparent differences after MP (pre-MP of 2 ± 1 vs. post-MP of 2 ± 1). Three post-MP biopsies (2 peripheral, 1 core) showed signs of apoptosis, as evidenced by the presence of Councilman bodies (all scored 1 out of 4).

DISCUSSION

This study sought to demonstrate the feasibility of a portable MP device that meets the flow and pressure demands considered suitable for preservation of a liver graft while retaining dependability and port- ability. We have shown that these demands can be met using an oxygen-driven pump system.

We examined both biochemical (AST, LDH) and histological parameters to assess the damage profile after MP (Figure 4). During perfusion, the biochemical parameters showed a gradual increase, as usually found in a recirculating perfusion device. These values are in agreement with earlier reports on porcine and clinical liver MP when corrected for circulating volume, indicating minimal hepatocellular injury [Guarrera et al., 2010; van der Plaats, 2006].

Histologically, we have shown preservation of architectural integrity of the parenchyma and absence of edema after 20-h MP. The ultimate test is

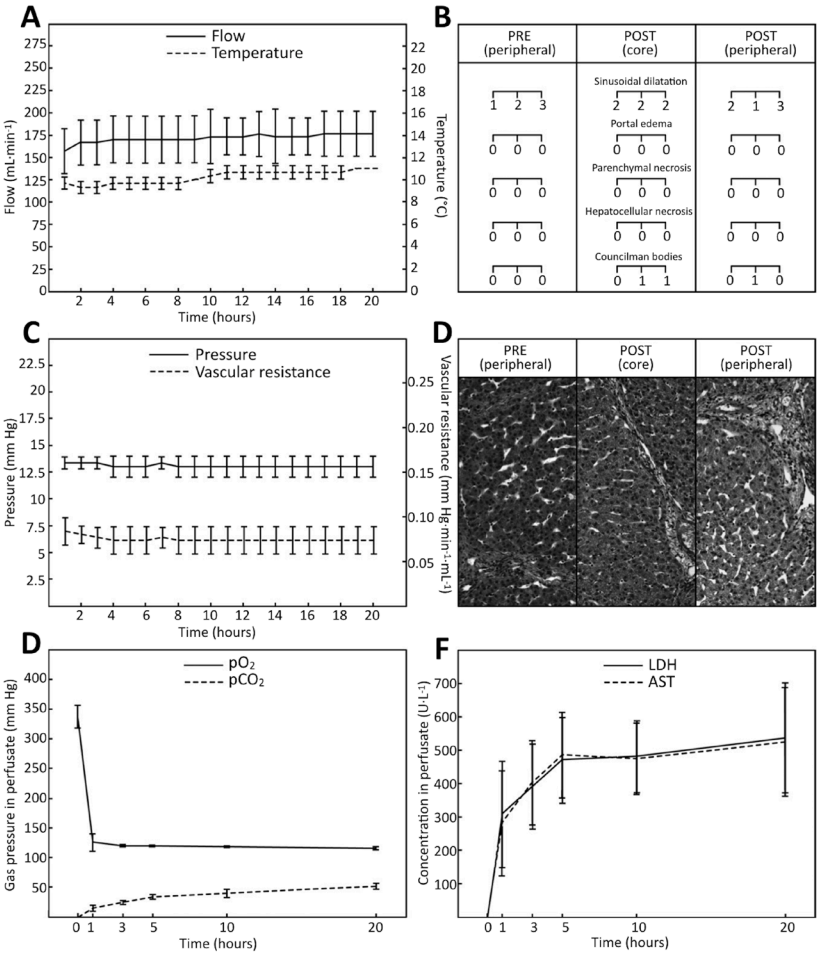

Figure. 4. (A) Perfusion flow (mL/min) and temperature (°C). (B) Histological scores: sinusoidal dilatation: 0, absent; 1, less than 1/3 of parenchyma; 2, less than 2/3; 3, more than 2/3. Portal edema: 0, absent; 1, less than 25%; 2, between 25–50%; 3, between 50–75%; 4, more than 75%. Areas of confluent parenchymal necrosis: 0, absent; 1, affecting less than 25% of parenchyma; 2, affecting 25–50%; 3, affecting 50–75%; 4, affecting >75%. Hepatocellular mitosis: 0, absent; 1, in case of <2 foci per 8 fields (40x objective); 2, in case of 2–4 foci; 3, in case of 5–10 foci; 4, in case of >10 foci. Councilman bodies (cytosegresome formation): 0, absent; 1, in case of <2 foci (10x objective); 2, in case of 2–4 foci; 3, in case of 5–10 foci; 4, in case of >10 foci. (C) Pressure (mm Hg) and vascular resistance (mm Hg/min/mL). (D) Representative hematoxylin and eosin-stained liver sections. (E) Perfusate pO_2 and pCO_2 (mm Hg). (F) Perfusate aspartate aminotransferase (AST) and lactate dehydrogenase (LDH) concentrations (U/L). All values are depicted as mean ± SD.

graft outcome in a large animal liver transplantation model. In large animal kidney transplantation, MP using the Airdrive has proven to be beneficial over conventional cold storage in pre-damaged kidney grafts [Schreinemachers et al., 2010]. However, large animal liver transplantation encompasses surgical restrictions (e.g., absence of collateral hepatic circulation) that make the model less comparative.

One of the main concerns in the use of an MP system, as reflected by the technical diversity of the experimental and commercial systems produced to date, is implementation of the pump. Currently, most available MP systems are based on a roller pump mechanism to recirculate the perfusate [Horpácsy et al., 1979; Moers et al., 2009; Guarrera et al., 2004; Metcalfe et al, 2002]. However, a significant technical obstacle associated with roller-type pumps is their extensive power consumption, which imposes considerable restrictions on portable systems [Guarrera et al., 2010; Brockmann et al., 2009]. To circumvent this major hurdle, the Airdrive makes use of a 2-L oxygen cylinder to drive the pump while sustaining an average PV flow of >150 mL/min for up to 20 h.

The current configuration of perfusion dynamics is aimed at perfusion via the PV only. It is arguable that a dual pump system could provide flow for both the portal venous system as well as the HA system. It can be conceived that dual MP can be beneficial due to oxygenation of the biliary system [Michels, 1966]. However, studies assessing this effect in a clinically representative model are yet to be conducted.

The required flow through a liver graft during MP remains a subject of debate and can be of critical importance for optimal preservation of the graft. Hypothermia causes an initial afferent vasoconstriction resulting from surgical handling and a reduced Ca^{2+}-ATPase activity in vascular smooth muscle cells [Jackson et al., 2000]. Therefore, hypothermic MP has been suggested to be safe at 25% of physiological flow [‘t Hart et al., 2007; Debbaut et al., 2011]. Given the fact that physiological portal flows at normothermic temperatures are typically around 1000 mL/min, the recorded perfusate flow of 177 ± 25 mL/min in our study is consistent with a safe range [Jakimowicz et al., 1998].

Preservation of organs at 4°C constitutes the gold standard in organ preservation. In this study, the MP system showed moderately higher

temperatures during perfusion, reaching an average of 10 ± 0.5°C. In our experiments, metabolic activity was evident from the increase in perfusate pCO_2 and decrease in pO_2, collectively typifying a metabolically active organ. Taking this into consideration, it is arguable whether extreme lowering of metabolism is required during MP as nutrients and oxygen are continuously available. And, in line with this view, there is growing consensus on the use of (sub)normothermic preservation temperatures during MP. The preservation of suboptimal organs, such as those from elderly or nonheart-beating donors as well as steatotic livers, may benefit from MP and from preservation at higher temperatures [Hessheimer et al., 2012]. In that respect, the Airdrive MP system is capable of operating at any temperature within the spectrum of hypothermic and (sub)normothermic perfusion. However, this study has merely demonstrated the feasibility of the Airdrive as a liver MP system. A possible benefit of MP using marginal livers cannot be presumed based on these findings and remains to be shown in the Airdrive.

Allocation of organs is rarely restricted to a single center, making portability of an MP system essential to its implementation. By using disposable light-weight materials, the Airdrive weight remains below 15 kg when operational (i.e., including embedded oxygen cylinder), which is below the maximum one-person manual handling weight enforced by occupational health codes in many countries.

This study has demonstrated the feasibility of a portable machine perfusion system for preservation of the liver. Using an oxygen-driven pump system, continuous perfusion via the pulmonary can be maintained for a clinically relevant preservation time without notable preservation damage to the organ. These results support further research on the use of the Airdrive for marginal liver grafts.

SUPPLEMENT

Supplemental Table S1

T_b body temperature
T_a ambient temperature (<10 T_a reported values, no mean value)
n^1 group size for T_b data
n^2 group size for T_a data

Agent	Category	n^1 Species	$\Delta T_b \pm SD$	$\Delta T_a \pm SD$	n^2
5'-Hydroxytryptophan	Amino acid	20 Rat	-1,0 ± 2,1 °C	23,1 ± 6,2 °C	19
5'-Hydroxytryptophan	Amino acid	10 Mouse	-0,4 ± 3,6 °C		<10
5'-Hydroxytryptophan	Amino acid	38 Rabbit	0,8 ± 1,3 °C	21,8 ± 1,3 °C	25
Acetaminophen	Antipyretic	13 Mouse	-4,9 ± 3,3 °C		<10
Acetaminophen	Antipyretic	10 Rat	-1,9 ± 2,0 °C		<10
Acetylcholine	Acetylcholine agonist	18 Rat	-0,7 ± 1,0 °C	18,9 ± 9,8 °C	17
Acetylstrophanthidin	Glycoside	11 Primate	-2,2 ± 3,6 °C	24,0 ± 0 °C	11
ACTH	Peptide	12 Rabbit	-0,6 ± 0,6 °C	22,7 ± 3,4 °C	12
Amantadine	Dopamine receptor agonist	12 Mouse	-2,5 ± 2,5 °C		<10
Aminobutyric Acid	Amino acid	54 Mouse	-2,6 ± 2,9 °C	22,0 ± 6,7 °C	21
Aminobutyric Acid	Amino acid	27 Rat	-1,1 ± 2,5 °C	24,6 ± 7 °C	17
Aminopyrine	Antipyretic	13 Rabbit	-1,6 ± 1,1 °C		<10
Amitriptyline	Tricyclic antidepressant	14 Mouse	-1,6 ± 2,0 °C		<10
Amphetamine	Amphetamine	197 Mouse	0,5 ± 3,0 °C	21,4 ± 5,4 °C	171
Amphetamine	Amphetamine	272 Rat	0,6 ± 2,4 °C	18,7 ± 9,1 °C	210
Amphetamine	Amphetamine	22 Rabbit	2,0 ± 1,2 °C	22,1 ± 1,6 °C	11
Amphetamine	Amphetamine	10 Dog	2,3 ± 1,5 °C		<10
Angiotensin	Peptide	15 Primate	-0,1 ± 0,6 °C		<10
Apomorphine	Dopamine receptor agonist	144 Mouse	-3,9 ± 2,1 °C	29,9 ± 1,5 °C	124
Apomorphine	Dopamine receptor agonist	145 Rat	-1,2 ± 1,3 °C	19,2 ± 7,4 °C	115
Apomorphine	Dopamine receptor agonist	37 Rabbit	1,5 ± 1,1 °C	21,4 ± 4,8 °C	24
Arachidonic Acid	Prostaglandin precursor	16 Rat	0,8 ± 0,8 °C	21,8 ± 0,8 °C	14
Arachidonic Acid	Prostaglandin precursor	11 Rabbit	1,0 ± 1,3 °C		<10
Arecoline	Acetylcholine agonist	54 Rat	-1,0 ± 1,8 °C		<10
Arecoline	Acetylcholine agonist	10 Cat	0,4 ± 0,9 °C		<10
Aspirin	Antipyretic	26 Rat	-0,6 ± 1,1 °C		<10
Aspirin	Antipyretic	12 Rabbit	0,1 ± 0,7 °C		<10

Atropine	Muscarinic blocking agent	22 Mouse	-0,5 ± 1,4 °C	22,2 ± 6,8 °C	18
Atropine	Muscarinic blocking agent	47 Rat	-0,1 ± 1,3 °C	19,7 ± 9 °C	44
Atropine	Muscarinic blocking agent	17 Rabbit	-0,1 ± 0,6 °C	20,7 ± 8,2 °C	14
Bombesin	Peptide	64 Rat	-1,9 ± 2,5 °C	13,5 ± 11,3 °C	61
Bromocriptine	Dopamine receptor agonist	16 Rat	-2,7 ± 4,1 °C		<10
Calcium Chloride	Cation	12 Rat	-1,0 ± 0,9 °C	22,6 ± 1,1 °C	12
Calcium Chloride	Cation	10 Rabbit	-1,0 ± 1,2 °C		<10
Calcium Chloride	Cation	12 Cat	-0,8 ± 0,7 °C		<10
Cannabidol	Hallucinogen	13 Mouse	-1,6 ± 1,3 °C		<10
Cannabis	Hallucinogen	14 Rat	-2,1 ± 2,0 °C		<10
Capsaicin	Capsaicinoid	11 Rat	-1,9 ± 3,6 °C		<10
Carbachol	Acetylcholine agonist	10 Rat	-1,5 ± 2,6 °C	19,3 ± 8,5 °C	10
Carbachol	Acetylcholine agonist	10 Sheep	0,6 ± 0,7 °C	21,5 ± 8,3 °C	10
Carbon Dioxide	Gas	28 Rat	-3,3 ± 6,1 °C	23,5 ± 12,8 °C	28
Carbon Dioxide	Gas	14 Guinea Pig	-1,7 ± 2,1 °C	21,4 ± 5,6 °C	14
Ceruletide	Peptide	20 Mouse	-1,4 ± 1,1 °C		<10
Chloroamphetamine	Amphetamine	14 Rabbit	1,0 ± 2,1 °C		<10
Chlorophenylalanine	Presynaptic aminergic alt. agent	18 Mouse	-0,5 ± 1,6 °C	19,8 ± 7,4 °C	14
Chlorophenylalanine	Presynaptic aminergic alt. agent	18 Rabbit	-0,2 ± 0,3 °C	21,5 ± 5,4 °C	15
Chlorophenylalanine	Presynaptic aminergic alt. agent	50 Rat	-0,2 ± 1,3 °C	21,1 ± 8,9 °C	45
Chlorpromazine	Neuroleptic	101 Mouse	-4,4 ± 4,1 °C	23,6 ± 7,9 °C	82
Chlorpromazine	Neuroleptic	205 Rat	-4,0 ± 5,0 °C	21,5 ± 20,7 °C	157
Chlorpromazine	Neuroleptic	12 Guinea Pig	-2,0 ± 1,2 °C		<10
Chlorpromazine	Neuroleptic	46 Rabbit	-1,1 ± 1,0 °C	21,1 ± 5,9 °C	26
Cimetidine	H2 receptor antagonist	11 Rat	-0,3 ± 0,4 °C	21,3 ± 1,3 °C	11
Clomipramine	Tricyclic antidepressant	11 Mouse	-1,4± 1,3 °C		<10
Clomipramine	Tricyclic antidepressant	16 Rat	-0,6 ± 1,3 °C	21,5 ± 6,8 °C	21
Clonidine	Adrenergic agonist	27 Mouse	-2,6 ± 1,4 °C	21,3 ± 1 °C	24
Clonidine	Adrenergic agonist	72 Rat	-2,2 ± 1,7 °C	21,1 ± 7,5 °C	64
Cobaltous Chloride	Cation	11 Mouse	-3,4 ± 1,9 °C	23,9 ± 3,8 °C	11
Cocaine	Uptake inhibitor	16 Rat	-1,0 ± 1,8 °C	19,3 ± 6,6 °C	15
Cocaine	Uptake inhibitor	11 Mouse	0,2 ± 2,0 °C	26,6 ± 4,9 °C	11
Cocaine	Uptake inhibitor	12 Primate	0,3 ± 1,2 °C		<10
Cyproheptadine	Serotonin antagonist	10 Rabbit	-0,6 ± 0,6 °C		<10
Cyproheptadine	Serotonin antagonist	20 Rat	0,0 ± 1,1 °C	20,9 ± 6,5 °C	19
d-Ala-2-Met-Enkephalinamide	Peptide	20 Cat	1,1 ± 2,0 °C	19,2 ± 8,7 °C	19
Desipramine	Tricyclic antidepressant	22 Mouse	-0,7 ± 1,3 °C	22,8 ± 3,3 °C	19
Desipramine	Tricyclic antidepressant	21 Rat	-0,4 ± 3,0 °C	18,4 ± 7 °C	17
Diethyldithiocarbamate	Dopamine β-hydroxylase inhibitor	12 Rat	-1,6 ± 1,8 °C	22,5 ± 6,3 °C	12
Dihydroxyphenylalanine	Amino acid	13 Mouse	-1,6 ± 2,8 °C	22,1 ± 1,6 °C	12
Dihydroxyphenylalanine	Amino acid	18 Rabbit	0,5 ± 0,9 °C	21,2 ± 8,5 °C	15

Dihydroxytryptamine	Tryptamine	23 Rat	-0,1 ± 1,0 °C	21,8 ± 9,2 °C	23
Dinitrophenol	Uncoupling agent	25 Rat	1,3 ± 1,4 °C	22,0 ± 8,4 °C	19
Dinitrophenol	Uncoupling agent	24 Rabbit	1,4 ± 0,9 °C		<10
Dinitrophenol	Uncoupling agent	18 Dog	1,9 ± 2,0 °C		<10
Diphenhydramine	H1 receptor antagonist	15 Mouse	-1,4 ± 1,4 °C	22,5 ± 2,6 °C	12
DMSO	Organosulfic	18 Rat	-8,6 ± 10,5 °C	12,5 ± 10,3 °C	17
DMSO	Organosulfic	11 Mouse	-1,9 ± 2,6 °C		<10
Dopamine	Dopamine receptor agonist	14 Mouse	-0,9 ± 2,7 °C		<10
Dopamine	Dopamine receptor agonist	53 Rat	-0,9 ± 1,4 °C	19,5 ± 4,7 °C	41
Dopamine	Dopamine receptor agonist	21 Rabbit	0,9 ± 1,2 °C	21,5 ± 4,6 °C	21
Ephedrine	Adrenergic agonist	15 Mouse	0,2 ± 2,7 °C	24,4 ± 6,5 °C	14
Epinephrine	Adrenergic agonist	18 Mouse	-3,7 ± 6,4 °C	20,9 ± 6,5 °C	11
Epinephrine	Adrenergic agonist	26 Rat	-0,4 ± 2,4 °C	21,1 ± 6,2 °C	25
Epinephrine	Adrenergic agonist	24 Rabbit	0,4 ± 1,6 °C		<10
Ergotamine	Ergot alkaloid	13 Rabbit	-1,9 ± 2,3 °C		<10
Ergotoxine	Ergot alkaloid	14 Rabbit	0,9 ± 3,9 °C		<10
Ethanol	Anesthetic	52 Mouse	-2,4 ± 2,4 °C	23,4 ± 4,9 °C	48
Ethanol	Anesthetic	28 Rat	-1,3 ± 1,2 °C	23,4 ± 7,5 °C	12
Fenfluramine	Amphetamine	25 Rat	1,2 ± 2,1 °C	25,6 ± 5,9 °C	23
Fenfluramine	Amphetamine	12 Rabbit	1,5 ± 0,6 °C	22,6 ± 1,8 °C	12
Guanethidine	Uptake inhibitor	13 Rat	-0,2 ± 2,3 °C	20,7 ± 8,2 °C	13
Haloperidol	Neuroleptic	28 Mouse	-2,3 ± 2,9 °C	21,3 ± 4 °C	19
Haloperidol	Neuroleptic	69 Rat	-0,4 ± 1,5 °C	19,3 ± 8,1 °C	56
Haloperidol	Neuroleptic	18 Rabbit	-0,3 ± 0,7 °C	21,3 ± 6,8 °C	12
Halothane	Anesthetic	23 Pig	2,6 ± 2,2 °C		<10
Harmaline	Hallucinogen	10 Rat	-2,2 ± 1,7 °C	23,8 ± 0,9 °C	10
Helium	Gas	21 Hamster	-18,3 ± 12,7 °C	10,4 ± 13,3 °C	21
Histamine	Neuromuscular blocking agent	21 Mouse	-2,3 ± 2,6 °C	22,8 ± 4,9 °C	16
Histamine	Neuromuscular blocking agent	57 Rat	-0,9 ± 1,6 °C	22,3 ± 4,7 °C	47
Histamine	Neuromuscular blocking agent	12 Cat	-0,5 ± 1,3 °C	21,9 ± 7,2 °C	10
Histamine	Neuromuscular blocking agent	10 Sheep	0,2 ± 0,3 °C		<10
Histidine	Amino acid	10 Rat	-0,4 ± 0,6 °C		<10
Hydroxydopamine	Uptake altering agent	14 Mouse	-1,2 ± 1,3 °C	20,7 ± 5 °C	14
Hydroxydopamine	Uptake altering agent	70 Rat	-0,7 ± 1,6 °C	16,3 ± 12 °C	62
Imipramine	Tricyclic antidepressant	24 Rat	-0,9 ± 1,3 °C	21,3 ± 7,3 °C	19
Imipramine	Tricyclic antidepressant	23 Mouse	-0,8 ± 1,1 °C	22,4 ± 2,4 °C	16
Imipramine	Tricyclic antidepressant	12 Rabbit	1,0 ± 1,9 °C		<10
Indomethacin	Antipyretic	11 Mouse	-0,5 ± 1,3 °C	18,2 ± 13,8 °C	11
Indomethacin	Antipyretic	28 Rat	-0,3 ± 0,6 °C	22,4 ± 4,7 °C	25
Indomethacin	Antipyretic	15 Rabbit	-0,1 ± 0,2 °C	21,8 ± 1,7 °C	13
Insulin	Hormone	10 Mouse	-5,3 ± 4,4 °C	24,1 ± 5,2 °C	10

Isoflurophate	Anticholinesterase	30 Rat	-3,5 ± 2,3 °C	23,3 ± 2,8 °C	15
Isoproterenol	adrenergic agonist	14 Mouse	-1,2 ± 3,8 °C	21,1 ± 6,7 °C	14
Isoproterenol	adrenergic agonist	56 Rat	0,4 ± 1,6 °C	23,0 ± 5,3 °C	52
LRH	Peptide	10 Rat	-0,1 ± 1,0 °C	20,4 ± 7,5 °C	10
Lysergide	Hallucinogen	10 Mouse	-0,3 ± 2,0 °C		<10
Lysergide	Hallucinogen	25 Rat	0,3 ± 1,5 °C	25,9 ± 7,9 °C	16
Lysergide	Hallucinogen	88 Rabbit	1,5 ± 0,7 °C	22,7 ± 5,3 °C	48
Melanostatin	Peptide	10 Mouse	-0,5 ± 1,1 °C		<10
Meperidine	Narcotic analgesic	27 Mouse	-2,1 ± 3,2 °C	22,7 ± 5,3 °C	23
Meperidine	Narcotic analgesic	13 Rat	-1,2 ± 1,5 °C	20,4 ± 2,9 °C	11
Meperidine	Narcotic analgesic	11 Rabbit	0,6 ± 1,2 °C		<10
Met-Enkephalin	Peptide	11 Rat	0,4 ± 0,9 °C		<10
Metamphetamine	Amphetamine	23 Mouse	0,2 ± 3,2 °C	24,8 ± 5,4 °C	21
Methacholine	Acetylcholine agonist	11 Rat	-1,8 ± 1,7 °C	20,5 ± 8,5 °C	11
Methadone	Narcotic analgesic	10 Mouse	-3,3 ± 6,4 °C	23,9 ± 2,8 °C	11
Methadone	Narcotic analgesic	41 Rat	-1,0 ± 2,1 °C	20,3 ± 6,7 °C	27
Methylatropine	Muscarinic blocking agent	11 Rat	-0,9 ± 2,5 °C		<10
Methyldopa	Uptake altering agent	10 Rat	-2,7 ± 2,4 °C		<10
Methyldopa	Uptake altering agent	11 Mouse	-0,8 ± 1,9 °C		<10
Methysergide	Serotonin antagonist	28 Rat	-0,3 ± 0,9 °C	18,7 ± 8,3 °C	25
Metyrosine	Uptake altering agent	41 Rat	-1,9 ± 3,1 °C	22,7 ± 7,5 °C	29
Morphine	Narcotic analgesic	32 Dog	-1,4 ± 1,6 °C		<10
Morphine	Narcotic analgesic	10 Mouse	-1,2 ± 2,1 °C	23,0 ± 3,6 °C	92
Morphine	Narcotic analgesic	330 Rat	-0,0 ± 2,1 °C	22,3 ± 5,1 °C	273
Morphine	Narcotic analgesic	37 Cat	1,6 ± 1,4 °C	18,8 ± 8,7 °C	24
Morphine	Narcotic analgesic	35 Rabbit	-0,3 ± 1,3 °C	21,7 ± 6,5 °C	15
Muramyl-dipeptide	Peptide	25 Rabbit	1,4 ± 0,8 °C		<10
Nalorphine	Narcotic analgesic	11 Mouse	0,3 ± 0,4 °C	24,0 ± 6,6 °C	10
Naloxone	Narcotic analgesic	29 Mouse	-1,0 ± 3,4 °C	21,7 ± 5,6 °C	25
Naloxone	Narcotic analgesic	81 Rat	-0,1 ± 0,5 °C	19,4 ± 7,4 °C	67
Naltrexone	Narcotic analgesic	11 Rat	-0,7 ± 1,4 °C		<10
Neurotensin	Peptide	40 Mouse	-2,8 ± 2,8 °C	20,1 ± 8,5 °C	40
Neurotensin	Peptide	77 Rat	-1,2 ± 1,1 °C	18,8 ± 8,3 °C	59
Nicotine	Acetylcholine agonist	26 Mouse	-2,6 ± 2,6 °C	20,7 ± 7,1 °C	24
Norepinephrine	Adrenergic agonist	35 Mouse	-1,3 ± 2,2 °C	20,9 ± 9,7 °C	32
Norepinephrine	Adrenergic agonist	38 Cat	-1,0 ± 0,9 °C	23,1 ± 4,8 °C	27
Norepinephrine	Adrenergic agonist	13 Primate	-0,6 ± 0,9 °C	22,7 ± 7,5 °C	10
Norepinephrine	Adrenergic agonist	223 Rat	-0,0 ± 1,8 °C	22,7 ± 7,9 °C	155
Norepinephrine	Adrenergic agonist	21 Sheep	0,4 ± 1,2 °C	21,4 ± 12,8 °C	21
Norepinephrine	Adrenergic agonist	15 Guinea Pig	0,7 ± 0,5 °C	26,2 ± 7,2 °C	14
Norepinephrine	Adrenergic agonist	55 Rabbit	0,8 ± 1,1 °C	24,3 ± 21,7 °C	42

Oxotremorine	Acetylcholine agonist	89 Mouse	-7,7 ± 3,6 °C	21,4 ± 3,5 °C	86
Oxotremorine	Acetylcholine agonist	33 Rat	-2,8 ± 3,9 °C	19,2 ± 4,8 °C	21
Oxygen	Gas	11 Rat	-3,1 ± 3,2 °C		<10
Oxytocin	Peptide	11 Rat	1,1 ± 0,6 °C	20,0 ± 9,1 °C	10
Pargyline	Monoamine oxidase inhibitor	20 Rat	-1,3 ± 1,3 °C	18,2 ± 10,2 °C	19
Pentazocine	Narcotic analgesic	18 Cat	-0,3 ± 1,6 °C	17,6 ± 10,9 °C	17
Pentobarbital	Barbiturate	16 Mouse	-6,4 ± 5,6 °C	21,9 ± 7,1 °C	11
Pentobarbital	Barbiturate	12 Dog	-3,9 ± 4,1 °C		<10
Pentobarbital	Barbiturate	10 Cat	-3,4 ± 3,2 °C		<10
Pentobarbital	Barbiturate	35 Rat	-2,0 ± 3,2 °C	20,0 ± 9,6 °C	35
Pentylenetetrazole	Analeptic	10 Rat	-2,3 ± 1,1 °C	21,9 ± 7,1 °C	10
Phenacetin	Antipyretic	12 Rat	-0,5 ± 1,4 °C		<10
Phenoxybenzamine	α-adrenergic antagonist	20 Mouse	-3,5 ± 3,5 °C	23,0 ± 1,8 °C	18
Phenoxybenzamine	α-adrenergic antagonist	26 Rat	-1,9 ± 2,9 °C	17,4 ± 8 °C	24
Phenoxybenzamine	α-adrenergic antagonist	20 Rabbit	-0,6 ± 0,7 °C	21,8 ± 1,5 °C	15
Phentolamine	α-adrenergic antagonist	65 Rat	-1,2 ± 1,7 °C	19,2 ± 8,4 °C	63
Phentolamine	α-adrenergic antagonist	14 Mouse	-1,0 ± 1,6 °C	23,7 ± 5,1 °C	12
Physostigmine	Anticholinesterase	12 Mouse	-2,9 ± 2,1 °C	22,1 ± 4,1 °C	12
Physostigmine	Anticholinesterase	26 Rat	-1,3 ± 1,4 °C	22,1 ± 5,8 °C	18
Pilocarpine	Acetylcholine agonist	29 Rat	-1,7 ± 0,8 °C	22,1 ± 3,7 °C	19
Pilocarpine	Acetylcholine agonist	22 Mouse	-1,6 ± 1,5 °C	23,5 ± 5,2 °C	20
Pimozide	Neuroleptic	54 Rat	0,1 ± 0,9 °C	18,2 ± 8,3 °C	51
Piribedil	Dopamine receptor agonist	14 Mouse	-4,1 ± 1,7 °C		<10
Piribedil	Dopamine receptor agonist	16 Rat	-2,7 ± 1,6 °C	16,2 ± 8,9 °C	15
Promazine	Neuroleptic	26 Mouse	-5,8 ± 5,8 °C	25,4 ± 8,1 °C	19
Promethazine	Neuroleptic	10 Mouse	-2,9 ± 1,8 °C	22,8 ± 2,6 °C	10
Propranolol	β-adrenergic antagonist	29 Mouse	-1,5 ± 2,7 °C	19,8 ± 10,3 °C	29
Propranolol	β-adrenergic antagonist	11 Guinea Pig	-1,4 ± 4,2 °C	20,6 ± 19,2 °C	11
Propranolol	β-adrenergic antagonist	67 Rat	-0,7 ± 1,1 °C	18,9 ± 8,5 °C	63
Propranolol	β-adrenergic antagonist	14 Rabbit	0,2 ± 0,7 °C	21,5 ± 2,9 °C	14
Prostaglandin D2	Prostaglandin	14 Rat	-0,1 ± 0,8 °C	22,7 ± 1,3 °C	13
Prostaglandin E1	Prostaglandin	43 Rat	0,4 ± 2,0 °C	21,6 ± 5,2 °C	33
Prostaglandin E1	Prostaglandin	52 Rabbit	0,9 ± 0,5 °C	23,4 ± 16,5 °C	42
Prostaglandin E1	Prostaglandin	24 Cat	1,6 ± 1,2 °C	22,0 ± 4,2 °C	22
Prostaglandin E2	Prostaglandin	16 Rabbit	1,0 ± 0,4 °C	23,2 ± 2,9 °C	15
Prostaglandin E2	Prostaglandin	57 Rat	1,4 ± 1,2 °C	20,7 ± 6,4 °C	41
Prostaglandin E2	Prostaglandin	11 Mouse	1,6 ± 0,9 °C		<10
Prostaglandin F2	Prostaglandin	24 Rat	1,3 ± 1,3 °C		<10
Quinine	Glycoside	11 Rat	-3,3 ± 1,8 °C	19,2 ± 8,1 °C	11
Reserpine	Uptake altering agent	152 Mouse	-7,9 ± 4,8 °C	22,1 ± 6,2 °C	56
Reserpine	Uptake altering agent	82 Rat	-2,6 ± 4,2 °C	20,0 ± 7,8 °C	66

Reserpine	Uptake altering agent	35 Rabbit	-0,5 ± 2,3 °C	23,7 ± 1,2 °C	20
Serotonin	Tryptamine	27 Mouse	-3,4 ± 2,4 °C	23,0 ± 4 °C	24
Serotonin	Tryptamine	114 Rat	-0,8 ± 1,5 °C	21,9 ± 6,8 °C	103
Serotonin	Tryptamine	20 Sheep	-0,5 ± 0,4 °C	18,4 ± 13,7 °C	19
Serotonin	Tryptamine	22 Cat	0,4 ± 0,9 °C	25,1 ± 6,3 °C	19
Serotonin	Tryptamine	54 Rabbit	0,5 ± 1,3 °C	21,0 ± 6,5 °C	40
Sodium Chloride	Cation	16 Rat	-0,0 ± 1,0 °C	21,5 ± 1,6 °C	15
Sodium Chloride	Cation	12 Cat	0,8 ± 1,4 °C	20,1 ± 9,9 °C	10
Sodium Salicylate	Antipyretic	34 Rat	-1,1 ± 1,4 °C	23,0 ± 6,3 °C	15
Sodium Salicylate	Antipyretic	17 Rabbit	-0,1 ± 0,3 °C		<10
Soman	Anticholinesterase	18 Rat	-3,3 ± 1,9 °C	22,2 ± 4 °C	15
Somatostatin	Peptide	27 Rat	0,9 ± 1,6 °C		<10
Substance P	Peptide	17 Rat	-0,2 ± 1,7 °C	10,7 ± 10,2 °C	10
Succinylcholine	Neuromuscular blocking agent	16 Pig	1,8 ± 1,7 °C		<10
Taurine	Amino acid	18 Rat	-2,2 ± 3,6 °C	21,4 ± 9,4 °C	16
Taurine	Amino acid	17 Rabbit	-2,0 ± 2,6 °C	19,8 ± 7 °C	16
Terodotoxin	Toxin	11 Cat	-2,4 ± 1,9 °C	14,7 ± 8,2 °C	10
Thyroxine	Hormone	12 Rat	1,0 ± 1,9 °C	16,7 ± 14,6 °C	13
Tranyclypromine	Monoamine oxidase inhibitor	19 Rat	-0,8 ± 2,2 °C	21,6 ± 1,9 °C	16
Tranyclypromine	Monoamine oxidase inhibitor	13 Rabbit	0,8 ± 1,5 °C		<10
Tremorine	Acetylcholine agonist	12 Rat	-6,9 ± 6,9 °C	15,5 ± 11 °C	11
Tremorine	Acetylcholine agonist	35 Mouse	-6,7 ± 2,7 °C	21,1 ± 2,5 °C	35
TRH	Peptide	50 Rat	0,4 ± 0,9 °C	19,3 ± 7,8 °C	38
TRH	Peptide	35 Mouse	0,5 ± 2,1 °C	19,3 ± 6,7 °C	29
TRH	Peptide	25 Rabbit	0,8 ± 0,7 °C		<10
Tryptophan	Amino acid	13 Rat	-1,3 ± 1,9 °C	16,3 ± 9,7 °C	13
Tyramine	Adrenergic agonist	23 Rat	1,5 ± 1,0 °C	24,9 ± 8,3 °C	23
Urethan	Anesthetic	13 Rat	-3,0 ± 5,2 °C	23,0 ± 9,4 °C	12
Vasopressin	Peptide	23 Rat	-0,3 ± 1,2 °C		<10
Yohimbine	α-adrenergic antagonist	15 Rat	-1,0 ± 1,5 °C	22,1 ± 2,6 °C	15
β-Endorphin	Peptide	34 Mouse	-0,4 ± 4,2 °C	19,9 ± 9,3 °C	30
β-Endorphin	Peptide	97 Rat	-0,3 ± 1,9 °C	18,9 ± 8,8 °C	82
β-Tetrahydronaphthalamine	Adrenergic agonist	11 Rat	0,3 ± 2,8 °C		<10
β-Tetrahydronaphthalamine	Adrenergic agonist	21 Rabbit	2,5 ± 1,7 °C		<10
Δ8-THC	Hallucinogen	18 Mouse	-2,6 ± 1,4 °C	22,6 ± 0,3 °C	18
Δ9-THC	Hallucinogen	103 Mouse	-3,7 ± 2,9 °C	22,7 ± 6 °C	90
Δ9-THC	Hallucinogen	75 Rat	-1,7 ± 1,6 °C	22,3 ± 3,6 °C	63
Δ9-THC	Hallucinogen	12 Cat	-1,1 ± 1,4 °C	24,0 ± 0 °C	14

Supplemental table S2

Species	Number of reports
Alpaca	9
Armadillo	1
Bear	2
Cat	720
Cattle	36
Crab	1
Crayfish	1
Deer	1
Desert rat	19
Dog	368
Duck	7
Echnida	9
Fish	42
Frog	3
Gerbil	44
Goat	65
Goose	2
Ground squirrel	86
Guinea pig	281
Hamster	101
Hedgehog	4
Horse	16
Human	1285
Leopard	1
Lion	1
Lizard	10
Lobster	1
Mouse	3549
Pigeon	238
Pig	78
Primate	328
Quail	5
Rabbit	2008
Rat	6154
Salamander	13
Scorpion	2
Sheep	251
Shrimp	1
Toad	1
Turkey	3
Turtle	2
Woodchuck	5
Zebu	1

Contributing authors

Department of Surgery
Academic Medical Center Amsterdam, Amsterdam, The Netherlands
- T.M. van Gulik
- M. Heger
- S.D. Hemelrijk
- I.C.J.H. Post

Department of Translational Physiology
Academic Medical Center Amsterdam, Amsterdam, The Netherlands
- R. Bezemer
- D.M.J. Milstein

Department of Pathology
Academic Medical Center Amsterdam, Amsterdam, The Netherlands
- J. Verheij

Department of Nuclear Medicine
Academic Medical Center Amsterdam, Amsterdam, The Netherlands
- R.J. Bennink
- K.M. de Bruin

Department of Anesthesiology
Academic Medical Center Amsterdam, Amsterdam, The Netherlands
- M.H.N. van Velzen

Department of Blood Cell Research
Sanquin Blood Supply Foundation, Amsterdam, The Netherlands
- D. de Korte

List of Publications

Post ICJH, **Dirkes MC**, Heger M, van Loon JP, Swildens B, Huijzer GM, van Gulik TM. Appraisal of the porcine kidney autotransplantation model. Front Biosci (Elite Ed) 2012 Jan 1; 4: 1345-1357.

Post ICJH, **Dirkes MC**, Heger M, Bezemer, van 't Leven RJ, van Gulik TM. Optimal flow and pressure management in machine perfusion systems for organ preservation. Ann Biomed Eng 2012 Dec; 40(12): 2698-2707.

Dirkes MC, Post ICJH, Heger M, van Gulik TM. A novel oxygenated machine perfusion system for preservation of the liver. Artif Organs 2013 Aug; 37(8): 719-724.

Post ICJH, **Dirkes MC**, Heger M, Verheij J, de Bruin KM, de Korte D, Bennink RJ, van Gulik TM. Efficacy of liver graft washout as a function of the perfusate, pressure, and temperature. Liver Transpl 2013 Aug; 19(8): 843-851.

Dirkes MC, Milstein DM, Heger M, van Gulik TM. Absence of hydrogen sulfide-induced hypometabolism in pigs: a mechanistic explanation in relation to small nonhibernating mammals. Eur Surg Res 2015; 54(3-4): 178-191.

Dirkes MC, Gulik TM, Heger M. Survey and critical appraisal of Pharmacological agents with potential thermo-modulatory properties in the context of artificially induced hypometabolism. J Clin Transl Res 2015(1):6-21.

Dirkes MC, Gulik TM, Heger M. The physiology of artificial hibernation. J Clin Transl Res 2015(2): 78-93.

Bereiter-Hahn J, Helmaier G, Carey HV, Herwig A, Coukèr A, Henning RH, Cerri M, Hut R, Ruf T, **Dirkes MC**, Singer D, Drew KL, Vya-Zouskiy V. ESA Topical Team "Hibernation and Torpor" Recommendations to ESA. ESA, ESTECT, Noordwijk, The Netherlands 2015

Olthoff PB, Reniers MJ, **Dirkes MC**, Gulik TM, Heger M, van Golen RF. Protective mechanisms of hypothermia in liver surgery and transplantation. Mol Med 2015 Nov; 21: 833-846.

Hemelrijk SD*, **Dirkes MC***, van Velzen MHN, Bezemer R, van Gulik TM, Heger M. Exogenous hydrogen sulfide gas does not induce hypothermia in normoxic mice. Sci Rep 2018 Mar 1;8(1): 3855

* Authors contributed equally

PhD Portfolio

PhD student	Marcel C. Dirkes
PhD period	January 2009 – March 2013
PhD supervisor	Prof. Dr. T.M. van Gulik
PhD co-supervisor	Dr. M. Heger

PhD training	Year	ECTS
Seminars		
Department seminars at Experimental Surgery		
One day on Liver Surgery Symposia		
Teaching		
Bachelor students		
Rianne Meijer	2009	0.5
Erhan Ceylann	2009	0.5
Hella Muijsers	2010	0.5
Steven van der Werff	2010	0.5
Jende Zijlmans	2012	0.5
Derya Aydemirli	2012	0.5
Sophie de Ruijter	2012	0.5
Master students		
Wadim de Boon	2012	0.5
Peter Albers	2011	1.0
Wadim de Boon	2011	1.0
Sanne Smit	2012	1.0
Sebastiaan Hemelrijk	2012	1.0
TU Delft, Dept. of Industrial Design. "design considerations in transplantation surgery"	2011	0.5
Oral presentations		
European Society for Surgical Research		
• Hydrogen sulfide does not induce hypometabolism in pigs	2010	0.5
Symposium Experimental Research Surgical Specialisms		
• Hydrogen sulfide (H2S) does not induce hypometabolism in pigs	2010	0.5
• Effect of temperature on indocyanine green (ICG) clearance	2012	0.5
• Temperature dependence of indocyanine green clearance	2012	0.5
Poster presentations		
Symposium Experimental Research Surgical Specialisms		
• Bloodretention after washout of the rat liver with different preservation solutions	2009	0.5
European Society for Surgical Research		
• The Airdrive: a disposable hypothermic oxygenated machine perfusion system for the liver	2010	0.5
International Hepato-Pancreatico Billiary Association		
• Erythrocyte retention after wash-out of the rat liver using different preservation solutions	2011	0.5
• Temperature dependence of indocyanine green clearance	2012	0.5

SUMMARIES

SUMMARY

The work described in this dissertation, On the Physiology of Artificial Hibernation, aims to translate insights from the physiology of natural hibernators to a model of artificial hibernation that could aid clinical applications.

In **Part I**, the governing physiological elements that are responsible for the induction of (artificial) hibernation are discussed. Translation of natural hibernation to its artificial counterpart is currently hampered by incomplete understanding of the exact mechanisms responsible for induction of hibernation.

To facilitate this translation, in **Chapter 1**, a model was developed that identifies the necessary physiological changes for induction of artificial hibernation. This model encompasses six essential components: metabolism (anabolism and catabolism), body temperature, thermoneutral zone, substrate, ambient temperature, and hibernation-inducing agents. The individual components are interrelated and collectively govern the induction and sustenance of a hypometabolic state. To illustrate the potential validity of this model, various pharmacological agents (hibernation induction trigger, delta-opioid, hydrogen sulfide, 5'-adenosine monophosphate, thyronamine, 2-deoxyglucose, magnesium) are described in terms of their influence on specific components of the model and corollary effects on metabolism.

Then, **Chapter 2** dives deeper into one of the critical elements to gain control over induction of (artificial) hibernation, to achieve a significant and sustained reduction in body temperature. A reduction in body temperature can be achieved by a downward adjustment of the thermoneutral zone, a process also described as anapyrexia. Pharmacological induction of anapyrexia could enable numerous applications in medicine. To identify the potential of pharmacological agents to induce anapyrexic signaling, experimental findings of over a thousand pharmacologically active compounds are analyzed for their ability to induce anapyrexia in animals. Based on this analysis, eight agents (helium, dimethyl sulfoxide, reserpine, (oxo)tremorine, pentobarbital, (chlor)promazine, insulin, and acetaminophen) are identified as potential anapyrexia-inducing compounds and discussed in detail, along with the

translational pitfalls for each candidate compound. Of the agents discussed, reserpine, (oxo)tremorine, and (chlor)promazine may possess true anapyrexic properties based on their ability to either affect the thermoneutral zone or its effectors and facilitate hypothermic signaling.

In **Part II**, the effects of a popular biochemical agent for inducing artificial hibernation, hydrogen sulfide (H_2S), are evaluated for use in large and small non-hibernating animals.

Chapter 3 starts with a series of experiments that demonstrated several adverse effects of H_2S in a large-animal model. Numerous studies in small rodents have demonstrated that H_2S induces hypometabolism, supposedly as a result of histotoxic hypoxia. However, other studies have shown that the induction of hypometabolism by H_2S is absent in large animals. To determine the cause of this animal size-dependent discrepancy in H_2S pharmacodynamics, the effects of sodium H_2S on systemic, pneumocardial, hematological, biochemical, microvascular (sublingual), and histological parameters are investigated in pigs. After four hours following H_2S administration, no effects are observed with respect to systemic, pneumocardial, hematological, biochemical, and histological parameters. However, H_2S does trigger significant hyperperfusion in the sublingual microcirculation, as evidenced by an increased blood vessel diameter, total vessel density, and perfused vessel density. These phenomena are consistent with microvascular changes that occur during a panting response; an important heat loss mechanism (i.e., thermoregulatory effector) in pigs that is controlled by the thermoneutral zone (Z_{tn}). On the basis of our findings and the literature, a mechanistic explanation is provided for the differential manifestation of hypometabolism between small and large animals. In large animals, H_2S does not act via histotoxic hypoxia but likely triggers carotid bodies to transmit a hypoxic signal, which subsequently lowers the Z_{tn} and activates heat loss mechanisms (e.g., panting) to align ATP consumption with ATP production through hypothermia. Since large animals have a small surface:size ratio, the cooling rate is too inefficient to accommodate hypothermia and subsequent hypometabolism. This is why large animals do not exhibit hypometabolism, despite the activation of thermoregulatory effectors. This is also a reason for the poor translatability of artificial hypometabolism to the clinical setting.

Chapter 4, subsequently, goes back to a small-animal model (mice) and compares the effects of H_2S to – what turns out to be – the more potent effects of hypoxia for the induction of artificial hibernation. H_2S gas in an atmosphere of mild hypoxia reportedly induces suspended animation in mice; a state analogous to hibernation entailing hypothermia and hypometabolism. However, using non-invasive thermographic imaging, we demonstrate that mice exposed to more severe hypoxia reduce their body temperature to ambient temperature, while mice exposed to H_2S gas under normoxic conditions did not exhibit this behavior. This suggests that mice undergo hypothermia in response to hypoxia, not as a direct effect of H_2S gas, which contradicts many of the previously reported findings and putative contentions.

Part III ends with a description of practical systems and strategies for bringing this model to single organ application in the liver, ultimately to be used to improve organ viability and transplantation success rates in clinical scenarios.

Chapter 5 describes the necessary preparations to the liver to maintain stable extracorporeal hepatic physiological function. In this context, an important aspect is donor graft washout, which can be impaired by colloids in organ preservation solutions that increase the viscosity and agglutinative propensity of red blood cells (RBCs) and potentially decrease organ function. Here, the colloid-induced agglutinative effects on RBCs and RBC retention after liver washout with Ringer's lactate (RL), histidine tryptophan ketoglutarate solution, University of Wisconsin solution, and Polysol are determined as a function of the washout pressure and temperature in a rat liver washout model with radiolabeled RBCs. Colloids (polyethylene glycol in Polysol and hydroxyethyl starch in University of Wisconsin) induce RBC agglutination, regardless of the solution composition. A single portal washout with any of the solutions does not result in differences in the degree of RBC retention, regardless of the temperature or pressure. After simultaneous arterial and portal washout at 37°C and 100 mm Hg of perfusion pressure, RL is associated with the lowest degree of radiolabeled RBC retention, and also required the shortest washout time.

Chapter 6 closes with the proposal of a machine perfusion system that

allows extended extracorporeal control of several of the model's elements. A potential method to increase the donor pool for organ transplantation is machine perfusion (MP). However, MP systems for liver grafts remain difficult to use because of organ-specific demands. Here, a novel, portable, pressure-regulated, oxygenating MP system for hypothermic preservation of the liver is developed, perfusing liver grafts via the portal vein (PV). In three porcine livers undergoing twenty hours of hypothermic perfusion using Belzer MP solution, the perfusate flow, temperature, venous pressure, and pO_2 and pCO_2 are monitored and biochemical and histological parameters are analyzed to determine post-preservation organ damage. Perfusate flow through the PV increases over time, while the PV pressure remains stable, and the perfusate temperature increases slightly. Aspartate aminotransferase and lactate dehydrogenase are increase significantly post-perfusion. Blood gas analysis shows a stable pO_2 before perfusion of the liver, which significantly reduces during MP, accompanied by a significantly increasing pCO_2. This demonstrates the feasibility of a portable MP system for preservation of the liver and shows that continuous perfusion via the PV can be maintained with an oxygen-driven pump system without notable preservation damage of the organ.

SAMENVATTING

Het onderzoek in dit proefschrift, On the Physiology of Artificial Hibernation, richt zich op het vertalen van inzichten uit de fysiologie van natuurlijke winterslapers naar een model voor kunstmatige winterslaap dat kan bijdragen aan orgaanpreservatie bij klinische toepassingen.

In **Deel I** worden de elementen die verantwoordelijk zijn voor de inductie van (kunstmatige) winterslaap besproken. Onvolledige kennis van de exacte mechanismen die verantwoordelijk zijn voor de inductie van winterslaap beperkt tot op heden de vertaling van een natuurlijke naar een kunstmatige winterslaap.

Om deze vertaling te faciliteren is in **Hoofdstuk 1** een model ontwikkeld dat de vereiste fysiologische factoren voor inductie van kunstmatige winterslaap identificeert. Dit model bestaat uit zes essentiële componenten: metabolisme (anabolisme en catabolisme), lichaamstemperatuur, thermoneutrale zone, substraat, omgevingstemperatuur, en winterslaap-inducerend middel. Deze individuele bouwstenen staan onderling met elkaar in verband en bepalen samen de inductie en de instandhouding van een hypometabole staat. Om de impact van dit model te illustreren, worden verschillende winterslaap-inducerende middelen beschreven – hibernation induction trigger, delta-opoiden, waterstof sulfide, 5'-adenosine monofosfaat, thyronamine, 2-deoxyglucose en magnesium – en hun werking op de verschillende elementen van het model, alsmede de daaropvolgende metabolische effecten.

Vervolgens gaat **Hoofdstuk 2** dieper in op één van de essentiële factoren die controle geven over de inductie van (kunstmatige) winterslaap: anapyrexie. Een daling in lichaamstemperatuur kan worden bewerkstelligd door het naar beneden bijstellen van de thermoneutrale zone, een proces dat wordt beschreven als anapyrexie. Farmacologische inductie van anapyrexie maakt talrijke medische toepassingen mogelijk. Om het vermogen van farmacologische middelen om anapyrexie te induceren te identificeren, heeft deze studie via literatuuronderzoek een analyse van meer dan duizend farmacologische middelen gemaakt. Hierbij is het vermogen om anapyrexie te induceren in verschillende diermodellen getoetst. Op basis van deze

analyse zijn acht middelen geïdentificeerd die over de potentie beschikken om anapyrexie te induceren, namelijk helium, dimethyl sulfoxide, reserpine, (oxo)tremorine, pentobarbital, (chlor)promazine, insuline en acetaminophen. Elk van deze middelen wordt in detail besproken, en in relatie tot de valkuilen van translatie. Van de besproken middelen is bij reserpine, (oxo)tremorine, en (chlor)promazine op basis van de effecten op de thermoneutrale zone aanleiding om ervan uit te gaan dat deze middelen anapyrexie kunnen induceren, of faciliteren via hypotherme signallering.

In **Deel II** worden de effecten van het veelgebruikte biochemische winterslaap-inducerend middel waterstofsulfide (H_2S) geëvalueerd voor gebruik in grote en kleine dieren zonder natuurlijke winterslaap.

Hoofdstuk 3 begint met een serie experimenten die de nadelige effecten van H_2S in grote dieren demonstreren. Talrijke studies lieten al eerder zien dat H_2S hypometabolisme in kleine dieren kan induceren, vermoedelijk als resultaat van histotoxische hypoxie. Andere studies laten echter zien dat deze inductie in grote dieren afwezig is bij het gebruik van H_2S. Om te bepalen wat de oorzaak is van deze discrepantie in de resultaten tussen kleine en grote dieren, zijn de effecten van natrium H_2S onderzocht in een varkensmodel op systemisch, pneumocardiaal, hematologisch, biochemisch, microvasculair (sublinguaal) en histologisch niveau. Na vier uur blootstelling aan H_2S werden geen effecten geobserveerd op systemisch, pneumocardiaal, hematologisch, biochemisch, en histologisch niveau. Op microvasculair niveau liet H_2S echter subliguale hypoperfusie zien in de vorm van toename in bloedvat diameter, totale vaatdichtheid en dichtheid van geperfuseerde vaten. Dit fenomeen is in overeenkomst met de microvasulaire veranderingen die plaatsvinden bij hijgen; een belangrijk mechanisme om warmte kwijt te raken bij varkens (ook wel thermoregulatoire effector genoemd), dat onder controle staat van de thermoneutrale zone (Z_{tn}). Op basis van deze bevindingen en de literatuur geeft dit hoofdstuk een mechanistische verklaring voor de verschillende manifestaties van hypometabolisme in kleine en grote dieren. In grote dieren werkt H_2S niet via de histotoxische hypoxie, maar vermoedelijk via transmissie van een hypoxisch signaal vanuit chemoreceptoren in de carotiden. Dit signaal heeft een Z_{tn}-verlagend effect welke aanzet tot mechanismen om warmte kwijt te raken, zoals hijgen, met als doel om de energieconsumptie

met energieproductie te balanceren via hypothermie. Aangezien grote dieren een relatief kleine oppervlakte:inhoud ratio hebben, is de snelheid van afkoelen niet efficiënt genoeg om de lichaamstemperatuur te doen dalen voor hypometabolisme. Dit is waarom grote dieren geen hypometabolisme laten zien, ondanks activatie van thermoregulatoire effectoren. Dit is ook de reden waarom kunstmatige winterslaap slecht om te zetten is naar de klinische situatie.

Hoofdstuk 4 gaat vervolgens terug naar kleinere dieren (muis), om de effecten van H_2S te vergelijken met de – naar zal blijken potentere – effecten van hypoxia voor de inductie van kunstmatige winterslaap. Blootstelling aan H_2S gas met milde hypoxie veroorzaakt naar verluidt een staat van suspended animation in muizen; een staat die analoog is aan winterslaap met karakteristieke effecten als hypothermie en hypometabolisme. Echter, door middel van niet-invasieve thermografische imaging demonstreren we dat muizen die worden blootgesteld aan sterkere hypoxie hun lichaamstemperatuur laten dalen tot de omgevingstemperatuur. Dit in tegenstelling tot muizen die worden blootgesteld aan H_2S gas met een normaal zuurstofgehalte (normoxie), die dit gedrag niet laten zien. Dit suggereert dat muizen hypothermie ondergaan in reactie op hypoxie, en niet als direct effect van H_2S. Dit komt niet overeen met eerder gepubliceerde bevindingen en vermeende stellingen.

Deel III eindigt met een beschrijving van praktische systemen en strategieën die dit model vertalen naar de toepassing op één enkel orgaan, de lever. Het doel hiervan is de optimalisatie van donororgaankwaliteit en de verhoogde slagingskans van transplantaties in klinische scenario's.

Hoodstuk 5 beschrijft de noodzakelijke voorbereidingen om de lever buiten het lichaam in een stabiele staat te kunnen bewaren met behoud van de fysiologische functie. Het schoonwassen van een graft is in deze situatie belangrijk, maar kan beïnvloed worden door colloiden die in orgaanpreservatievloeistoffen zitten. Colloiden kunnen de viscositeit en agglutinatie-eigenschappen van rode bloedcellen versterken, en uiteindelijk de orgaanfunctie beperken. Na het spoelen van de lever met Ringer lactaat (RL), histidine tryptofaan ketogluteraat (HTK), University of Wisconsin (UW) en Polysol (PS), worden hier colloid-geïnduceerde agglutinatie-effecten van

rode bloedcellen, en retentie van deze cellen in de lever, bepaald als functie van druk en temperatuur in het ratmodel met radioactief gelabelde rode bloedcellen. Colloiden (polythyleen glycol in PS en hydroxyethyl starch in UW) induceren agglutinatie van rode bloedcellen, ongeacht de samenstelling van de vloeistof. Spoeling via de vena porta laat geen verschillende uitkomsten zien in retentie van rode bloedcellen tussen de verschillende vloeistoffen, ongeacht de temperatuur en/of de druk. Na gelijktijdige spoeling via de vena porta en arteria hepatica op 37 °C met 100 mm Hg druk, laat RL de laagste retentie van gelabelde rode bloedcellen zien, met de kortste spoelingstijd.

Hoodstuk 6 sluit met een voorstel voor een perfusiemachine die langdurige extra-corporale controle biedt van verschillende elementen uit het model. Een potentiële manier voor het vergroten van de poel van organen voor transplantatie is het gebruik van machineperfusie (MP). Echter, MP van de lever blijft moeilijk vanwege de orgaanspecifieke eisen. In dit hoofdstuk wordt een nieuw, draagbaar, druk-gereguleerd, en geoxygeneerd MP systeem voorgesteld dat is ontwikkeld voor gebruik van de lever met perfusie via de vena porta. In het bijbehorende onderzoek werden stroomsnelheid van perfusaat, temperatuur, veneuze druk, pO_2 en pCO_2 bepaald tijdens 20 uur perfusie van drie varkenslevers met Belzer MP vloeistof. Biochemische en histologische parameters werden gebruikt om preservatieschade vast te stellen. Stroomsnelheid via de vena porta liep geleidelijk terug, bij een stabiele druk en licht stijgende temperatuur. Aspertaat aminotransferase en lactaat dehydrogenase stegen significant na de perfusie. Bloedgasanalyse liet een stabiele pO_2 zien voor aanvang van perfusie, en een significante daling tijdens perfusie die samenging met een significante stijging in pCO_2. Deze studie demonstreert de haalbaarheid van draagbare machineperfusie voor preservatie van de lever, en laat zien dat perfusie via de vena porta behouden kan blijven via een zuurstof-gedreven pompsysteem zonder noemenswaardige schade aan het orgaan.

REFERENCES

REFERENCES

Abbotts B, Wang LC, Glass JD. Absence of evidence for a hibernation "trigger" in blood dialysate of Richardson's ground squirrel. Cryobiology 1979 Apr; (16(2): 179-183

Abello R, Haynie TP, Kim EE. Pitfalls of a 99mTc-RBC bleeding study due to gallbladder and ileal-loop visualization. Gastrointest Radiol 1991; 16: 32-34.

Al-Badry KS, Taha HM. Hibernation-hypothermia and metabolism in hedgehogs. Changes in water and electrolytes. Comp Biochem Physiol A Comp Physiol 1983; 74: 435-441.

Ali MY, Ping CY, Mok YY, Ling L, Whiteman M, Bhatia M, Moore PK. Regulation of vascular nitric oxide in vitro and in vivo; a new role for endogenous hydrogen sulphide? Br J Pharmacol 2006; 149: 625-634.

Almeida MC, Hew-Butler T, Soriano RN, Rao S, Wang W, Wang J, Tamayo N, Oliveira DL, Nucci TB, Aryal P, Garami A, Bautista D, Gavva NR, Romanovsky AA. Pharmacological blockade of the cold receptor TRPM8 attenuates autonomic and behavioral cold defenses and decreases deep body temperature. J Neurosci 2012; 32: 2086-2099.

Althaus M, Urness KD, Clauss WG, Baines DL, Fronius M. The gasotransmitter hydrogen sulphide decreases Na+ transport across pulmonary epithelial cells. Br J Pharmacol 2012; 166: 1946-1963.

Ananiadou OG, Bibou K, Drossos GE, Bai M, Haj-Yahia S, Charchardi A, Johnson EO. Hypothermia at 10 degrees C reduces neurologic injury after hypothermic circulatory arrest in the pig. J Card Surg 2008; 23: 31-38.

Armitage WJ, Dale W, Alexander EA. Protocols for thawing and cryoprotectant dilution of heart valves. Cryobiology 2005; 50: 17-20.

Arrhenius SA. Über die Dissociationswärme und den Einfluß der Temperatur auf den Dissociationsgrad der Elektrolyte. Zeitschrift für Phys Chemie 1889; 4, 96-116.

Asfar P, Calzia E, Radermacher P. Is pharmacological, H2S-induced 'suspended animation' feasible in the ICU? Crit Care 2014; 18, 215.

Aslami H, Schultz MJ, Juffermans NP. Potential applications of hydrogen sulfide-induced suspended animation. Curr Med Chem 2009; 16: 1295-1303.

Aslami H, Heinen A, Roelofs JJ, Zuurbier CJ, Schultz MJ, Juffermans NP. Suspended animation inducer hydrogen sulfide is protective in an in vivo model of ventilator-induced lung injury. Intensive Care Med 2010; 36: 1946-1952.

Aslami H, Beurskens CJ, de Beer FM, Kuipers MT, Roelofs JJ, Hegeman MA, van der Sluijs KF, Schultz MJ, Juffermans NP. A short course of infusion of a hydrogen sulfide-donor attenuates endotoxemia induced organ injury via stimulation of anti-inflammatory pathways, with no additional protection from prolonged infusion. Cytokine 2013; 61, 614-621.

Avery DD. Intrahypothalamic adrenergic and cholinergic injection effects on temperature and ingestive behavior in the rat. Neuro-pharmacology 1971; 10: 753-763.

Aw TY, Jones DP. Secondary bioenergetic hypoxia. Inhibition of sulfation and glucuronidation reactions in isolated hepatocytes at low O2 concentration. J Biol Chem 1982; 257: 8997-9004.

Axelrod YK, Diringer MN. Temperature management in acute neurologic disorders. Neurol Clin 2008; 26: 585-603.

Ayoub SS, Botting RM, Goorha S, Colville-Nash PR, Willoughby DA, Ballou LR. Acetaminophen-induced hypothermia in mice is mediated by a prostaglandin endoperoxide synthase 1 gene-derived protein. Proc Natl Acad Sci U S A 2004; 101: 11165-11169.

Azoulay D, Eshkenazy R, Andreani P, Castaing D, Adam R, Ichai P, Naili S, Vinet E, Saliba F, Lemoine A, Gillon MC, Bismuth H. In situ hypothermic perfusion of the liver versus standard total vascular exclusion for complex liver resection. Ann Surg 2005; 241: 277-285.

Bakar B, Kose EA, Sonal S, Alhan A, Kilinc K, Keskil IS. Evaluation of the neurotoxicity of DMSO infused into the carotid artery of rat. Injury 2012; 43: 315-322.

Barnas GM, Rautenberg W. Shivering and cardiorespiratory responses during normocapnic hypoxia in the pigeon. J Appl Physiol (1985) 1990; 68: 84-87.

Basile DP, Friedrich JL, Spahic J, Knipe N, Mang H, Leonard EC, Changizi-Ashtiyani S, Bacallao RL, Molitoris BA, Sutton TA. Impaired endothelial proliferation and mesenchymal transition contribute to vascular rarefaction following acute kidney injury. Am J Physiol Renal Phys 2011; 300: F721-F733.

Baumgart K, Wagner F, Gröger M, Weber S, Barth E, Vogt JA, Wachter U, Huber-Lang M, Knöferl MW, Albuszies G, Georgieff M, Asfar P, Szabó C, Calzia E, Radermacher P, Simkova V. Cardiac and metabolic effects of hypo- thermia and inhaled hydrogen sulfide in anesthetized and ventilated mice. Crit Care Med 2010; 38: 588-595.

Beauchamp RO, Jr., Bus JS, Popp JA, Boreiko CJ, Andjelkovich DA. A critical review of the literature on hydrogen sulfide toxicity. Crit Rev Toxicol 1984; 13: 25-97.

Beaudry JL, McClelland GB. Thermogenesis in CD-1 mice after combined chronic hypoxia and cold acclimation. Comp Biochem Physiol B Biochem Mol Biol 2010; 157: 301-309.

Bechtold DA, Sidibe A, Saer BR, Li J, Hand LE, Ivanova EA, Darras VM, Dam J, Jockers R, Luchman SM, Loudon AS. A role for the melatonin-related receptor GPR50 in leptin signaling, adaptive thermogenesis, and torpor. Curr Biol 2012; 22, 70-7.

Benamar K, Rawls SM, Geller EB, Adler MW. Intrahypothalamic injection of deltorphin-II alters body temperature in rats. Brain Res 2004; 1019: 22-27.

Bereiter-Hahn J, Helmaier G, Carey HV, Herwig A, Coukèr A, Henning RH, Cerri M, Hut R, Ruf T, Dirkes MC, Singer D, Drew KL, Vya-Zouskiy V. ESA Topical Team "Hibernation and Torpor" Recommendations to ESA. ESA, ESTECT, Noordwijk, The Netherlands 2015

Bernard SA, Gray TW, Buist MD, Jones BM, Silvester W, Gutteridge G, Smith K. Treatment of comatose survivors of out-of-hospital cardiac arrest with induced hypothermia. N Engl J Med 2002; 346: 557-563.

Bessems M, Doorschodt BM, van Marle J, Vreeling H, Meijer AJ, van Gulik TM. Improved machine perfusion preservation of the non-heart-beating donor rat liver using Polysol: a new machine perfusion preservation solution. Liver Transpl 2005; 11: 1379-1388.

Bessems M, 't Hart NA, Tolba R, Doorschodt BM, Leuvenink HG, Ploeg RJ, Minor T, van Gulik TM. The isolated perfused rat liver: standardization of a time-honoured model. Lab Anim 2006; 40: 236-246. (a)

Bessems M, Doorschodt BM, Albers PS, Meijer AJ, van Gulik TM. Wash-out of the non-heart-beating donor liver: a matter of flush solution and temperature? Liver Int 2006; 26: 880-888. (b)

Bishop JJ, Nance PR, Popel AS, Intaglietta M, Johnson PC. Effect of erythrocyte aggregation on velocity profiles in venules. Am J Physiol Heart Circ Physiol 2001; 280: H222-H236.

Bito LZ, Roberts JC. The effects of hibernation on the chemical composition of cerebrospinal and intraocular fluids, blood plasma and brain tissue of the woodchuck (Marmota monax). Comp Biochem Physiol A Comp Physiol 1974; 47: 183-193.

Blackstone E, Morrison M, Roth MB. H2S induces a suspended animation-like state in mice. Science 2005; 308: 518.

Blackstone E, Roth MB. Suspended animation-like state protects mice from

lethal hypoxia. Shock 2007; 27: 370-372.

Bonventre JV, Cheung JY. Effects of metabolic acidosis on viability of cells exposed to anoxia. Am J Physiol 1985; 249(pt 1): C149-C159.

Bos EM, Leuvenink HG, Snijder PM, Kloosterhuis NJ, Hillebrands JL, Leemans JC, Florquin S, van Goor H. Hydrogen sulfide-induced hypometabolism prevents renal ischemia/ reperfusion injury. J Am Soc Nephrol 2009; 20: 1901-1905.

Boissier JR, Giudicelli JF, Larno S, Advenier C. Differential inotropic-chronotropic action of thyronamine. Eur J Pharmacol 1973 May; 22(2): 141-149.

Boulant JA. Role of the preoptic anterior hypothalamus in thermoregulation and fever. Clin Infect Dis 2000; 31 Suppl 5: S157- S161.

Bradham GB, Sample JJ. The vascular and thermal effects of dimethyl sulfoxide. Ann N Y Acad Sci 1967; 141: 225-230.

Branco LG. Effects of 2-deoxy-D-glucose and insulin on plasma glucose levels and behavioral thermoregulation of toads. Am J Physiol 1997; 272: R1-R5.

Branco LG, Carnio EC & Barros RC. Role of the nitric oxide pathway in hypoxia-induced hypothermia of rats. Am J Physiol 1997; 273, R967-71.

Braulke LJ, Klingenspor M, DeBarber A, Tobias SC, Grandy DK, Scanlan TS, Heldmaier G. 3-Iodothyronamine: a novel hormone controlling the balance between glucose and lipid utilisation. J Comp Physiol B 2008; 178: 167-177.

Brill DR. Gallbladder visualization during technetium- 99m-labeled red cell scintigraphy for gastrointestinal bleeding. J Nucl Med 1985; 26: 1408-1411.

Broccardo M, Improta G. Hypothermic effect of D-Ala-deltorphin II, a selective delta opioid receptor agonist. Neurosci Lett 1992; 139: 209-212.

Brockmann J, Reddy S, Coussios C, Pigott D, Guirriero D, Hughes D, Morovat A, Roy D, Winter L, Friend PJ. Normothermic perfusion: a new paradigm for organ preservation. Ann Surg 2009; 250: 1-6.

Brodie BB, Finger KF, Orlans FB, Quinn GP, Sulser F. Evidence that tranquilizing action of reserpine is associated with change in brain serotonin and not in brain norepinephrine. J Pharmacol Exp Ther 1960; 129: 250-256.

Brodsky SV, Yamamoto T, Tada T, Kim B, Chen J, Kajiya F, Goligorsky MS. Endothelial dysfunction in ischemic acute renal failure: rescue by transplanted endothelial cells. Am J Physiol Renal Physiol 2002; 282: F1140-F1149.

Bruce DS, Cope GW, Elam TR, Ruit KA, Oeltgen PR, Su TP. Opioids and hibernation. I. Effects of naloxone on bear HIT'S depression of guinea pig ileum contractility and on induction of summer hibernation in the ground squirrel. Life Sci 1987; 41: 2107-2113.

Bruce DS, Darling NK, Seeland KJ, Oeltgen PR, Nilekani SP. Is the polar bear (Ursus maritimus) a hibernator? Continued studies on opioids and hibernation. Pharmacol Biochem Behav 1990 Mar; 35(3): 705-711.

Bruce DS, Bailey EC, Setran DP, Tramell MS, Jacobson D, Oeltgen PR, Horton ND, Hellgren EC. Circannual variations in bear plasma albumin and its opioid-like effects on guinea pig ileum. Pharmacol Biochem Behav 1996; 53: 885-889.

Buchanan TA, Cane P, Eng CC, Sipos GF, Lee C. Hypothermia is critical for survival during prolonged insulin-induced hypoglycemia in rats. Metabolism 1991; 40: 330-334.

Buckler KJ, Williams BA, Honore E. An oxygen-, acid- and anaesthetic-sensitive TASK-like background potassium channel in rat arterial chemoreceptor cells. J Physiol 2000; 525 Pt 1: 135-142.

Cannon B, Nedergaard J. Brown adipose tissue: function and physiological significance. Physiol Rev 2004; 84: 277-359.

References

Cereijo-Santalo R. Osmotic pressure and ATPase activity of rat liver mitochondria. Arch Biochem Biophys 1972; 152: 78-82.

Cerri M, Zamboni G, Tupone D, Dentico D, Luppi M, Martelli D, Perez E, Amici R. Cutaneous vasodilation elicited by disinhibition of the caudal portion of the rostral ventromedial medulla of the free-behaving rat. Neuroscience 2010; 165: 984-995.

Cerri M, Mastrotto M, Tupone D, Martelli D, Luppi M, Perez E, Zamboni G, Amici R. The inhibition of neurons in the central nervous pathways for thermoregulatory cold defense induces a suspended animation state in the rat. J Neurosci 2013; 33: 2984-2993.

Chai CY, Fann YD, Lin MT. Hypothermic action of chlorpromazine in monkeys. Br J Pharmacol 1976; 57: 43-49.

Chiellini G, Frascarelli S, Ghelardoni S, Carnicelli V, Tobias SC, DeBarber A, Brogioni S, Ronca-Testoni S, Cerbai E, Grandy DK, Scanlan TS, Zucchi R. Cardiac effects of 3-iodothyronamine: a new aminergic system modulating cardiac function. FASEB J 2007; 21: 1597-1608.

Cho AK, Haslett WL, Jenden DJ. The peripheral actions of oxotremorine, a metabolite of tremorine. J Pharmacol Exp Ther 1962; 138: 249-257.

Clapham JC. Central control of thermogenesis. Neuropharmacology 2012; 63, 111–123.

Clark WG. Changes in body temperature after administration of amino acids, peptides, dopamine, neuroleptics and related agents. Neurosci Biobehav Rev 1979; 3: 179-231.

Clark WG, Clark YL. Changes in body temperature after administration of acetylcholine, histamine, morphine, prostaglandins and related agents. Neurosci Biobehav Rev 1980; 4: 175- 240. (a)

Clark WG, Clark YL. Changes in body temperature after administration of adrenergic and serotonergic agents and related drugs including antidepressants. Neurosci Biobehav Rev 1980; 4: 281-375. (b)

Clark WG, Clark YL. Changes in body temperature after
administration of antipyretics, LSD, delta 9-THC, CNS depressants
and stimulants, hormones, inorganic ions, gases, 2,4-DNP and
miscellaneous agents. Neurosci Biobehav Rev 1981; 5: 1-136.

Clark WG, Lipton JM. Changes in body temperature after administration of amino acids, peptides, dopamine, neuroleptics and related agents: II. Neurosci Biobehav Rev 1985; 9: 299-371. (a)

Clark WG, Lipton JM. Changes in body temperature after administration of acetylcholine, histamine, morphine, prostaglandins and related agents: II. Neurosci Biobehav Rev 1985; 9: 479-552. (b)

Clark WG, Lipton JM. Changes in body temperature after administration of adrenergic and serotonergic agents and related drugs including antidepressants. II. Neurosci Biobehav Rev 1986; 10: 153-220.

Clark WG. Changes in body temperature after administration of antipyretics, LSD, delta 9-THC and related agents. II. Neurosci Biobehav Rev 1987; 11: 35-96.

Clausen G, Storesund A. Electrolyte distribution and renal function in the hibernating hedgehog. Acta Physiol Scand 1971; 83: 4-12.

Collman JP, Ghosh S, Dey A, Decréau RA. Using a functional enzyme model to understand the chemistry behind hydrogen sulfide induced hibernation. Proc Natl Acad Sci 2009; 106: 22090–22095.

Cooper CE, Brown GC. The inhibition of mitochondrial cytochrome oxidase by the gases carbon monoxide, nitric oxide, hydrogen cyanide and hydrogen sulfide: chemical mechanism and physiological significance. J Bioenerg Biomembr 2008; 40: 533–539.

Côté P, Polumbo RA, Harrison DC. Thyronamine, a new inotropic agent: its cardiovascular effects and mechanism of action. Cardiovasc Res 1974 Nov; 8(6): 721-730.

Cox B, Tha SJ. The role of dopamine and noradrenaline in temperature control of normal and reserpine-pretreated mice. J Pharm Pharmacol 1975; 27: 242-247.

Cox B. Pharmacologic control of temperature regulation. Annu Rev Pharmacol Toxicol 1977; 17: 341-353.

Crawshaw L, Grahn D, Wollmuth L, Simpson L. Central nervous regulation of body temperature in vertebrates: comparative aspects. Pharmacol Ther 1985; 30: 19-30.

Cuevasanta E, Denicola A, Alvarez B, Moller MN. Solubility and permeation of hydrogen sulfide in lipid membranes. PLoS One 2012; 7: e34562.

Dage RC. A centrally mediated prolonged hypotension produced by oxotremorine or pilocarpine. Br J Pharmacol 1979; 65: 15-21.

Daniels IS, Zhang J, O'Brien WG, III, Tao Z, Miki T, Zhao Z, Blackburn MR, Lee CC. A role of erythrocytes in adenosine monophosphate initiation of hypometabolism in mammals. J Biol Chem 2010; 285: 20716-20723.

Danzl DF, Pozos RS. Accidental hypothermia. N Engl J Med 1994; 331: 1756-1760.

Dark J, Miller DR, Zucker I. Reduced glucose availability induces torpor in Siberian hamsters. Am J Physiol 1994; 267: R496-R501.

Dark J, Miller DR, Licht P, Zucker I. Glucoprivation counteracts effects of testosterone on daily torpor in Siberian hamsters. Am J Physiol 1996; 270: R398-R403.

Dawe AR, Spurrier WA. Hibernation induced in ground squirrels by blood transfusion. Science 1969; 163: 298-299.

Dawe AR, Spurrier WA, Armour JA. Summer hibernation induced by cryogenically preserved blood "trigger". Science 1970; 168: 497-498.

Dawe AR, Spurrier WA. Summer hibernation of infants (six week old) 13-lined ground squirrels, Citellus tridecemlineatus. Cryobiology 1974 Feb; 11(1): 33-43.

Debbaut C, Monbaliu D, Casteleyn C, Cornillie P, van Loon D, Masschaele B, Pirenne J, Simoens P, van Hoorebeke L, Segers P. From vascular corrosion cast to electrical analog model for the study of human liver hemodynamics and perfusion. IEEE Trans Biomed Eng 2011; 58: 25–35.

Decima EE, Rand RW. Oxotremorine induced tremor in the decorticated cat. Int J Neuropharmacol 1965; 4: 139-148.

Del CJ, Engbaek L. The nature of the neuromuscular block produced by magnesium. J Physiol 1954; 124: 370-384.

Derwall M, Francis RC, Kida K, Bougaki M, Crimi E, Adrie C, Zapol WM, Ichinose F. Administration of hydrogen sulfide via extracorporeal membrane lung ventilation in sheep with partial cardiopulmonary bypass perfusion: a proof of concept study on metabolic and vasomotor effects. Crit Care 2011; 15: R51.

Deshpande R, Heaton N. Can non-heart-beating donors replace cadaveric heart-beating liver donors? J Hepatol 2006; 45: 499-503.

Dewanjee MK. Binding of 99mTc ion to hemoglobin. J Nucl Med 1974; 15: 703-706.

Dhillo WS, Bewick GA, White NE, Gardiner JV, Thompson EL, Bataveljic A, Murphy KG, Roy D, Patel NA, Scutt JN, Armstrong A, Ghatei MA, Bloom SR. The thyroid hormone derivative 3-iodothyronamine increases food intake in rodents. Diabetes Obes Metab 2009 Mar; 11(3): 251-260.

Dinant S, Roseboom HJ, Levi M, van Vliet AK, van Gulik TM. Hypothermic in situ perfusion of the porcine liver using Celsior or Ringer-lactate solution. Langenbecks Arch Surg

2009; 394: 143-150.

Dippel DW, van Breda EJ, van der Worp HB, van Gemert HM, Kappelle LJ, Algra A, Koudstaal PJ. Timing of the effect of acetaminophen on body temperature in patients with acute ischemic stroke. Neurology 2003; 61: 677-679.

Dirkes MC, Post IC, Heger M, van Gulik TM. A novel oxygenated machine perfusion system for preservation of the liver. Artif Organs 2013; 37: 719-724.

Dirkes MC, Milstein DM, Heger M, van Gulik TM. Absence of hydrogen sulfide-induced hypometabolism in pigs: a mechanistic explanation in relation to small nonhibernating mammals. Eur Surg Res 2015; 54: 178-191.

Dirkes MC, van Gulik TM, Heger M. Survey and critical appraisal of pharmacological agents with potential thermo-regulatory properties in the context of artificially induced hypometabolism. J Clin Transl Res 2015(1): 6-12.

Donatti AF, Soriano RN, Sabino JP, Branco LGS. Involvement of endogenous hydrogen sulfide (H2S) in the rostral ventrolateral medulla (RVLM) in hypoxia-induced hypothermia. Brain Res Bull 2014; 108, 94–9.

Dorman DC, Brenneman KA, Struve MF, Miller KL, James RA, Marshall MW, Foster PM. Fertility and developmental neurotoxicity effects of inhaled hydrogen sulfide in Sprague-Dawley rats. Neurotoxicol Teratol 2000; 22: 71–84.

Doyle KP, Suchland KL, Ciesielski TM, Lessov NS, Grandy DK, Scanlan TS, Stenzel-Poore MP. Novel thyroxine derivatives, thyronamine and 3-iodothyronamine, induce transient hypothermia and marked neuroprotection against stroke injury. Stroke 2007; 38: 2569-2576.

Drabek T, Kochanek PM, Stezoski J, Wu X, Bayir H, Morhard RC, Stezoski SW, Tisherman SA. Intravenous hydrogen sulfide does not induce hypothermia or improve survival from hemorrhagic shock in pigs. Shock 2011; 35: 67-73.

Dupre RK, Owen TL. Behavioral thermoregulation by hypoxic rats. J Exp Zool 1992; 262: 230-235.

Duterte-Boucher D, Panissaud C, Michael-Titus A, Costentin J. Stimulation of central D1 dopamine receptors reverses reserpine-induced hypothermia in mice. Neuropharmacology 1989; 28: 419-421.

Ebel H, Gunther T. Magnesium metabolism: a review. J Clin Chem Clin Biochem 1980; 18: 257-270.

Edwards BA, Munday KA. Electrolyte metabolism in the hibernating hedgehog (Erinaceus europaeus). Comp Biochem Physiol 1969; 31: 329-335.

Feldberg W, Myers RD, Veale WL. Perfusion from cerebral ventricle to cisterna magna in the unanaesthetized cat. Effect of calcium on body temperature. J Physiol 1970; 207: 403-416.

Feng L, Zhao N, Yao X, Sun X, Du L, Diao X, Li S, Li Y. Histidine-tryptophan-ketoglutarate solution vs. University of Wisconsin solution for liver transplantation: a systematic review. Liver Transpl 2007; 13: 1125-1136.

Ferren LG, South FE, Jacobs HK. Calcium and magnesium levels in tissues and serum of hibernating and cold-acclimated hamsters. Cryobiology 1971; 8: 506-508.

Fox RH, Davies TW, Marsh FP, Urich H. Hypothermia in a young man with an anterior hypothalamic lesion. Lancet 1970; 2: 185-188.

Frank SM, Higgins MS, Breslow MJ, Fleisher LA, Gorman RB, Sitzmann JV, Raff H, Beattie C. The catecholamine, cortisol, and hemodynamic responses to mild perioperative hypothermia. A randomized clinical trial. Anesthesiology 1995; 82: 83-93.

Frankenhaeuser B, Meves H. The effect of magnesium and calcium on the frog

myelinated nerve fibre. J Physiol 1958; 142: 360-365.

Frappell P, Lanthier C, Baudinette RV, Mortola JP. Metabolism and ventilation in acute hypoxia: a comparative analysis in small mammalian species. Am J Physiol 1992; 262: R1040-R1046.

Ganster F, Burban M, de la Bourdonnaye M, Fizanne L, Douay O, Loufrani L, Mercat A, Calès P, Radermacher P, Henrion D, Asfar P, Meziani F. Effects of hydrogen sulfide on hemodynamics, inflammatory response and oxidative stress during resuscitated hemorrhagic shock in rats. Crit Care 2010; 14(5): R165.

Gastaca M. Biliary complications after orthotopic liver transplantation: a review of incidence and risk factors. Transplant Proc 2012; 44: 1545-1549.

Gautier H, Bonora M, M'Barek SB, Sinclair JD. Effects of hypoxia and cold acclimation on thermoregulation in the rat. J Appl Physiol (1985) 1991; 71: 1355-1363.

Gautier H. Interactions among metabolic rate, hypoxia, and control of breathing. J Appl Physiol 1996; 81, 521-7.

Geiser F, Ruf T. Hibernation versus daily torpor in mammals and birds-physiological variables and classification of torpor patterns. Physiological Zoology 1995; 68: 935-966.

Geiser F. Metabolic rate and body temperature reduction during hibernation and daily torpor. Annu Rev Physiol 2004; 66: 239-274.

Giesbrecht GG, Fewell JE, Megirian D, Brant R, Remmers JE. Hypoxia similarly impairs metabolic responses to cutaneous and core cold stimuli in conscious rats. J Appl Physiol (1985) 1994; 77: 726-730.

Giordano A, Frontini A, Castellucci M, Cinti S. Presence and distribution of cholinergic nerves in rat mediastinal brown adipose tissue. J Histochem Cytochem 2004; 52: 923-930.

Gleeson M, Barnas GM, Rautenberg W. The effects of hypoxia on the metabolic and cardiorespiratory responses to shivering produced by external and central cooling in the pigeon. Pflugers Arch 1986; 407: 312-319.

Goedhart PT, Khalilzada M, Bezemer R, Merza J, Ince C. Sidestream dark field (SDF) imaging: a novel stroboscopic LED ring-based imaging modality for clinical assessment of the microcirculation. Opt Express 2007; 15: 15101-15114.

Gómez G, Pikal MJ, Rodríguez-Hornedo N. Effect of initial buffer composition on pH changes during far-from-equilibrium freezing of sodium phosphate buffer solutions. Pharm Res 2001; 18: 90-97.

Gonzalez C, Almaraz L, Obeso A, Rigual R. Carotid body chemo-receptors: from natural stimuli to sensory discharges. Physiol Rev 1994; 74: 829-898.

Goodwin M. Good laboratory practice 30 years on: challenges for industry. Ann Ist Super Sanita 2008; 44: 369-373.

Gordon CJ, Mohler FS, Watkinson WP, Rezvani AH. Temperature regulation in laboratory mammals following acute toxic insult. Toxicology 1988; 53: 161-178.

Gordon CJ, Fogelson L. Comparative effects of hypoxia on behavioral thermoregulation in rats, hamsters, and mice. Am J Physiol 1991; 260: R120-R125.

Gordon CJ. The therapeutic potential of regulated hypothermia. Emerg Med J 2001; 18: 81-89.

Griffiths AP, Henderson M, Penn ND, Tindall H. Haematological, neurological and psychiatric complications of chronic hypothermia following surgery for craniopharyngioma. Postgrad Med J 1988; 64: 617-620.

Guarrera JV, Polyak M, O'Mar Arrington B, Kapur S, Stubenbord WT, Kinkhabwala M. Pulsatile machine perfusion with vasosol solution improves early graft function

after cadaveric renal transplantation. Transplantation 2004; 77: 1264-1268.

Guarrera JV, Karim NA. Liver preservation: is there anything new yet? Curr Opin Organ Transplant 2008; 13: 148-154.

Guarrera JV, Henry SD, Samstein B, Odeh-Ramadan R, Kinkhabwala M, Goldstein MJ, Ratner LE, Renz JF, Lee HT, Brown RS Jr, Emond JC. Hypothermic machine preservation in human liver transplantation: the first clinical series. Am J Transplant 2010; 10: 372-381.

Haggag G, Raheem KA, Khalil F. Hibernation in reptiles. I. Changes in blood electrolytes. Comp Biochem Physiol 1965; 16: 457-465.

Hahin R, Campbell DT. Simple shifts in the voltage dependence of sodium channel gating caused by divalent cations. J Gen Physiol 1983; 82: 785-805.

Hammel HT, Hardy JD, Fusco MM. Thermoregulatory responses to hypothalamic cooling in unanesthetized dogs. Am J Physiol 1960; 198: 481–486.

Han W, Dong Z, Dimitropoulou C, Su Y. Hydrogen sulfide ameliorates tobacco smoke-induced oxidative stress and emphysema in mice. Antioxid Redox Signal 2011; 15: 2121–2134.

Haouzi P, Notet V, Chenuel B, Chalon B, Sponne I, Ogier V, Bihain B. H2S induced hypometabolism in mice is missing in sedated sheep. Respir Physiol Neurobiol 2008; 160: 109-115.

Haouzi P, Bell HJ, Notet V, Bihain B. Comparison of the metabolic and ventilatory response to hypoxia and H2S in unsedated mice and rats. Respir Physiol Neurobiol 2009; 167: 316-322.

Hart ME, Suchland KL, Miyakawa M, Bunzow JR, Grandy DK, Scanlan TS. Trace amine-associated receptor agonists: synthesis and evaluation of thyronamines and related analogues. J Med Chem 2006; 49: 1101-1112.

't Hart NA, van der Plaats A, Leuvenink HG, Wiersema- Buist J, Olinga P, van Luyn MJ, Verkerke GJ, Rakhorst G, Ploeg RJ. Initial blood wash-out during organ procurement determines liver injury and function after preservation and reperfusion. Am J Transplant 2004; 4: 1836-1844.

't Hart NA, der van Plaats A, Leuvenink HG, van Goor H, Wiersema-Buist J, Verkerke GJ, Rakhorst G, Ploeg RJ. Determination of an adequate perfusion pressure for continuous dual vessel hypothermic machine perfusion of the rat liver. Transpl Int 2007; 20: 343-352.

Hascalik S, Celik O, Kekilli E, Elter K, Karakas HM, Aydin NE. Novel noninvasive detection method for endometriosis: research and development of scintigraphic survey on endometrial implants in rats. Fertil Steril 2008; 90: 209-213.

Hayden P, Lindberg RG. Hypoxia-induced torpor in pocket mice (genus: Perognathus). Comp Biochem Physiol 1970; 33: 167-179.

He Z, Yamawaki T, Yang S, Day AL, Simpkins JW, Naritomi H. Experimental model of small deep infarcts involving the hypothalamus in rats: changes in body temperature and postural reflex. Stroke 1999; 30: 2743-2751.

Heagy FC, Burton AC. Effect of intravenous injection of magnesium chloride on the body temperature of the unanesthetized dog, with some observations on magnesium levels and body temperature in man. Am J Physiol 1948; 152: 407-416.

Heger M, Marsman HA, Bezemer R, Cloos MA, van Golen RF, van Gulik TM. Non-invasive quantification of triglyceride content in steatotic rat livers by (1)H-MRS: when water meets (too much) fat. Acad Radiol 2011; 18: 1582–1592.

Heldmaier G, Ortmann S, Elvert R. Natural hypometabolism during hibernation and daily torpor in mammals. Respir Physiol Neurobiol 2004; 141, 317-329.

Heller HC, Colliver GW. CNS regulation of body temperature during hibernation. Am J Physiol 1974; 227, 583-9.

Heller HC, Colliver GW, Bread J. Thermoregulation during entrance into hibernation. Pflugers Arch 1977; 369, 55-9.

Heller HC. Hibernation: neural aspects. Annu Rev Physiol 1979; 41: 305-321.

Hemelrijk SD, Dirkes MC, van Velzen MHN, Bezemer R, van Gulik TM, Heger M. Exogenous hydrogen sulfide gas does not induce hypothermia in normoxic mice. Sci Rep 2018 Mar; 8(1): 3855

Hemingway A, Nahas GG. Effect of varying degrees of hypoxia on temperature regulation. Am J Physiol 1952; 170: 426-433.

Hessheimer AJ, Fondevila C, García-Valdecasas JC. Extracorporeal machine liver perfusion: are we warming up? Curr Opin Organ Transplant 2012; 17: 143-147.

Hill JR. The oxygen consumption of new-born and adult mammals. Its dependence on the oxygen tension in the inspired air and on the environmental temperature. J Physiol 1959; 149: 346- 373.

Hill BC, Woon TC, Nicholls P, Peterson J, Greenwood C, Thomson AJ. Interactions of sulphide and other ligands with cytochrome c oxidase. An electron-paramagnetic-resonance study. Biochem J 1984; 224: 591-600.

Hinrichsen CF, Maskrey M, Mortola JP. Ventilatory and metabolic responses to cold and hypoxia in conscious rats with discrete hypothalamic lesions. Respir Physiol 1998; 111: 247-256.

Hochachka PW, Buck LT, Doll CJ, Land SC. Unifying theory of hypoxia tolerance: molecular/metabolic defense and rescue mechanisms for surviving oxygen lack. Proc Natl Acad Sci U S A 1996; 93: 9493-9498.

Holzer M, Behringer W. Therapeutic hypothermia after cardiac arrest and myocardial infarction. Best Pract Res Clin Anaesthesiol 2008; 22: 711-728.

Horpácsy G, Scholz D, Althaus P, May G. Clinical experiences in the Gambro-preservation unit: analysis of 101 human cadaver kidneys. Eur Surg Res 1979; 11: 50–60.

Horstman DH, Banderet LE. Hypoxia-induced metabolic and core temperature changes in the squirrel monkey. J Appl Physiol Respir Environ Exerc Physiol 1977; 42: 273-278.

Horton ND, Kaftani DJ, Bruce DS, Bailey EC, Krober AS, Jones JR, Turker M, Khattar N, Su TP, Bolling SF, Oeltgen PR. Isolation and partial characterization of an opioid-like 88 kDa hibernation-related protein. Comp Biochem Physiol B Biochem Mol Biol 1998; 119: 787-805.

Hsieh AC, Carlson LD. Role of adrenaline and noradrenaline in chemical regulation of heat production. Am J Physiol 1957; 190: 243-246.

Hudson JW, Scott IM. Daily torpor in the laboratory mouse, Mus- musculus var. albino. Physiological Zoology 1979; 52: 205-218.

Hughes JD, Chen C, Mattar SG, Someren A, Noe B, Suwyn CR, Lumsden AB. Normothermic renal artery perfusion: a comparison of perfusates. Ann Vasc Surg 1996; 10: 123-130.

Humphreys RB, Hawkins M, Lipton JM. Effects of anesthetic injected into brainstem sites on body temperature and behavioral thermoregulation. Physiol Behav 1976; 17: 667-674.

Hutton KE, Goodnight CJ. Variations in the blood chemistry of turtles under active and hibernating conditions. Physiological Zoology 1957; 3: 198-207.
Ingram DL. Stimulation of cutaneous glands in the pig. J Comp Pathol 1967; 77: 93-98.

Ivanov KP. Physiological blocking of the mechanisms of cold death: theoretical and experimental considerations. J Therm Biol 2000; 25: 467-479.

Izumizaki M, Pokorski M, Homma I. Role of the carotid bodies in chemosensory ventilatory responses in the anesthetized

mouse. J Appl Physiol 2004; 97, 1401-7.

Jackson DC, Heisler N. Intracellular and extracellular acid-base and electrolyte status of submerged anoxic turtles at 3 degrees C. Respir Physiol 1983; 53: 187-201.

Jackson WF. Ion channels and vascular tone. Hypertension 2000; 35(Pt 2) :173-8.

Jakimowicz J, Stultiëns G, Smulders F. Laparoscopic insufflation of the abdomen reduces portal venous flow. Surg Endosc 1998; 12: 129-132.

Jinka TR, Toien O, Drew KL. Season primes the brain in an arctic hibernator to facilitate entrance into torpor mediated by adenosine A(1) receptors. J Neurosci 2011; 31: 10752-10758.

Johnson KG. Thermoregulatory changes induced by cholinomimetic substances introduced into the cerebral ventricles of sheep. Br J Pharmacol 1975; 53: 489-497.

Ju H, So H, Ha K, Park K, Lee JW Ching CM, Choi I. Sustained torpidity following multi-dose administration of 3-iodothyronamine in mice. J Cell Physiol 2011 Apr; 226(4): 853-858.

Jurkovich GJ, Greiser WB, Luterman A, Curreri PW. Hypothermia in trauma victims: an ominous predictor of survival. J Trauma 1987; 27: 1019-1024.

Kanosue K, Yanase-Fujiwara M, Hosono T. Hypothalamic network for thermoregulatory vasomotor control. Am J Physiol 1994; 267, R283-8.

Kasner SE, Wein T, Piriyawat P, Villar-Cordova CE, Chalela JA, Krieger DW, Morgenstern LB, Kimmel SE, Grotta JC. Acetaminophen for altering body temperature in acute stroke: a randomized clinical trial. Stroke 2002; 33: 130-134.

Kawashima Y, Ohwada S, Sakata K, Ohya T, Tomizawa N, Takeyoshi I, Morishita Y. Effects of a phosphate buffered extracellular (Ep4) solution in preservation and reperfusion injury in the canine liver. Tohoku J Exp Med 1999; 187: 99-110.

Kemp PJ, Telezhkin V. Oxygen sensing by the carotid body: is it all just rotten eggs? Antioxid Redox Signal 2014; 20: 794-804.

Kenny AD, Musacchia XJ. Influence of season and hibernation on thyroid calcitonin content and plasma electrolytes in ground-squirrel. Comp Biochem Physiol A Comp Physiol 1977; 57: 485-489.

Kindermann W, Pleschka K. Local blood flow and metabolism of the tongue before and during panting in the dog. Eur J Physiol 1973; 340: 251–262.

Kirkpatrick WE, Lomax P. Temperature changes induced by chlorpromazine and N-methyl chlorpromazine in the rat. Neuropharmacology 1971; 10: 61-66.

Kizilirmak S, Karakas SE, Akca O, Ozkan T, Yavru A, Pembeci K, Sessler DI, Telci L. Magnesium sulfate stops postanesthetic shivering. Ann N Y Acad Sci 1997; 813: 799-806.

Kleiber M. Body size and metabolism. J Agric Sci 1932; 11: 6.

Kleiber M. Body size and metabolic rate. Physiol Rev 1947; 27: 511-541.

Kliche K, Jeggle P, Pavensta€dt H, Oberleithner H. Role of cellular mechanics in the function and life span of vascular endothelium. Pflugers Arch 2011; 462: 209-217.

Klöppel K, Gerlach J, Neuhaus P. Addition of an osmotic agent to liver preservative solutions in a model of in vitro preservation of hepatocytes. Langenbecks Arch Chir 1994; 379: 329-334.

Kocsis JJ, Harkaway S, Snyder R. Biological effects of the metabolites of dimethyl sulfoxide. Ann N Y Acad Sci 1975; 243: 104-109.

Kollias J, Bullard RW. The influence of

chlorpromazine on physical and chemical mechanisms of temperature regulation in the rat. J Pharmacol Exp Ther 1964; 145: 373-381.

Kotlyarov EV, Mattay VS, Reba RC. Gallbladder visualization during technetium-99m RBC blood pool imaging. Case report and literature review. Clin Nucl Med 1988; 13: 515-516.

Kottke FJ, Phalen JS. Effect of hypoxia upon temperature regulation of mice, dogs, and man. Am J Physiol 1948; 153: 10-15.

Kubo S, Doe I, Kurokawa Y, Nishikawa H, Kawabata A. Direct inhibition of endothelial nitric oxide synthase by hydrogen sulfide: contribution to dual modulation of vascular tension. Toxicology 2007; 232, 138-146.

Kuhnen G, Wloch B, Wunnenberg W. Effects of acute-hypoxia and or hypercapnia on body temperatures and cold induced thermogenesis in the golden-hamster. Journal of Thermal Biology 1987; 12: 103-107.

Kwiatkoski M, Soriano RN, Francescato HD, Batalhao ME, Coimbra TM, Carnio EC, Branco LG: Hydrogen sulfide as a cryogenic mediator of hypoxia-induced anapyrexia. Neuroscience 2012; 201: 146-156

Lammens M, Lissoir F, Carton H. Hypothermia in three patients with multiple sclerosis. Clin Neurol Neurosurg 1989; 91: 117-121.

Lee CC. Is human hibernation possible? Annu Rev Med 2008; 59: 177-186.

Lee ZW, Zhou J, Chen CS, Zhao Y, Tan CH, Li L, Moore PK, Deng LW: The slow-releasing hydrogen sulfide donor, GYY4137, exhibits novel anti-cancer effects in vitro and in vivo. PLoS One 2011; 6: e21077.

Letsou GV, Breznock EM, Whitehair J, Kurtz RS, Jacobs R, Leavitt ML, Sternberg H, Shermer S, Kehrer S, Segall JM, Voelker MA, Waitz HD, Segall PE. Resuscitating hypothermic dogs after 2 hours of circulatory arrest below 6 degrees C. J Trauma 2003; 54: S177- S182.

Levac B, Parlow JL, van Vlymen J, James P, Tuttle A, Shepherd L. Ringer's lactate is compatible with saline-adenine-glucose-mannitol preserved packed red blood cells for rapid transfusion. Can J Anaesth 2010;57: 1071-1077.

Li J, Zhang G, Cai S, Redington AN. Effect of inhaled hydrogen sulfide on metabolic responses in anesthetized, paralyzed, and mechanically ventilated piglets. Pediatr Crit Care Med 2008; 9: 110-112. (a)

Li S, Dou W, Tang Y, Goorha S, Ballou LR, Blatteis CM. Acetaminophen: antipyretic or hypothermic in mice? In either case, PGHS-1b (COX-3) is irrelevant. Prostaglandins Other Lipid Mediat 2008; 85: 89-99. (b)

Li Q, Sun B, Wang X, Jin Z, Zhou Y, Dong L, Jiang LH, Rong W. A crucial role for hydrogen sulfide in oxygen sensing via modulating large conductance calcium-activated potassium channels. Antioxid Redox Signal 2010; 12: 1179-1189.

Lifson JD, Rubinstein EH, Sonnenschein RR. Hypoxic tachycardia in the rat. Experientia 1977; 33, 476-7.

Lim JJ, Liu YH, Khin ESW, Bian JS. Vasoconstrictive effect of hydrogen sulfide involves downregulation of cAMP in vascular smooth muscle cells. Am J Physiol Cell Physiol 2008; 295, C1261-C1270.

Lin MT, Chern YF, Wang Z, Wang HS. Effects of apomorphine on thermoregulatory responses of rats to different ambient tempera- tures. Can J Physiol Pharmacol 1979; 57: 469-475.

Lin MT. Effects of sodium pentobarbital on thermoregulatory responses in the rat. Neuropharmacology 1981; 20: 693-698.

Lomax P. The hypothermic effect of pentobarbital in the rat: sites and mechanisms of action. Brain Res 1966; 1: 296-302.

Lomax P, Jenden DJ. Hypothermia following systematic and intracerebral injection

of oxotremorine in the rat. Int J Neuropharmacol 1966; 5: 353-359.

Lomax P, Foster RS, Kirkpatrick WE. Cholinergic and adrenergic interactions in the thermoregulatory centers of the rat. Brain Res 1969; 15: 431-438.

Lopez A, Prior M, Yong S, Albassam M, Lillie LE. Biochemical and cytologic alterations in the respiratory tract of rats exposed for 4 hours to hydrogen sulfide. Fundam Appl Toxicol 1987; 9, 753-762.

Lotti VJ, Lomax P, George R. Temperature responses in the rat following intracerebral microinjection of morphine. J Pharmacol Exp Ther 1965; 150: 135-139.

Luecke RH, Gray EW, South FE. Simulation of passive thermal behavior of a cooling biological system: entry into hibernation. Pflugers Arch 1971; 327: 37-52.

Lysakowski C, Dumont L, Czarnetzki C, Tramer MR. Magnesium as an adjuvant to postoperative analgesia: a systematic review of randomized trials. Anesth Analg 2007; 104: 1532-1539.

Madden CJ, Morrison SF. Hypoxic activation of arterial chemoreceptors inhibits sympathetic outflow to brown adipose tissue in rats. J Physiol 2005; 566: 559-573.

Madden JA, Ahlf SB, Dantuma MW, Olson KR, Roerig DL. Precursors and inhibitors of hydrogen sulfide synthesis affect acute hypoxic pulmonary vasoconstriction in the intact lung. J Appl Physiol 2012; 112, 411-418.

Maingret F, Lauritzen I, Patel AJ, Heurteaux C, Reyes R, Lesage F, Lazdunski M, Honore E. TREK-1 is a heat-activated background K(+) channel. EMBO J 2000; 19: 2483-2491.

Margules DL, Goldman B, Finck A. Hibernation: an opioid- dependent state? Brain Res Bull 1979; 4: 721-724.

van Marken Lichtenbelt WD, Vanhommerig JW, Smulders NM, Drossaerts JM, Kemerink GJ, Bouvy ND, Schrauwen P, Teule GJ. Cold-activated brown adipose tissue in healthy men. N Engl J Med 2009; 360: 1500-1508.

Marshall, J. M. Peripheral chemoreceptors and cardiovascular regulation. Physiol Rev 1994; 74, 543–594.

Martinez D, Fiori CZ, Baronio D, Carissimi A, Kaminski RS, Kim LJ, Rosa DP, Bos A. Brown adipose tissue: is it affected by intermittent hypoxia? Lipids Health Dis 2010; 9: 121.

Mathews WB, Nakamoto Y, Abraham EH, Scheffel U, Hilton J, Ravert HT, Tatsumi M, Rauseo PA, Traughber BJ, Salikhova AY, Dannals RF, Wahl RL. Synthesis and biodistribution of [11C] adenosine 5'-monophosphate ([11C]AMP). Mol Imaging Biol 2005; 7: 203-208.

Mayer ML, Westbrook GL. Permeation and block of N-methyl-D-aspartic acid receptor channels by divalent cations in mouse cultured albumin and its opioid-like effects on guinea pig ileum. Pharmacol central neurones. J Physiol 1987; 394: 501-527.

Mayer-Gross W, Berliner F. Observations in hypoglycaemia: IV. Body temperature and coma. Br J Psychiatry 1942; 88: 419-427.

Mayfield KP, D'Alecy LG. Delta-1 opioid agonist acutely increases hypoxic tolerance. J Pharmacol Exp Ther 1994; 268: 683-688. (a)

Mayfield KP, D'Alecy LG. Delta-1 opioid receptor dependence of acute hypoxic adaptation. J Pharmacol Exp Ther 1994; 268: 74-77. (b)

Mayfield KP, Hong EJ, Carney KM, D'Alecy LG. Potential adaptations to acute hypoxia: Hct, stress proteins, and set point for temperature regulation. Am J Physiol 1994; 266: R1615-R1622.

McBirnie JE, Pearson FG, Trusler GA, Karachi HH, Bigelow WG. Physiologic studies of the groundhog (Marmota monax). Can J Med Sci 1953; 31: 421-430.

Mellergard P. Changes in human intracerebral

temperature in response to different methods of brain cooling. Neurosurgery 1992; 31: 671-677.

Metcalfe MS, Waller JR, Hosgood SA, Shaw M, Hassanein W, Nicholson ML. A paired study comparing the efficacy of renal preservation by normothermic autologous blood perfusion and hypothermic pulsatile perfusion. Transplant Proc 2002; 34: 1473-1474.

Michels NA. Newer anatomy of the liver and its variant blood supply and collateral circulation. Am J Surg 1966; 112: 337-347.

Milsom WK, Burleson ML. Peripheral arterial chemoreceptors and the evolution of the carotid body. Respir Physiol Neurobiol 2007; 157, 4–11.

Milstein DJ, Bezemer R, Ince C. Sidestream dark-field (SDF) video microscopy for clinical imaging of the micro-circulation; in Leahy MJ (ed): Microcirculation Imaging. Weinheim, Wiley, 2012, pp 37–52.

Moers C, Smits JM, Maathuis MH, Treckmann J, van Gelder F, Napieralski BP, van Kasterop-Kutz M, van der Heijde JJ, Squifflet JP, van Heurn E, Kirste GR, Rahmel A, Leuvenink HG, Paul A, Pirenne J, Ploeg RJ. Machine perfusion or cold storage in deceased-donor kidney transplantation. N Engl J Med 2009; 360: 7–19.

Molnar GW, Read RC. Hypoglycemia and body temperature. JAMA 1974; 227: 916-921.

Morariu AM, Vd Plaats A, V Oeveren W, 'T Hart NA, Leu- venink HG, Graaff R, Ploeg RJ, Rakhorst G. Hyperaggregating effect of hydroxyethyl starch components and University of Wisconsin solution on human red blood cells: a risk of impaired graft perfusion in organ procurement? Transplantation 2003; 76: 37-43.

Morrison SF, Nakamura K, Madden CJ. Central control of thermogenesis in mammals. Exp Physiol 2008; 93: 773-797.

Morrison SF, Nakamura K. Central neural pathways for thermoregulation. Front Biosci (Landmark Ed) 2011; 16: 74-104.

Mortola JP, Naso L. Thermogenesis in newborn rats after prenatal or postnatal hypoxia. J Appl Physiol (1985) 1998; 85: 84-90.

Mortola JP, Feher C. Hypoxia inhibits cold-induced huddling in rat pups. Respir Physiol 1998; 113: 213-222.

Mortola JP, Merazzi D, Naso L. Blood flow to the brown adipose tissue of conscious young rabbits during hypoxia in cold and warm conditions. Pflugers Arch 1999; 437: 255-260.

Mosbah IB, Franco-Gou R, Abdennebi HB, Hernandez R, Escolar G, Saidane D, Rosello-Catafau J, Peralta C. Effects of polyethylene glycol and hydroxyethyl starch in University of Wisconsin preservation solution on human red blood cell aggregation and viscosity. Transplant Proc 2006 Jun; 38(5): 1229-1235

Mrosovsky N, Barnes DS. Anorexia, food deprivation and hibernation. Physiol Behav 1974; 12: 265-270.

Muzzi M, Blasi F, Masi A, Coppi E, Traini C, Felici R, Pittelli M, Cavone L, Pugliese AM, Moroni F, Chiarugi A. Neurological basis of AMP-dependent thermoregulation and its relevance to central and peripheral hyperthermia. J Cereb Blood Flow Metab 2013; 33: 183- 190.

Myers JA, Millikan KW, Saclarides TJ. Common surgical diseases: An algorithmic approach to problem solving. 2nd ed, New York, Springer, 2008.

Myers RD, Yaksh TL. Control of body temperature in the unanaesthetized monkey by cholinergic and aminergic systems in the hypothalamus. J Physiol 1969; 202: 483-500.

Myers RD, Veale WL, Yaksh TL. Changes in body temperature of the unanaesthetized monkey produced by sodium and calcium ions perfused through the cerebral ventricles. J Physiol 1971; 217: 381- 392.

Myers RD, Veale WL. The role of sodium and calcium ions in the hypothalamus in the control of body temperature of the unanaesthetized cat. J Physiol 1971; 212: 411-430.

Myers RD, Yaksh TL. Thermoregulation around a new set-point established in the monkey by altering the ratio of sodium to calcium ions within the hypothalamus. J Physiol 1971; 218: 609- 633.

Myers RD, Brophy PD. Temperature changes in the rat produced by altering the sodium-calcium ratio in the cerebral ventricles. Neuropharmacology 1972; 11: 351-361.

Myers RD, Buckman JE. Deep hypothermia induced in the golden hamster by altering cerebral calcium levels. Am J Physiol 1972; 223: 1313-1318.

Myers RD, Simpson CW, Higgins D, Nattermann RA, Rice JC, Redgrave P, Metcalf G. Hypothalamic Na+ and Ca++ ions and temperature set-point: new mechanisms of action of a central or peripheral thermal challenge and intrahypothalamic 5-HT, NE, PGEi and pyrogen. Brain Res Bull 1976; 1: 301-327.

Myers RD, Oeltgen PR, Spurrier WA. Hibernation "trigger" injected in brain induces hypothermia and hypophagia in the monkey. Brain Res Bull 1981 Dec; 7(6): 691-705.

Nakamura K, Morrison SF. Central efferent pathways for cold-defensive and febrile shivering. J Physiol 2011; 589: 3641-3658.

Nakamura K. Central circuitries for body temperature regulation and fever. Am J Physiol Regul Integr Comp Physiol 2011; 301: R1207-R1228.

Nicholls P, Kim JK. Sulphide as an inhibitor and electron donor for the cytochrome c oxidase system. Can J Biochem 1982;60:613–623.

Nicholls P, Marshall DC, Cooper CE, Wilson MT. Sulfide inhibition of and metabolism by cytochrome c oxidase. Biochem Soc Trans 2013; 41, 1312–1316.

Nozari A, Safar P, Wu X, Stezoski WS, Henchir J, Kochanek P, Klain M, Radovsky A, Tisherman SA. Suspended animation can allow survival without brain damage after traumatic exsanguination cardiac arrest of 60 minutes in dogs. J Trauma 2004; 57: 1266-1275.

Oeltgen PR, Bergmann LC, Spurrier WA, Jones SB. Isolation of a hibernation inducing trigger(s) from the plasma of hibernating woodchucks. Prep Biochem 1978; 8: 171-188.

Oeltgen PR, Walsh JW, Hamann SR, Randall DC, Spurrier WA, Myers RD. Hibernation "trigger": opioid-like inhibitory action on brain function of the monkey. Pharmacol Biochem Behav 1982; 17: 1271-1274.

Oeltgen PR, Blouin RA, Spurrier WA, Myers RD. Hibernation "trigger" alters renal function in the primate. Physiol Behav 1985 Jan; 34(1): 79-81.

Oeltgen PR, Nilekani SP, Nuchols PA, Spurrier WA, Su TP. Further studies on opioids and hibernation: delta opioid receptor ligand selectively induced hibernation in summer-active ground squirrels. Life Sci 1988; 43: 1565-1574.

de Oliveira C, Garami A, Lehto SG , Pakai E, Tekus V, Pohoczky K, Youngblood BD, Wang W, Kort ME, Kym PR, Pinter E, Gavva NR, Romanovsky AA. Transient receptor potential channel ankyrin-1 is not a cold sensor for autonomic thermoregulation in rodents. J Neurosci 2014; 34: 4445-4452.

Olson JM, Jinka TR, Larson LK, Danielson JJ, Moore JT, Carpluck J, Drew KL. Circannual rhythm in body temperature, torpor, and sensitivity to A(1) adenosine receptor agonist in arctic ground squirrels. J Biol Rhythms 2013; 28: 201-207.

Ong PK, Jain S, Namgung B, Woo YI, Kim S. Cell-free layer formation in small arterioles at pathological levels of erythrocyte

aggregation. Microcirculation 2011; 18: 541-551.

Orlando MM, Panuska JA. Dimethylsulfoxide and thermore- gulation: studies on body temperature, metabolic rate and thyroid function. Cryobiology 1972; 9: 198-204.

Osipov RM, Robich MP, Feng J, Liu Y, Clements RT, Glazer HP, Sodha NR, Szabo C, Bianchi C, Sellke FW. Effect of hydrogen sulfide in a porcine model of myocardial ischemia-reperfusion: comparison of different administration regimens and characterization of the cellular mechanisms of protection. J Cardiovasc Pharmacol 2009; 54: 287-297.

Owens NC, Ootsuka Y, Kanosue K, McAllen RM. Thermoregulatory control of sympathetic fibres supplying the rat's tail. J Physiol 2002; 543, 849-858.

Panas HN, Lynch LJ, Vallender EJ, Xie Z, Chen GL, Lynn SK, Scanlan TS, Miller GM. Normal thermoregulatory responses to 3-iodothyronamine, trace amines and amphetamine-like psychostimulants in trace amine associated receptor 1 knockout mice. J Neurosci Res 2010; 88: 1962-1969.

Panuska JA. The effect of dimethylsulfoxide on behavioral temperature regulation. Proc Soc Exp Biol Med 1968; 127: 169-173

Parmeggiani PL, Azzaroni A, Calasso M. Behavioral state- dependent thermal feedback influencing the hypothalamic thermo- stat. Arch Ital Biol 2000; 138: 277-283.

Passias TC, Meneilly GS, Mekjavic IB. Effect of hypoglycemia on thermoregulatory responses. J Appl Physiol (1985) 1996; 80: 1021- 1032.

Pedemonte CH, Beauge L. Inhibition of (Na+,K+)-ATPase by magnesium ions and inorganic phosphate and release of these ligands in the cycles of ATP hydrolysis. Biochim Biophys Acta 1983; 748: 245-253.

Pegg DE, Jacobsen IA, Halasz NA, Society T. Organ Preservation: Basic and Applied Aspects. Lancaster, England: MTP Press; 1982.

Peleg M, Normand MD, Corradini MG. The Arrhenius equation revisited. Crit Rev Food Sci Nutr 2012; 52, 830-851.

Pelz KM, Routman D, Driscoll JR, Kriegsfeld LJ, Dark J. Monosodium glutamate-induced arcuate nucleus damage effects both natural torpor and 2DG-induced torpor-like hypothermia in Siberian hamsters. Am J Physiol Regul Intergr Comp Physiol 2008 Jan; 294(1): R255-265.

Peng YJ, Nanduri J, Raghuraman G, Souvannakitti D, Gadalla MM, Kumar GK, Snyder SH, Prabhakar NR. H2S mediates O2 sensing in the carotid body. Proc Natl Acad Sci USA 2010; 107: 10719- 10724.

Pengelley ET, Kelly KH. Plasma potassium and sodium concentrations in active and hibernating golden-mantled ground squirrels, Citellus lateralis. Comp Biochem Physiol 1967; 20: 299-305.

Pertwee RG, Marshall NR, Macdonald AG . Effects of subanesthetic doses of inert gases on behavioral thermoregulation in mice. J Appl Physiol (1985) 1986; 61: 1623-1633.

Petit L, Buu-Ho NP. A synthesis of thyronamine and its lower homolog. J Org Chem 1961; 26: 3832-3834.

Piantadosi CA, Thalmann ED. Thermal responses in humans exposed to cold hyperbaric helium-oxygen. J Appl Physiol Respir Environ Exerc Physiol 1980; 49: 1099-1106.

Pirenne J, Van Gelder F, Coosemans W, Aerts R, Gunson B, Koshiba T, Fourneau I, Mirza D, van Steenbergen W, Fevery J, Nevens F, MacMaster P. Type of donor aortic preservation solution and not cold ischemia time is a major determinant of biliary strictures after liver transplantation. Liver Transpl 2001; 7: 540-545.

van der Plaats A, Maathuis MH, 't Hart NA, Bellekom AA, Hofker HS, van der Houwen EB,

Verkerke GJ, Leuvenink HG, Verdonck P, Ploeg RJ, Rakhorst G. The Groningen hypothermic liver perfusion pump: functional evaluation of a new machine perfusion system. Ann Biomed Eng 2006; 34: 1924–34.

Planel E, Miyasaka T, Launey T, Chui DH, Tanemura K, Sato S, Murayama O, Ishiguro K, Tatebayashi Y, Takashima A. Alterations in glucose metabolism induce hypothermia leading to tau hyperphosphorylation through differential inhibition of kinase and phosphatase activities: implications for Alzheimer's disease. J Neurosci 2004; 24, 2401–11.

Platner WS. Effects of low temperature on magnesium content of blood, body fluids and tissues of goldfish and turtle. Am J Physiol 1950; 161: 399-405.

Platner WS, Hosko MJ, Jr. Mobility of serum magnesium in hypothermia. Am J Physiol 1953; 174: 273-276.

Polderman KH. Application of therapeutic hypothermia in the intensive care unit. Opportunities and pitfalls of a promising treatment modality-Part 2: Practical aspects and side effects. Intensive Care Med 2004; 30: 757-769.

Polderman KH. Mechanisms of action, physiological effects, and complications of hypothermia. Crit Care Med 2009; 37: S186-S202.

Post IC, Dirkes MC, Heger M, Bezemer R, van 't Leven J, van Gulik TM. Optimal flow and pressure management in machine perfusion systems for organ preservation. Ann Biomed Eng 2012; 40: 2698-2707.

Pozsgai G, Hajna Z, Bagoly T, Boros M, Kemény Á, Materazzi S, Nassini R, Helyes Z, Szolcsányi J, Pintér E. The role of transient receptor potential ankyrin 1 (TRPA1) receptor activation in hydrogen-sulphide-induced CGRP-release and vasodilation. Eur J Pharmacol 2012; 689: 56–64.

Prabhakar NR. Oxygen sensing by the carotid body chemoreceptors. J Appl Physiol (1985) 2000; 88: 2287-2295.

Prabhakar NR. Hydrogen sulfide (H2S): a physiologic mediator of carotid body response to hypoxia. Adv Exp Med Biol 2012; 758: 109-113.

Prabhakar NR, Semenza GL. Gaseous messengers in oxygen sensing. J Mol Med (Berl) 2012; 90: 265-272.

Pratihar S, Kundu JK. Increased serum magnesium and calcium and their regulation during hibernation in the indian common toad, Duttaphrynus melanostictus (Schneider, 1799). S Am J Herpetol 2009; 4: 51-54.

Prior MG, Sharma AK, Yong S, Lopez A. Concentration-time interactions in hydrogen sulphide toxicity in rats. Can J Vet Res 1988; 52, 375-9.

Queva C, Bremner-Danielsen M, Edlund A, Ekstrand AJ, Elg S, Erickson S, Johansson T, Lehmann A, Mattsson JP. Effects of GABA agonists on body temperature regulation in GABA (B1)-/- mice. Br J Pharmacol 2003; 140: 315-322.

Ratigan ED, McKay DB. Exploring principles of hibernation for organ preservation. Transplant Rev (Orlando) 2016 Jan; 30(1): 13-9.

Reese SA, Crocker CE, Jackson DC, Ultsch GR. The physiology of hibernation among painted turtles: the midland painted turtle (Chrysemys picta marginata). Respir Physiol 2001; 124: 43-50.

Reiniers MJ, van Golen RF, Heger M, Mearadji B, Bennink RJ, Verheij J, van Gulik TM. In situ hypothermic perfusion with retrograde outflow during right hemihepatectomy: first experiences with a new technique. J Am Coll Surg 2014; 218: e7-16.

Rewerski WJ, Jori A. Microinjection of chlorpromazine in different parts of rat brain. Int J Neuropharmacol 1968; 7: 359-364.

Riedesel ML. Serum magnesium levels in

mammalian hibernation. Trans Kans Acad Sci 1957; 62: 99-141.

Riedesel ML, Folk GE, Jr. Serum magnesium changes in cold- exposed mammals. J Mammal 1957; 38: 423-424.

Riedesel ML, Folk GE, Jr. Serum electrolyte levels in hibernating mammals. Am Nat 1958; 92: 307-312.

Ríos-González BB, Román-Morales EM, Pietri R, López-Garriga J. Hydrogen sulfide activation in hemeproteins: the sulfheme scenario. J Inorg Biochem 2014; 133, 78–86.

Robinson KA, Haymes EM. Metabolic effects of exposure to hypoxia plus cold at rest and during exercise in humans. J Appl Physiol (1985) 1990; 68: 720-725.
Rochelle RH, Chaffee RR, Greenleaf JE, Walker CD. The effects of magnesium on state 3 respiration of liver mitochondria from control and cold-acclimated rats and hamsters. Comp Biochem Physiol B 1978; 60: 267-269.

Rolfe DF, Brown GC. Cellular energy utilization and molecular origin of standard metabolic rate in mammals. Physiol Rev 1997; 77: 731-758.

Romanovsky AA, Ivanov AI, Shimansky YP. Selected contribution: ambient temperature for experiments in rats: a new method for determining the zone of thermal neutrality. J Appl Physiol (1985) 2002; 92: 2667-2679.

Rönert H, Pleschka K. Lingual blood flow and its hypothalamic control in the dog during panting. Eur J Physiol 1976; 367: 25-31.

Ros E. Nuts and novel biomarkers of cardiovascular disease. Am J Clin Nutr 2009; 89: 1649S-1656S.

Rosenbaum EE, Herschler RJ, Jacob SW. Dimethyl sulfoxide in musculoskeletal disorders. JAMA 1965; 192: 309-313.

Rudaya AY, Steiner AA, Robbins JR, Dragic AS, Romanovsky AA. Thermoregulatory responses to lipopolysaccharide in the mouse: dependence on the dose and ambient temperature. Am J Physiol Regul Integr Comp Physiol 2005; 289, R1244–R1252.

Rudelli R, Deck JH. Selective traumatic infarction of the human anterior hypothalamus. Clinical anatomical correlation. J Neurosurg 1979; 50: 645-654.

Ryu JH, Kang MH, Park KS, Do SH. Effects of magnesium sulphate on intraoperative anaesthetic requirements and postoperative analgesia in gynaecology patients receiving total intravenous anaesthesia. Br J Anaesth 2008; 100: 397-403.

Sadowski B, Szczepanska-Sadowska E. The effect of calcium ions chelation and sodium ions excess in the cerebrospinal fluid on body temperature in conscious dogs. Pflugers Arch 1974; 352: 61-68.

Sajid MS, Shakir AJ, Khatri K, Baig MK. The role of perioperative warming in surgery: a systematic review. Sao Paulo Med J 2009; 127: 231-237.

Salmi P, Kela J, Arvidsson U, Wahlestedt C. Functional interactions between delta- and mu-opioid receptors in rat thermoregulation. Eur J Pharmacol 2003; 458: 101-106.

Sato S, Kuwajima A, Watanabe S, Nagamoto M, Taki S, Murakami S, Hamada M. Delayed visualization of gall-bladder with in vivo labeled Tc-99m-red blood cell scintigraphy for gastrointestinal bleeding. Radiat Med 1988; 6: 159-161.

Saxena PN. Sodium and calcium ions in the control of temperature set-point in the pigeon. Br J Pharmacol 1976; 56: 187-192.

Scanlan TS, Suchland KL, Hart ME, Chiellini G, Huang Y, Kruzich PJ, Frascarelli S, Crossley DA, Bunzow JR, Ronca-Testoni S, Lin ET, Hatton D, Zucchi R, Grandy DK. 3-Iodothyronamine is an endogenous and rapid-acting derivative of thyroid hormone. Nat Med 2004; 10: 638-642.

Schreinemachers MCJM, Doorschodt BM, van Gulik TM. Machine perfusion

preservation of the liver: a worthwhile clinical activity? Curr Opin Organ Transplant 2007; 12: 224.

Schreinemachers MCJM, Doorschodt BM, Florquin S, van den Bergh MA, Zernecke A, Idu MM, Tolba RH, van Gulik TM. Pulsatile perfusion preservation of warm ischaemia-damaged experimental kidney grafts. Br J Surg 2010; 97: 349-358.

Scott RA, Schwartz JR, Cramer SP. Effect of cyanide binding on the copper sites of cytochrome c oxidase: an X-ray absorption spectroscopic study. J Inorg Biochem 1985; 23: 199-205.

Sekaran P, Ehrlich MP, Hagl C, Leavitt ML, Jacobs R, McCullough JN, Bennett-Guerrero E. A comparison of complete blood replacement with varying hematocrit levels on neurological recovery in a porcine model of profound hypothermic (<5 degrees C) circulatory arrest. Anesth Analg 2001; 92: 329-334.

Selzer A, Sudrann RB. Reliability of the determination of cardiac output in man by means of the Fick principle. Circ Res 1958; 6: 485- 490.

Seoane JR, Baile CA. Ionic changes in cerebrospinal fluid and feeding, drinking and temperature of sheep. Physiol Behav 1973; 10: 915-923.

Sgaragli G, Ninci R, Della CL, Valoti M, Nardini M, Andreoli V, Moneti G. Promazine. A major plasma metabolite of chlorpromazine in a population of chronic schizophrenics. Drug Metab Dispos 1986; 14: 263-266.

Sharif NA, Hughes J. Discrete mapping of brain Mu and delta opioid receptors using selective peptides: quantitative auto-radiography, species differences and comparison with kappa receptors. Peptides 1989; 10: 499-522.

Siebert N, Cantré D, Eipel C, Vollmar B. H2S contributes to the hepatic arterial buffer response and mediates vasorelaxation of the hepatic artery via activation of KATP channels. Am J Physiol Gastrointest Liver Physiol 2008 Dec; 295(6): G1266-G1273.

Simon F, Giudici R, Duy CN, Schelzig H, Oter S, Gröger M, Wachter U, Vogt J, Speit G, Szabó C, Radermacher P, Calzia E. Hemodynamic and metabolic effects of hydrogen sulfide during porcine ischemia/reperfusion injury. Shock 2008; 30: 359-364.

Sodha NR, Clements RT, Feng J, Liu Y, Bianchi C, Horvath EM, Szabo C, Stahl GL, Sellke FW. Hydrogen sulfide therapy attenuates the inflammatory response in a porcine model of myocardial ischemia/reperfusion injury. J Thorac Cardiovasc Surg 2009; 138: 977-984.

Som P, Yonekura Y, Oster ZH, Meyer MA, Pelletteri ML, Fowler JS, MacGregor RR, Russell JA, Wolf AP, Fand I, McNally WP, Brill AB. Quantitative autoradiography with radiopharmaceuticals, Part 2: Applications in radiopharmaceutical research: concise communication. J Nucl Med 1983; 24: 238-244.

Somerville AR, Whittle BA. The interrelation of hypothermia and depletion of noradrenaline, dopamine and 5-hydroxytryptamine from brain by reserpine, para-chlorophenylalanine and alpha-methylmetatyrosine. Br J Pharmacol Chemother 1967, 31: 120-131.

Song X, Körtner G, Geiser F. Reduction of metabolic rate and thermoregulation during daily torpor. J Comp Physiol B 1995; 165, 291-7.

Song X, Körtner G, Geiser F. Thermal relations of metabolic rate reduction in a hibernating marsupial. Am J Physiol 1997; 273, R2097-R2104.

Spencer RL, Hruby VJ, Burks TF. Alteration of thermoregulatory set point with opioid agonists. J Pharmacol Exp Ther 1990; 252: 696-705.

Spiegel HU, Schleimer K, Kranz D, Oldhafer KJ. Organ preservation with EC, HTK, and UW solutions in orthotopic liver transplantation in syngeneic rats. Part I: functional parameters. J Invest Surg 1998; 11: 49-56.

Spurrier WA, Folk GE Jr, Dawe AR. Induction of summer hibernation in the 13-lined ground squirrel shown by comparative serum transfusions from arctic mammals. Cryogiology 1976 Jun; 13(3): 368-374.

Stamper JL, Dark J. Metabolic fuel availability influences thermoregulation in deer mice (Peromyscus maniculatus). Physiol Behav 1997; 61: 521-524.

Stein A, Mao Z, Morrison JP, Fanucchi MV, Postlethwait EM, Patel RP, Krauw DW, Doeller JE, Bailey SM. Metabolic and cardiac signaling effects of inhaled hydrogen sulfide and low oxygen in male rats. J Appl Physiol 2012; 112, 1659-69.

Steiner AA, Branco LG. Hypoxia-induced anapyrexia: implications and putative mediators. Annu Rev Physiol 2002; 64: 263-288.

Stevens T, Fitzsimmons L. Effect of a standardized rewarming protocol and acetaminophen on core temperature after coronary artery bypass. Am J Crit Care 1995; 4: 189-197.

Stevens T. Managing postoperative hypothermia, rewarming, and its complications. Crit Care Nurs Q 1993; 16: 60-77.

Strek KS, Long MD, Gordon CJ. Effect of sodium pentobarbital on behavioral thermoregulation in rats and mice. Pharmacol Biochem Behav 1986; 24: 1147-1150.

Sugimura M, Hanamoto H, Boku A, Morimoto Y, Taki K, Kudo C, Niwa H. Influence of acute hypoxia combined with nitrous oxide on cardiovascular variability in conscious hypertensive rats. Auton Neurosci 2010; 156, 73-81.

Sullivan F, Hutchinson M, Bahandeka S, Moore RE. Chronic hypothermia in multiple sclerosis. J Neurol Neurosurg Psychiatry 1987; 50: 813-815.

Suomalainen P. Magnesium and calcium content of hedgehog serum during hibernation. Nature 1938; 141: 471.

Swan H, Jenkins D, Knox K. Metabolic torpor in Protopterus aethiopicus: an anti-metablic agent from the brain. The American Naturalist 1969 May-June; 103(931): 247-258.

Swan H, Schätte C. Antimetabolic extract from the brain of the hibernating ground squirrel Citellus tridecemlineatus. Science 1977 Jan; 195(4273): 84-85.

Swoap SJ, Rathvon M, Gutilla M. AMP does not induce torpor. Am J Physiol Regul Integr Comp Physiol 2007; 293: R468-R473.

Tan HP, Vyas D, Basu A, Randhawa P, Shah N, Donaldson J, Marcos A, Simmons RL, Starzl TE, Shapiro R. Cold heparinized lactated Ringers with procaine (HeLP) preservation fluid in 266 living donor kidney transplantations. Transplantation 2007; 83: 1134-1136.

Telezhkin V, Brazier SP, Cayzac S, Müller CT, Riccardi D, Kemp PJ. Hydrogen sulfide inhibits human BKCa channels. Adv Exp Med Biol 2009; 648: 65-72.

Tempel GE, Musacchia XJ. Renal function in the hibernating, and hypothermic hamster Mesocricetus auratus. Am J Physiol 1975; 228: 602-607.

Tempel GE, Wolinsky I, Musacchia XJ. Bone and serum-calcium in normothermic, cold-acclimated and hibernating hamsters. Comp Biochem Physiol A Comp Physiol 1978; 61: 145-147.

Tempel A, Zukin RS. Neuroanatomical patterns of the mu, delta, and kappa opioid receptors of rat brain as determined by quantitative in vitro autoradiography. Proc Natl Acad Sci U S A 1987; 84: 4308-4312.

Teppema LJ, Dahan A. The ventilatory response to hypoxia in mammals: Mechanisms, Measurement, and Analysis. Physiol Rev 2010; 90, 675-754.

Thompson DA, Lilavivathana U, Campbell RG, Welle SL, Craig AB. Thermoregulatory

and related responses to 2-deoxy-D-glucose administration in humans. Am J Physiol 1980; 239: R291-R295.

Thuillier R, Giraud S, Favreau F, Goujon JM, Desurmont T, Eugene M, Barrou B, Hauet T. Improving long-term outcome in allograft transplantation: role of ionic composition and polyethylene glycol. Transplantation 2011; 91: 605-614.

Tisone G, Vennarecci G, Baiocchi L, Negrini S, Palmieri GP, Angelico M, Dauri M, Casciani CU. Randomized study on in situ liver perfusion techniques: gravity perfusion vs high-pressure perfusion. Transplant Proc 1997; 29: 3460-3462.

Tojimbara T, Wicomb WN, Garcia-Kennedy R, Burns W, Hayashi M, Collins G, Esquivel CO. Liver transplantation from non-heart beating donors in rats: influence of viscosity and temperature of initial flushing solutions on graft function. Liver Transpl Surg 1997; 3: 39-45.

Tokunaga Y, Ozaki N, Wakashiro S, Ikai I, Kimoto M, Morimoto T, Shimahara Y, Kamiyama Y, Yamaoka Y, Ozawa K. Effects of perfusion pressure during flushing on the viability of the procured liver using non-invasive fluorometry. Transplantation 1988; 45: 1031-1035.

Toussaint K, Yang XC, Zielinski MA, Reigle KL, Sacavage SD, Nagar S, Raffa RB. What do we (not) know about how paracetamol (acetaminophen) works? J Clin Pharm Ther 2010; 35: 617- 638.

Treckmann J, Moers C, Smits JM, Gallinat A, Jochmans I, Squifflet JP, Pirenne J, **Ploeg** RJ, Paul A. Machine perfusion in clinical trials: "machine vs. solution effects". Transpl Int 2012; 25: e69-e70.

Tricklebank MD, Forler C, Fozard JR. The involvement of subtypes of the 5-HT1 receptor and of catecholaminergic systems in the behavioural response to 8-hydroxy-2-(di-n-propylamino) tetralin in the rat. Eur J Pharmacol 1984; 106: 271-282.

Trudell JR, Koblin DD, Eger EI. A molecular description of how noble gases and nitrogen bind to a model site of anesthetic action. Anesth Analg 1998; 87: 411-418.

Tsushima H, Mori M Matsuda T. Effects of D-Ala2-D-Leu5-enkephalin, microinjected into the supraoptic and paraventricular nuclei, on urine outflow rate. Jpn J Pharmacol 1993 Oct; 63(2): 181-186.

Tupone D, Madden CJ, Morrison SF. Central activation of the A1 adenosine receptor (A1AR) induces a hypothermic, torpor-like state in the rat. J Neurosci 2013; 33: 14512-14525. (a)

Tupone D, Madden CJ, Morrison SF. Highlights in basic autonomic neurosciences: central adenosine A1 receptor-the key to a hypometabolic state and therapeutic hypothermia? Auton Neurosci 2013; 176: 1-2. (b)

Ultsch GR, Hanley RW, Bauman TR. Responses to anoxia during simulated hibernation in northern and southern painted turtles. Ecology 1985; 66: 388-395.

Ultsch GR. Blood-Gases, Hematocrit, plasma ion concentrations, and acid-base status of musk turtles (Sternotherus-Odoratus) during simulated hibernation. Physiological Zoology 1988; 61: 78-94.

Ultsch GR, Carwile ME, Crocker CE, Jackson DC. The physiology of hibernation among painted turtles: the Eastern painted turtle Chrysemys picta picta. Physiol Biochem Zool 1999; 72: 493-501.

Virtanen KA, Lidell ME, Orava J, Heglind M, Westergren R, Niemi T, Taittonen M, **Laine** J, Savisto NJ, Enerback S, Nuutila P. Functional brown adipose tissue in healthy adults. N Engl J Med 2009; 360: 1518-1525.

Vitulli WF, Kaiser GA, Maranto DL, Blake SE, Storey TM, McPherson KP, Luper SL. Acetaminophen effects on behavioral thermoregulation in albino rats. Percept Mot Skills 1999; 88: 281-291.

Volpato GP, Searles R, Yu B, Scherrer-Crosbie M, Bloch KD, Ichinose F, Zapol WM. Inhaled hydrogen sulfide: a rapidly reversible inhibitor of cardiac and metabolic function in the mouse. Anesthesiology 2008; 108: 659-668.

Wadhwa A, Sengupta P, Durrani J, Akca O, Lenhardt R, Sessler DI, Doufas AG. Magnesium sulphate only slightly reduces the shivering threshold in humans. Br J Anaesth 2005; 94: 756-762.

Walton JB, Andrews JF. Torpor Induced by Food-Deprivation in the Wood Mouse Apodemus-Sylvaticus. Journal of Zoology 1981; 194: 260-263.

Weiner N, Perkins M, Sidman RL. Effect of reserpine on noradrenaline content of innervated and denervated brown adipose tissue of the rat. Nature 1962; 193: 137-138.

White KD, Scoones DJ, Newman PK. Hypothermia in multiple sclerosis. J Neurol Neurosurg Psychiatry 1996; 61: 369-375.

Willis JS, Goldman SS, Foster RF. Tissue K concentration in relation to the role of the kidney in hibernation and the cause of periodic arousal. Comp Biochem Physiol A Comp Physiol 1971; 39: 437-445.

Wilson CH, Wyrley-Birch H, Vijayanand D, Leea A, Car- ter NM, Haswell M, Cunningham AC, Talbot D. The influence of perfusion solution on renal graft viability assessment. Transplant Res 2012; 1: 18.

Wood MJ, Hennigan DB. Radionuclide tagged red blood cells in the gallbladder. Clin Nucl Med 1984; 9: 289-290.

Yakimova K, Sann H, Schmid HA, Pierau FK. Effects of GABA agonists and antagonists on temperature-sensitive neurones in the rat hypothalamus. J Physiol 1996; 494(Pt 1): 217-230.

Yamauchi JI, Richter S, Vollmar B, Menger MD, Minor T. Warm preflush with streptokinase improves microvascular procurement and tissue integrity in liver graft retrieval from non-heart-beating donors. Transplantation 2000; 69: 1780-1784.

Zatzman ML, South FE. Renal function of the awake and hibernating marmot Marmota flaviventris. Am J Physiol 1972; 222: 1035-1039.

Zhang H, Zhi L, Moore PK, Bhatia M. Role of hydrogen sulfide in cecal ligation and puncture-induced sepsis in the mouse. Am J Physiol Lung Cell Mol Physiol 2006; 290: L1193-L1201.

Zhang J, Kaasik K, Blackburn MR, Lee CC. Constant darkness is a circadian metabolic signal in mammals. Nature 2006; 439, 340-3.

Zhang F, Wang S, Luo Y, Ji X, Nemoto EM, Chen J. When hypothermia meets hypotension and hyperglycemia: the diverse effects of adenosine 5'-monophosphate on cerebral ischemia in rats. J Cereb Blood Flow Metab 2009; 29: 1022-1034.

Zhao WY, Xiong HY, Yuan Q, Zeng L, Wang LM, Zhu YH. In vitro effects of polyethylene glycol in University of Wisconsin preservation solution on human red blood cell aggregation and hemorheology. Clin Hemorheol Microcirc 2011; 47: 177-185.

Zweifler RM, Voorhees ME, Mahmood MA, Parnell M. Magnesium sulfate increases the rate of hypothermia via surface cooling and improves comfort. Stroke 2004; 35: 2331-2334.

ACKNOWLEDGEMENTS

Acknowledgements

In case of a personal copy you will find a hand-written acknowledgement below.